ROMA TRE
UNIVERSITÀ DEGLI STUDI

SCUOLA DOTTORALE IN GEOLOGIA DELL'AMBIENTE E DELLE RISORSE

XXIII CICLO

APPLICATION OF THE MODFLOW GROUNDWATER NUMERICAL MODEL TO HYDROGEOLOGICAL VOLCANIC UNITS

Sara Taviani
A.A. 2010/2011

Tutor: Prof. Giuseppe Capelli

Coordinatore: Prof. Domenico Cosentino

APPLICATION OF THE MODFLOW GROUNDWATER NUMERICAL MODEL TO HYDROGEOLOGICAL VOLCANIC UNITS

Tutor: prof. Giuseppe Capelli*

Co-tutors: Hans Jorgen Henriksen**

Carlo Rosa***

Dottoranda: Sara Taviani

* Laboratorio di Idrogeologia Numerica e Quantitativa, Dipartimento Scienze Geologiche, Università Roma Tre

** Geological Survey of Denmark and Greenland (GEUS), Copenhagen, Danimarca

***Fondazione Ing. Carlo Maurilio Lerici, Politecnico di Milano

a Cesare, curioso per le mie idee, mai banale nelle sue obiezioni
ed a Giusi, pronta nel trovare il bello della vita…papà e mamma

a Caterina, Filippo e Benni, allegri e stupefacenti

APPLICATIONS OF NUMERICAL GROUNDWATERS FLOW MODELS TO HYDROGEOLOGICAL VOLCANIC UNITS 6

APPLICATIONS OF NUMERICAL GROUNDWATERS FLOW MODELS TO HYDROGEOLOGICAL VOLCANIC UNITS

1. INTRODUCTION AND STUDY OBJECTIVES

This study is part of "multi step collaboration" between the Regional Groundwater Department (Autorità dei Bacini Regionali), the Regional Environmental Department (Assessorato all'Ambiente Regionale) and the University of Roma Tre. The aim of the projects overtaken in the last fifteen years has been the evaluation of the water resources.

Defining the study objectives is an important step in applying a ground water flow model. The objectives aid in determining the level of detail and accurancy required in the model simulation. Complete and detailed objectives would ideally be specified prior to any modelling activities. (ASTM, D5447-04)

The objectives of this work of study are:

To build a Bracciano conceptual model that could "contain" all the achieved information and analysis about a complex context. A conceptual model at basin scale (380 km2), that could on one side take in consideration all the complexities of the Bracciano volcanic deposits and on the other side that could arrive to a simplify representation. Bracciano hydrogeologic basin include: four caldera structures, two of these still occupied by lakes. There are two big withdrawal sites: one from lake and the other fed by drains on the northwest side of the Lake Bracciano. At the same time the area is exposed to a continuous exploitation and dewatering from effect of the several public and private pumping wells put in action in the last twenty years. Considering the Lake Bracciano relevance (since roman period Bracciano area constituted a water reservoir for the near city of Rome) the conceptual model should be focused on the lake-aquifer interactions.

To build a numerical groundwater model for the Bracciano hydrogeologic basin. By use of MODFLOW, set up a site specific regional groundwater model, which could be representative of the studied context at the scale decided. The mathematical model should be coherent with the conceptual model elaborated and it should be a constant critical reviewing of the mathematical model and then in consequences of the conceptual model to point to a better fit between them.
To construct a regional numerical groundwater flow whereby all the data and geological interpretations can be put together allowing quantitative evaluations of groundwater recharge, water balance for the lake and the aquifers. The idea with the numerical model is to try to evaluate whether the conceptual model can be confirmed by simulations and validation tests using data not used for calibration. Part of this objective is to find out how the conceptual model can be translated into a numerical model (simplified etc.), how boundary conditions can be introduced in the MODFLOW setup, rivers, drains, pumping wells, discretization, parameter zoning etc.

Further objective is to assess whether and to what extent the numerical modelling can be a powerful aid in the management of water resources for predictive simulations. It can be a powerful aid for different reasons. It can give feedback to data collection, conceptual model, process understanding, geological interpretation. It is a quantitative way of understanding groundwater levels and flow relationships. It can give input to local models etc.
It is important to understand if it is possible always think to use numerical hydrological modelling for management purposes and under what conditions. And if is not possible, which claims to give. Setting of a monitoring network could be of help in the improving of a model site building and in the validation of the model, necessary step for model that could be used with a predictive approach.

2. STUDY AREA

2.1 CONTEXT OF SABATINI VOLCANIC COMPLEX

2.1.1 Geographical setting

The region of Sabatini complex covers an area larger than 1690 km2 and it is located in the northern area of Rome (Central Italy). The volcanic activity conditions the morphological structure of the overall area.

The products of more distant volcanic activity belonging to the Vicano and Cimino complexes partially cover the northernmost part of this geographical area.

The study area belong to the Sabatini complex and it is constituted by the hydrogeologic basin of Bracciano Lake 380 km2 wide. Baccano, Polline, Stracciacappe, Martignano and Bracciano depressions are part of it (see Fig. 2.1).

Bracciano depression is the largest one (about 380 km2) and it was caused by a volcano-tectonic collapse. Other lower surface areas are presents, identified as small craters or calderas.

The depressions of Bracciano, Martignano and Monte Rosi are occupied by lakes, Their altitudes above sea level (a.s.l.) are 162, 205 and 237 m.and their depth 160, 54 and 5 m, respectively.

Until the 19th century some calderas were filled with water: there was a lake basin in the Stracciacappa caldera depression, drained by a tunnel connected to Bracciano Lake where another tunnel draining from Martignano joined; in the depression of Baccano caldera there was a swamp, drained by a tunnel in the south-southeast side of the valley.

Baccano valley is also open to the East and is connected to the Tevere River by the Curzio stream.

Aforementioned depressions are usually surrounded by a series of asymmetric topographic profile relieves with steep slopes inwards and more gentle slopes outwards.

In the northwest part, these depressions are surrounded by relieves: Rocca Romana (612 m a.s.l.), M. Raschio (554 m a.s.l), Monte Calvario (541 m a.s.l) and Poggio delle Forche (530 m a.s.l).

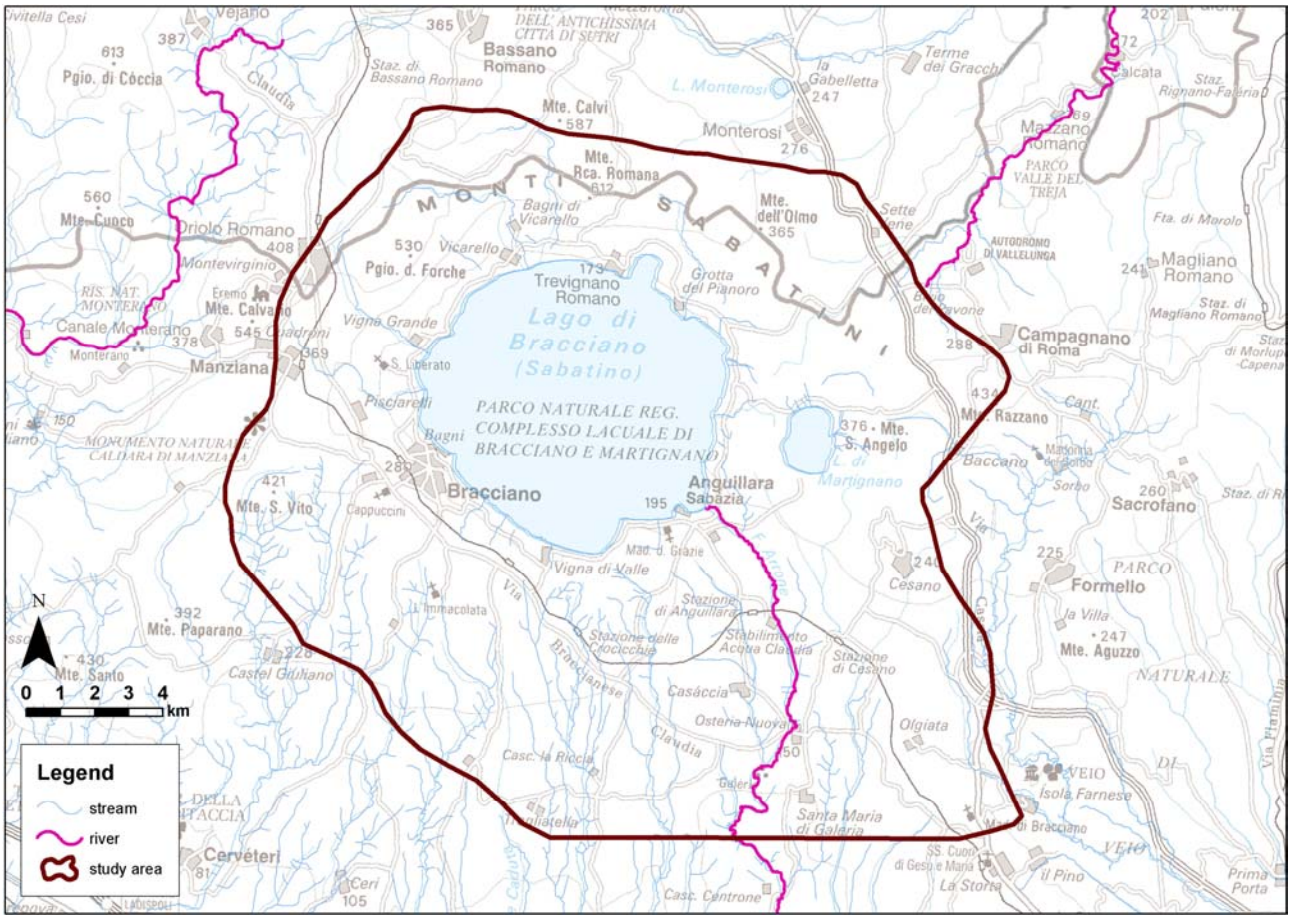

Figure 2.1: Topographic map of the study area

The relief, delimiting the Bracciano depression, has an opening at southeast (near Anguillara village) from which the lake effluent Arrone river originates.

In the east and southeast side the hills slope downwards to the Tevere valley and to the sea.

Some ridges develop radially towards the northeast, east and south, while numerous incisions, with valleys very close to each other and steep walls, generate a particular landscape characterized by young morphology and ongoing erosion.

Bracciano lake north perimeter relief is linked to Vicani relief.

The Tevere valley and the coastal plains has a completely different morphology with maximum heights of a few tens of meters with deep incisions.

2.1.2 Climate and hydrology

In this region the most important aspect of the climate is the peculiar precipitation regime. Precipitations (generally more than 900 mm/year) are usually concentrated in a restricted period of the year lasting between autumn and spring. They often occur in intervals of more consecutive days. Severe event are common. As a consequence, terrains soon reach saturation and generate runoff, main erosion contribution. The drainage pattern is generally radial towards the lake and with higher intensity in the south.

To summarize, severe erosion, affecting the river-beds on the volcanic edifice, is casued by three main concomitant factors: a) precipitation regime; b) high relief; c) lithologic heterogeneity.

In the period 1980-2000 observations at the SIMN (Serivizio Idrografico e Mareografico Nazionale) gauging stations showed an increase of annual mean temperature and a decrease of the annual precipitation (around 150-200 mm in 20 years) as shown in Fig. 2.2 and Fig. 2.3 (Capelli et al., 2005). Consequently, the impact of reduced rainfall and effective infiltration is not proportional to the average annual values, but depends on the combination of seasonal factors. For instance, the reduction of winter precipitation reduces the water supply in the period when evapotranspiration is minimal, thus introducing a net loss of effective infiltration. On the contrary, the availability of water in the warmer period results in increased evapotranspiration (see below). Similarly, the greatest temperature variations were in spring, when evapotranspiration reaches its maximum values.

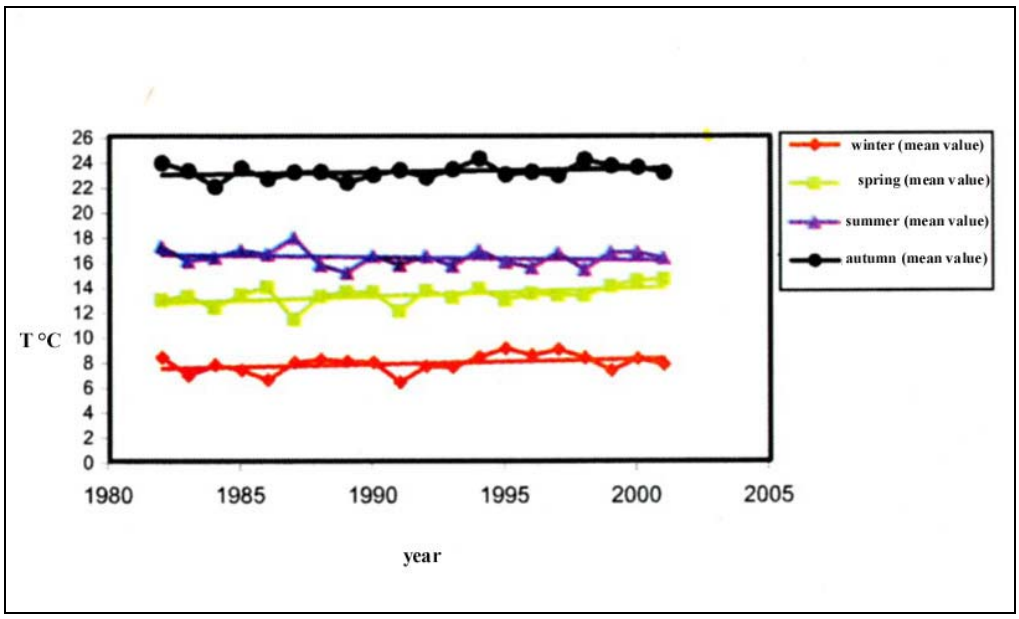

Figure 2.2: Seasonal temperature trend recorded by SIMN stations between 1980 and 2000 and relative regression curves.

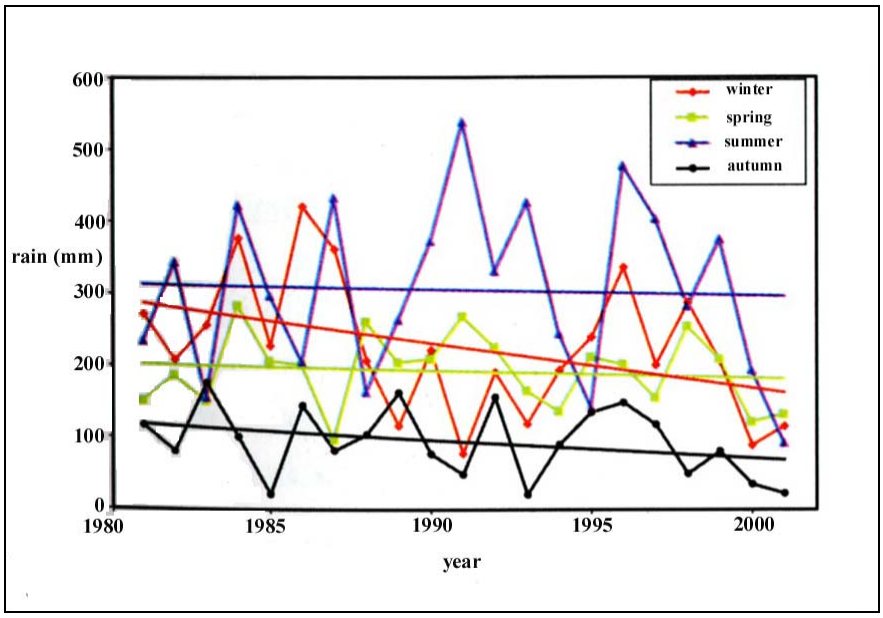

Figure 2.3: Seasonal rainfall trend recorded at SIMN stations between 1980 and 2000 and related regression curves.

The above considerations stress the need and the importance to examine the budget on monthly basis, ideally even daily, to take into account the climate factors variability during different years.

The hydrologic budget analysis also requires spatial extent for the abovementioned factors. Hence rainfall and temperature spatial reconstruction were needed.

Daily minimum, maximum and average temperature values and recorded rain by meteorological stations have been monthly aggregate and expressed as average value for the temperature and cumulative value for the rain measurements.

It was build a special macro to obtain cumulative rainfall and mean temperature by establishing criterion for the malfunctioning stations. It was defined a maximum number of days of not functioning, beyond which the monthly information was not considered for a specific station.

The hydrologic annual balance was analyzed on a monthly basis calculated from daily values, so it was possible to take into account the variability inside the year. The recharge has been calculated starting from the monthly estimate on cells 250x250 meters on two periods (1997 -2001 and 2002-2008), of the following parameters:

- Rainfall;
- Maximum temperature;
- Mean temperature;
- Minimum temperature.

The geostatistical method Random Function of K Order (IRFk) kriging (Chilès & Delfiner, 1999; Wakernagel, 1995; Bruno e Raspa, 1994; Matheron, 1973), which is valid in not-steady conditions, was applied to produce a set of maps describing parameters distribution;

The accuracy of the estimation is based on processes and data statistics derived from cross-validation by comparison with measured values. The cross-validation has been performed for all 4 parameters at each observation point and month (12 months for 5 years, 60 in total). After completion of cross-validation process, the variance of the relative errors has been calculated to assess the quality of the generated monthly maps.

The variance of rainfall is lower in the period 2000-2001 than 1997-99 (Fig. 2.4). Figure 2.5 indicates the frequency distribution of the relative standard deviation of the cross-validation errors. The value is lower than 0.5 for more than 80% of the cases and lower than 0.3 for 50% of the cases (months).

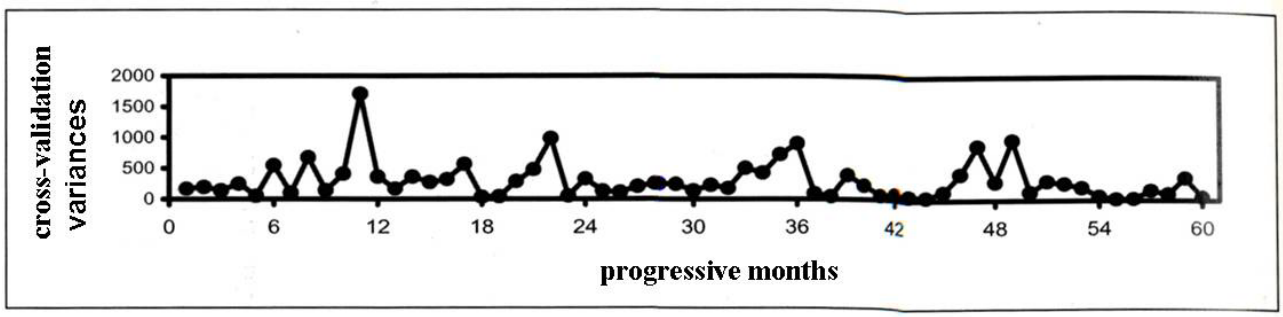

Figure 2.4: Temporal trend of cross-validation variances for monthly rainfall in the period 1997-2001.

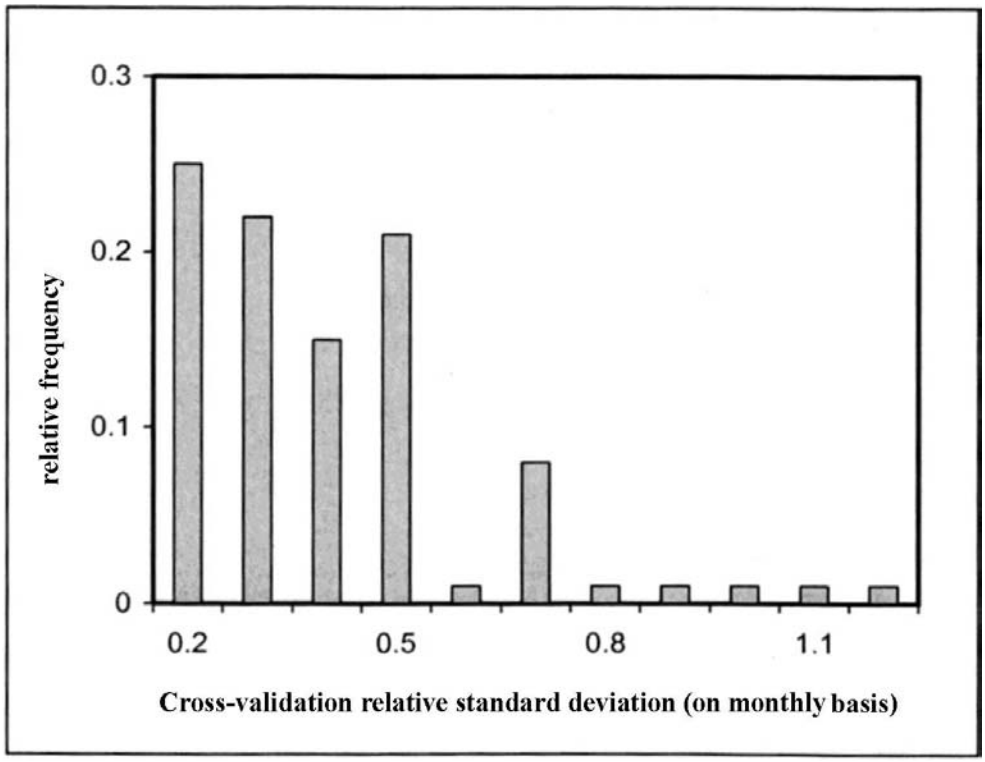

Figure 2.5: Histogram of cross-validation relative standard deviation (on monthly basis) of monthly precipitation in the period 1997-2001

Temperature cross-validation variance, excluding few months, oscillates between 1 and 2°C (Fig. 2.7). The frequency distribution of the relative standard deviation of cross-validation (Fig. 2.6) shows values ranging between 0.01 and 0.12. In 50% of the cases, values is lower than 0.05 and in 83% of the cases is lower than 0.08

The cross-validation was performed taking into account the estimation point elevation above the sea level to eliminate systematic errors otherwise introduced.

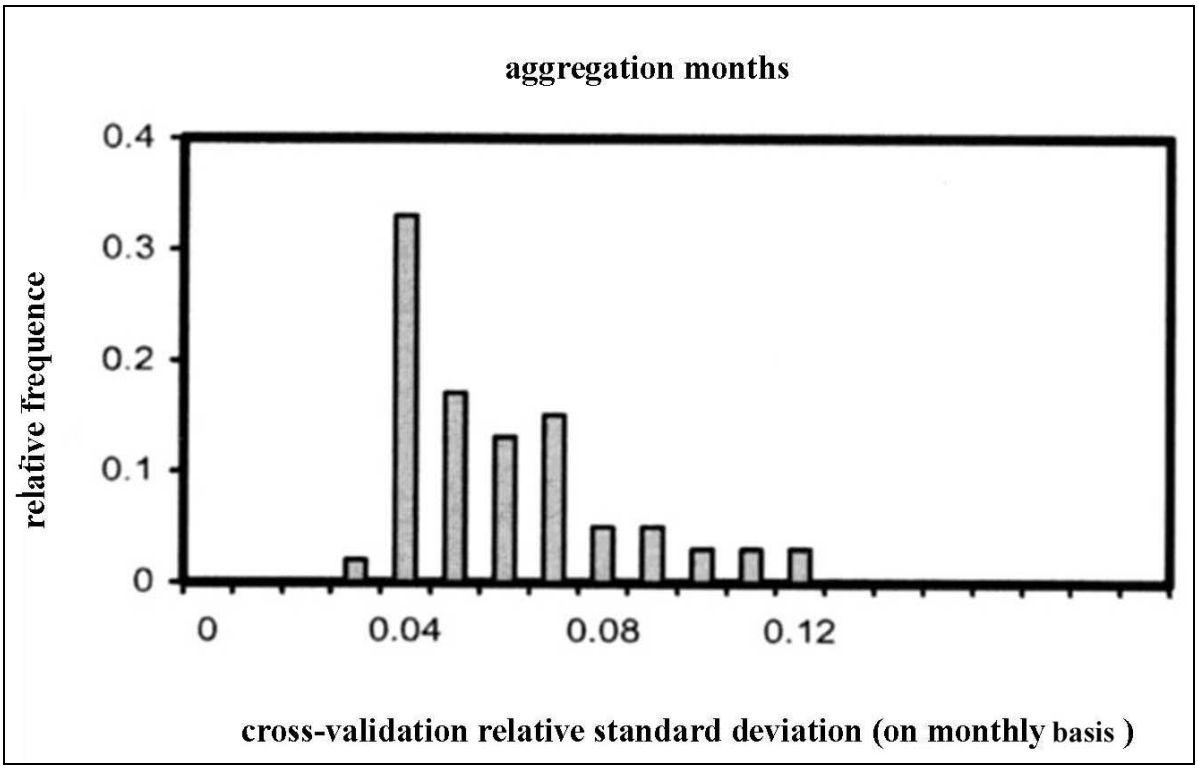

Figure 2.6: Histogram of cross-validation relative standard deviation (on monthly basis) of maximum temperature in the period 1997-2001

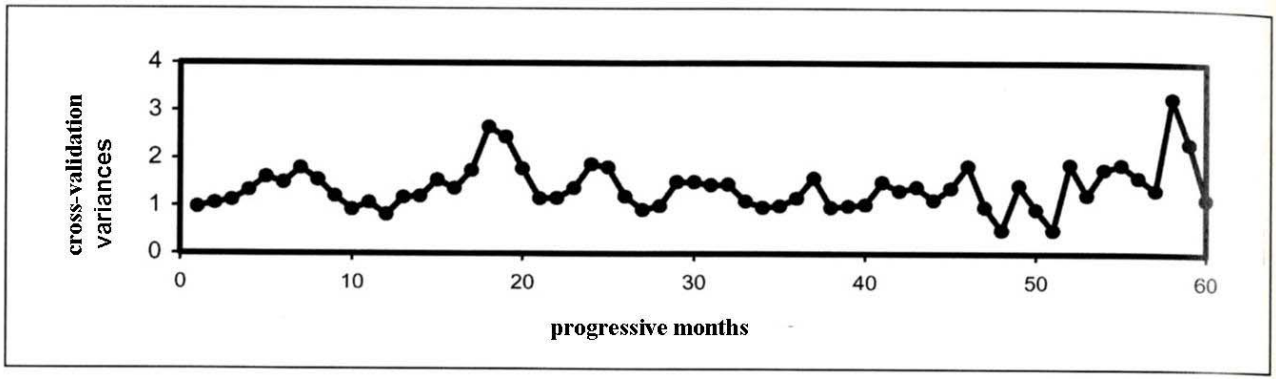

Figure 2.7 – Temporal trend of cross-validation variance of maximum monthly temperature in the period 1997-2001.

Figure 2.8 shows rainfall trend (for the years from 2000 to 2006) at 8 rain gauge stations present in the area (telemetric: Baccano, Bracciano, Castello Vici, Cerveteri, Formello, La Storta; automatic: Tragliatella and Trevignano Romano). There are periods without data due to malfunctioning of the instruments. The data were analyzed for the period 1951-2007, but measurements later than 2003 have not yet been validates by National Hydrographic Service (Servizio Idrografico Nazionale).

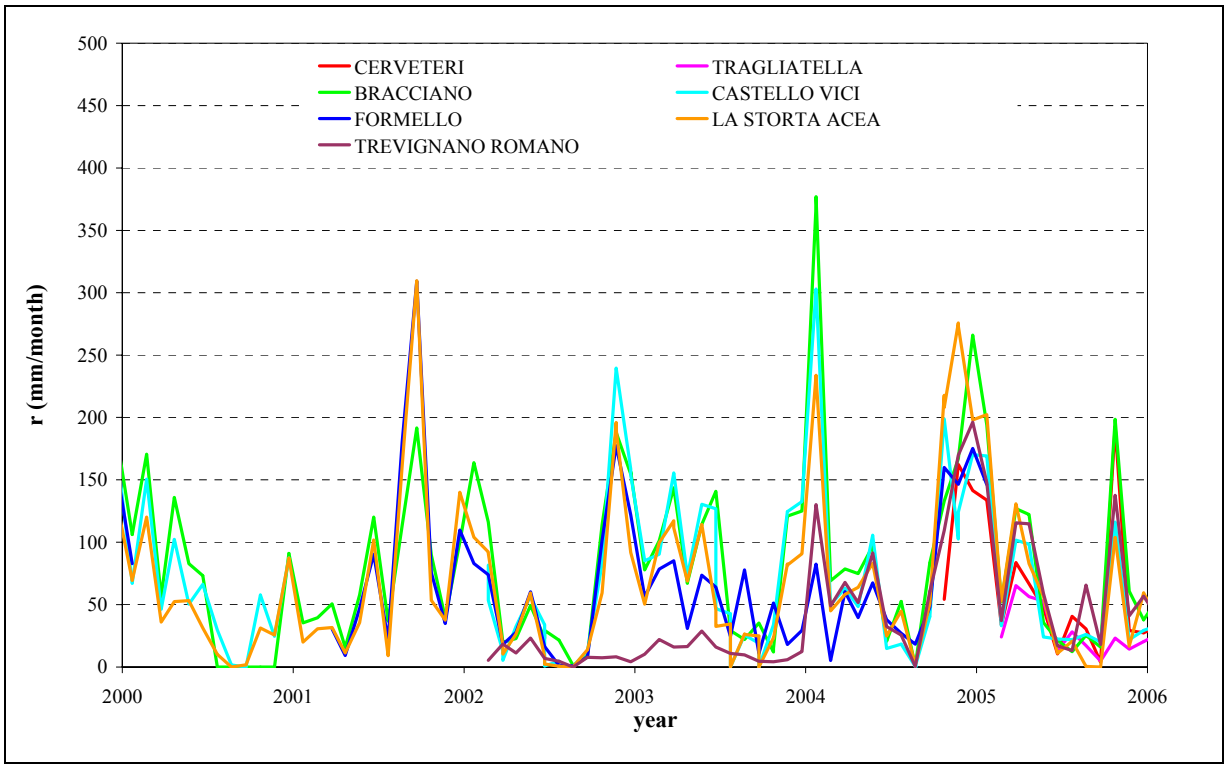

Figure 2.8: Rainfall patterns in the study area

2.1.2.1 Recharge

The recharge is represented by a raster map (250 x250 m cells) with each cell representing the corresponding calculated recharge. The recharge has been calculated using the "method of distribute

balance" as reported by Capelli et al.(2005). The annual recharge in each cell is the difference between precipitation, runoff and real evapotranspiration.

The effective infiltration is the portion of rain that contributes to aquifer recharge. In the case of aquifers where contributions of surface water and groundwater from adjacent areas can be considered as negligible, the effective infiltration corresponds to the amount of renewable resource, and thus available for the maintenance of underground and surface outflow/inflow basis of the waterways and for human activities.

In different areas of the hydrological basin, the recharge has different values according to:

- climate spatial and temporal distribution (temperature, rainfall, solar radiation, wind speed, humidity);
- morphology (slope, exposure, presence of drainage areas and/or semi-endorheic areas
- aquifer lithology (rock permeability);
- soil characteristics (available water capacity (AWC), effective porosity, etc.);
- vegetation cover and land use ;

The maximum size of computational cells must be comparable with the minimum size of considered cartographic elements (land use, lithological associations, morphology, AWC, etc.).

The timescale should allow to consider seasonal variability and, ultimately, distribution and intensity of meteorological events. The experimental data currently available made necessary monthly, in some case even daily, approach. It is always advisable to obtain the recharge as the sum of monthly or daily contributions, in order to take into account variability of regional and climate factors during several years.

In Table 2.1 is represented a scheme of the process of recharge calculation including the estimation of the main variables (temperatures, precipitation, runoff).

Table 2.1: scheme for calculating the distributed value of recharge

starting data	kinds of aggregation - other info	data processing	unit of measurement & maximum & minimun value	output	time depen-dent
Daily precipitation	monthly cumulate precipitation	kriging, FAI-k	mm	**P** distribuited value of monthly precipitation (grid)	yes
Maximum daily temperature	**Tmax monthly mean of the maximum daily temperature**	kriging FAI-k, with external drift	°C	**Tmax distribuited value of the monthly mean of the maximum daily temperature (grid)**	yes
Minimum daily temperature	**Tmin monthly mean of the minimum daily temperature**	kriging FAI-k, with external drift	°C	**Tmin distribuited value of the monthly mean of the minimum daily temperature (grid)**	yes
Mean daily temperature (obtained by the mean of the minimum and maximum daily temperature values)	**Tmean monthly mean of the medium daily temperatures**	kriging FAI-k, with external drift	°C	**Tmean distribuited value of the monthly mean of the medium daily temperatures (grid)**	yes
Corine land cover (shape poligon)		build specific legend correlate to fotointerpretation areas		**UTW (Unit of Territory Hydro exigency)** mapping units with homogeneous water requirement (poligon)	yes
colors ortophotos - scale 1:10.000 Regione Lazio flight 2000		fotointerpretation of colors ortophotos			
topographic map 1:10.000		draw perimeters UTW			
H=thickness of soil (m) -from geology map (1:25.000) poligon.shp P= gradient of stone (%) 120=mean unitary value of AWC for the considered soil (mm/y) F=correction factor for vulcanic soil	Value necessary in the estimation of the Evapotraspiration	**AWC= H*(1-P)*120 F Avaiable water capacity**	mm, from 0 to 235	distribuited value of the **AWC** (grid)	no
UTW(Unity of Territory Water Requirement)		a monthly value of kc is associated to every UTW class	from 0 to 1,1	**Kc -distribuited monthly value of the crop coefficent (grid)**	yes
hydraulic conductivity (geology)		assigning a percent value to each component	from 0 to 1	**Ck** -distribuited value of the Kennessey coefficent (grid)	almost no
topography slope (DEM)					
vegetal covering (UTW)					
RA solar radiation, it has an unic monthly value for the entire area	**EVR (evapotraspiration)**	**EVR= ETR (if there isn't deficit)**	**if P+Ui>ETR**	**ETP= 0,0023 (Tmean+17,8) (Tmax-Tmin)^{0,5} RA**	
			ETR= ETP*kc		
DF deficit		**EVR= P+ Ui (if there is deficit)**	**if P+Ui<ETR**		
Uim = (P- ETR+Ui)m-1; if Uim>AWC => Uim=AWC; if Uim<AWC=> Uim=Uim and DF= (Ui-ETR+P)m					
Surface Runoff	**SR(year) = Σ (Pmonth-EVRmonth)*Ck**				
Recharge	**R (year)= Σ (Pmonth- EVR month- SRmonth + Endo month)**				

Surface runoff: expressed as the sum of monthly difference between precipitation and evapotranspiration, multiplied by the average annual runoff coefficient (Kennessey coefficient, Ck) (See Ta-

ble 2.1 for the formula). The coefficient Ck has been calculated from the distributed balance given for a defined area and it is the sum of three factors changing according to the permeability of the outcropping rocks or terrains, the land cover and the surface slope. The coefficient is calculated taking also into account the aridity index (Ia), which relates the annual average temperature and rainfall to the driest month temperature and rainfall. Ck is yearly valid, therefore in the hydrologic balance the annual sum and not the monthly value is considered. In this way, Ck doesn't take into account the rainfall intensity distribution, introducing an error in runoff value estimation.

For instance, in the case of very intense rainfall, the evapotranspiration and the infiltration are negligible respect to the runoff but, being the daily precipitation averaged on the entire month, the Ck value is underestimated.

In urban areas, the surface runoff is larger compared to the not urbanized areas, with values higher than 270 mm/yr. During runoff model calibration, monthly and annual calculated runoff has been compared with the field data collected at SIMN measurement stations in Bracciano area. The gauging stations are on a limited number of streams and rivers, hence there are relevant lacks of data. However, the difference between simulated and observed values around 5% of the rainfall value on a single hydrographic basin.

During the past years experimental data have been collected (Gasparri, 1987 and Tarantino, 1991) in an adjacent basin to the study area (Cinque Bottini basin) similar to Bracciano basin from a geologic point of view.

Calibrated instruments were installed for flow measurement on a closed section of a watercourse. From the recorded data it was possible to distinguish runoff flow from the baseflow.

During the period 1984-1985 the mean calculated runoff was 94 mm, while in the period 1986-1987 was 55 mm.

The distributed recharge was calculated, not considering the lakes present in the study area (see Section 2.1.2.2 for the lake area). In Fig. 2.9 and 2.10 the visualization of the recharge for the periods 1997-2001 and 2002-2008. Mean recharge is 378 mm for 2002-2008 and 283 mm for 1997-2001.

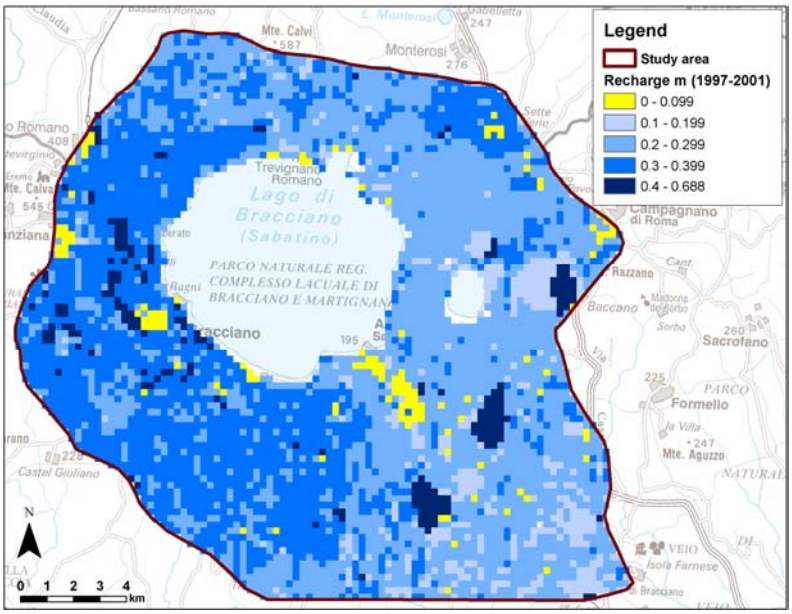

Figure 2.9: Distributed recharge (m) for the period 1997-2001

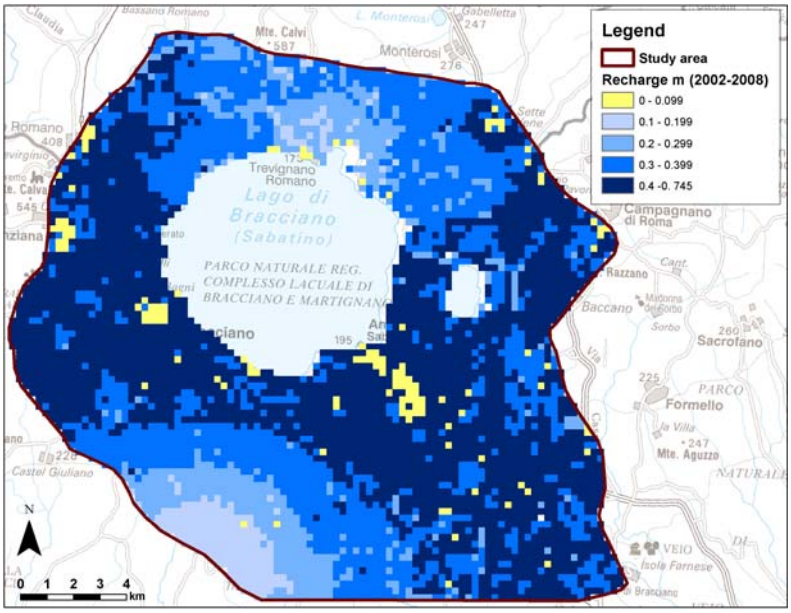

Figure 2.10: Distributed recharge (m) for the period 2002-20008.

2.1.2.2 Lakes

i) Bracciano Lake

Bracciano Lake represents a very important hydrogeologic unit. It occupies about one sixth of the study area (57 km2) with a maximum depth of 160 meters and a total volume about 484.78 m3. Bracciano Lake has a direct exchange with the volcanic aquifer. Lake level are available since 1952 until today (SIMN gauging stations). Figure 2.11 and Figure 2.12 evidence that lake level is almost stable, except the period from 1969 to 1971, where sudden level raise was recorded due to malfunctioning of the gauge stations. In the years 1978 and 1979 some gaps were recorded due to interrup-

tion of data recording. It can be observed that until 1989 the level of 163 m has been exceeded several times and the lower limit of 162 m has never been reached, while from 2002 to 2010 the upper limit never exceeded 163 m and several times the lower limit went below 162 m.. level, it is possible to observe a decreasing general trend.

From 1952 until 1994 the Anguillara Sabazia hydrometric station was operating and measured the lake level with a hydrometric zero of 161.74 m a.s.l. From 1995 this station was no longer working and Castello Vici hydrometric station, managed by ACEA Water Company, was operating with a different hydrometric zero corresponding to 161.79 m a.s.l, as considered in the below Figures. In 2008 the Hydrometric Regional Service installed a survey piezometer near the old Anguillara Sabazia station, but after a while it revealed a problem, due to the interference produced by a nearby private pumping well, as a consequence information relative to this piezometer were not considered.

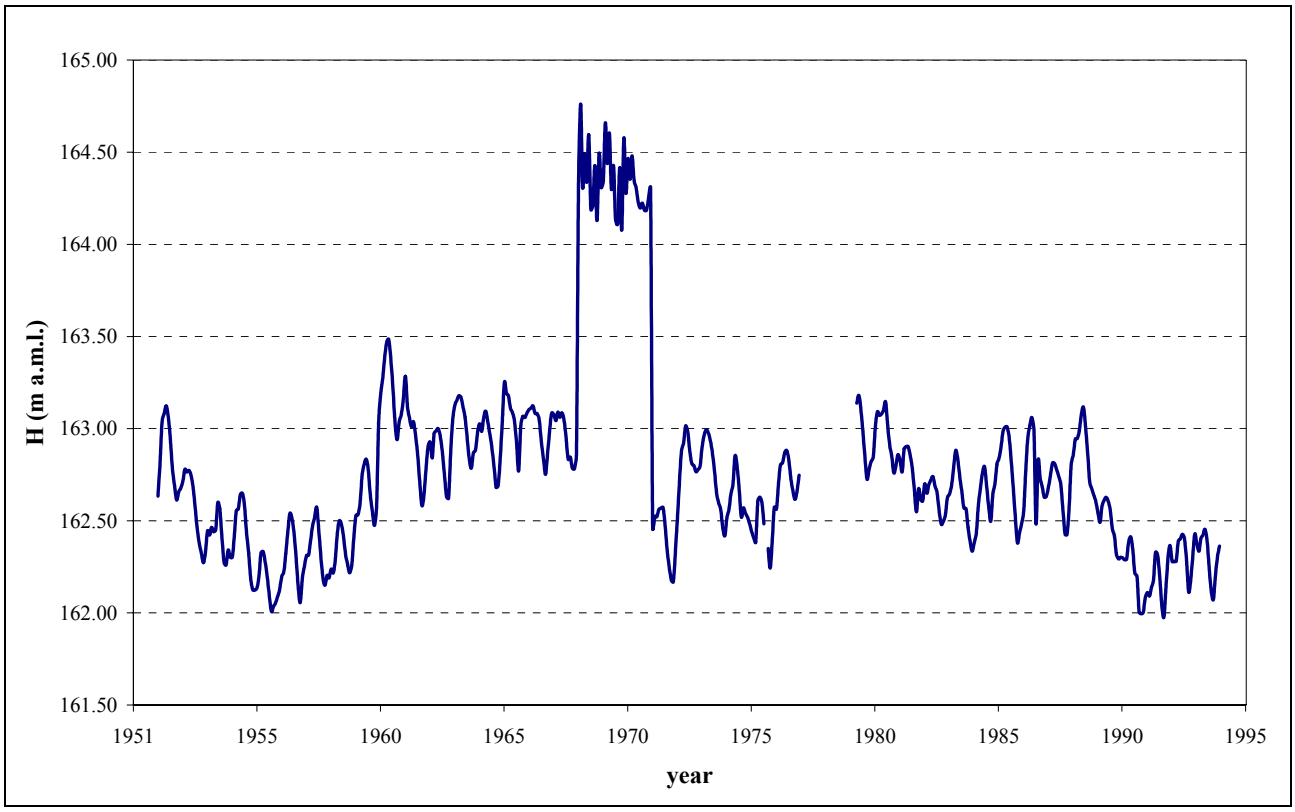

Figure 2.11: Hydrometric level of Bracciano Lake, monthly measurement values from National Hydrographic Service (Servizio Idrografico), from 1951 until 1994.

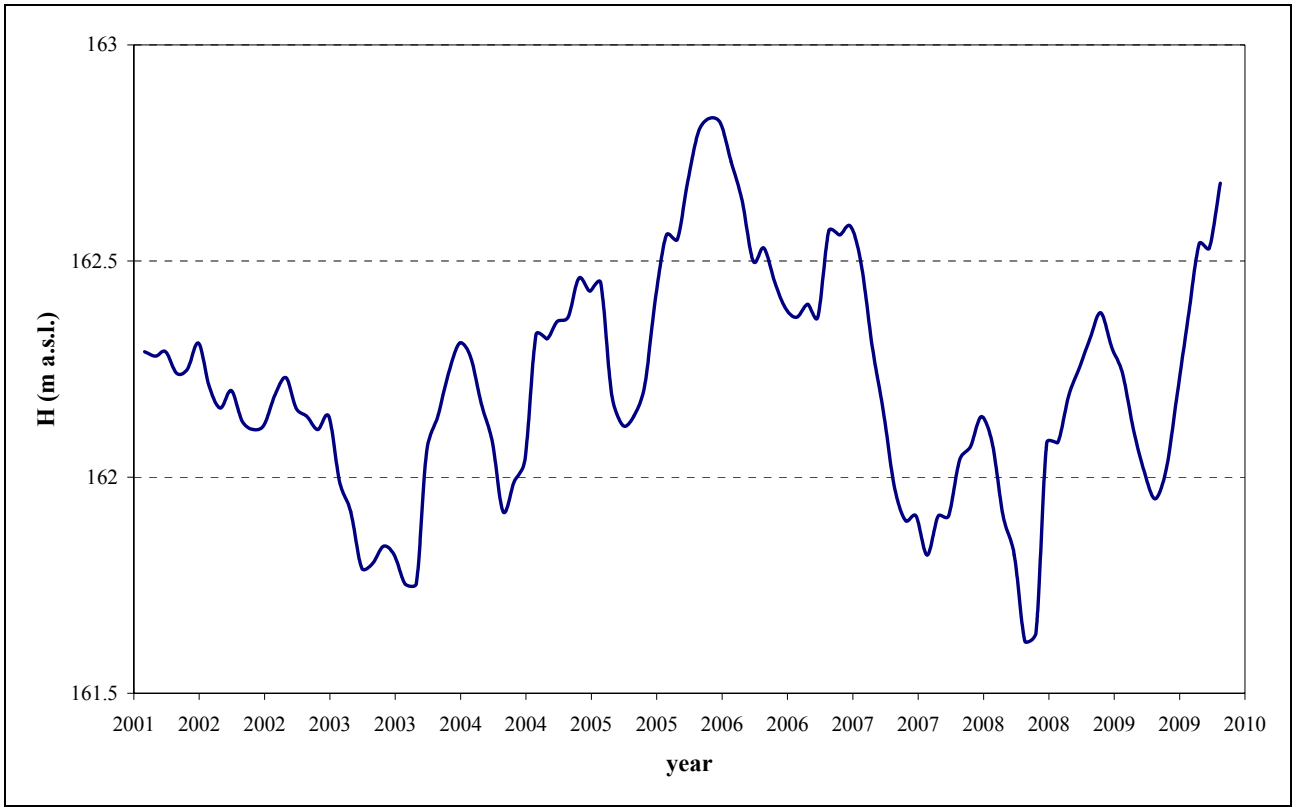

Figure 2.12**: Hydrometric level of Bracciano Lake, measurement values from ACEA (Mucicipal Agency Electricity and Water), from 2001 until 2010.**

Considering three SIMN gauging stations located around Bracciano Lake, the Vicentini formula was used to calculate the Evaporation on the lake:

$$E(t) = 5.33 * T(t) + 0.75[100 - U(t)] \quad \text{[mm/y]} \quad \text{Eq. 2.1}$$

Where

T(t) is monthly average temperature

U(t) is monthly average humidity

Figure 2.13 shows the location of the gauging stations. In Table 2.2 annual cumulative rain, annual average evaporation and annual cumulative runoff, calculated from monthly values, are reported. The difference between rain and evaporation is almost always negative, evidencing the prevalent role of the evaporation on the rain in the lake. Runoff value is not sufficient to restore the balance and it must therefore be assumed a component to lake recharge from the aquifer.

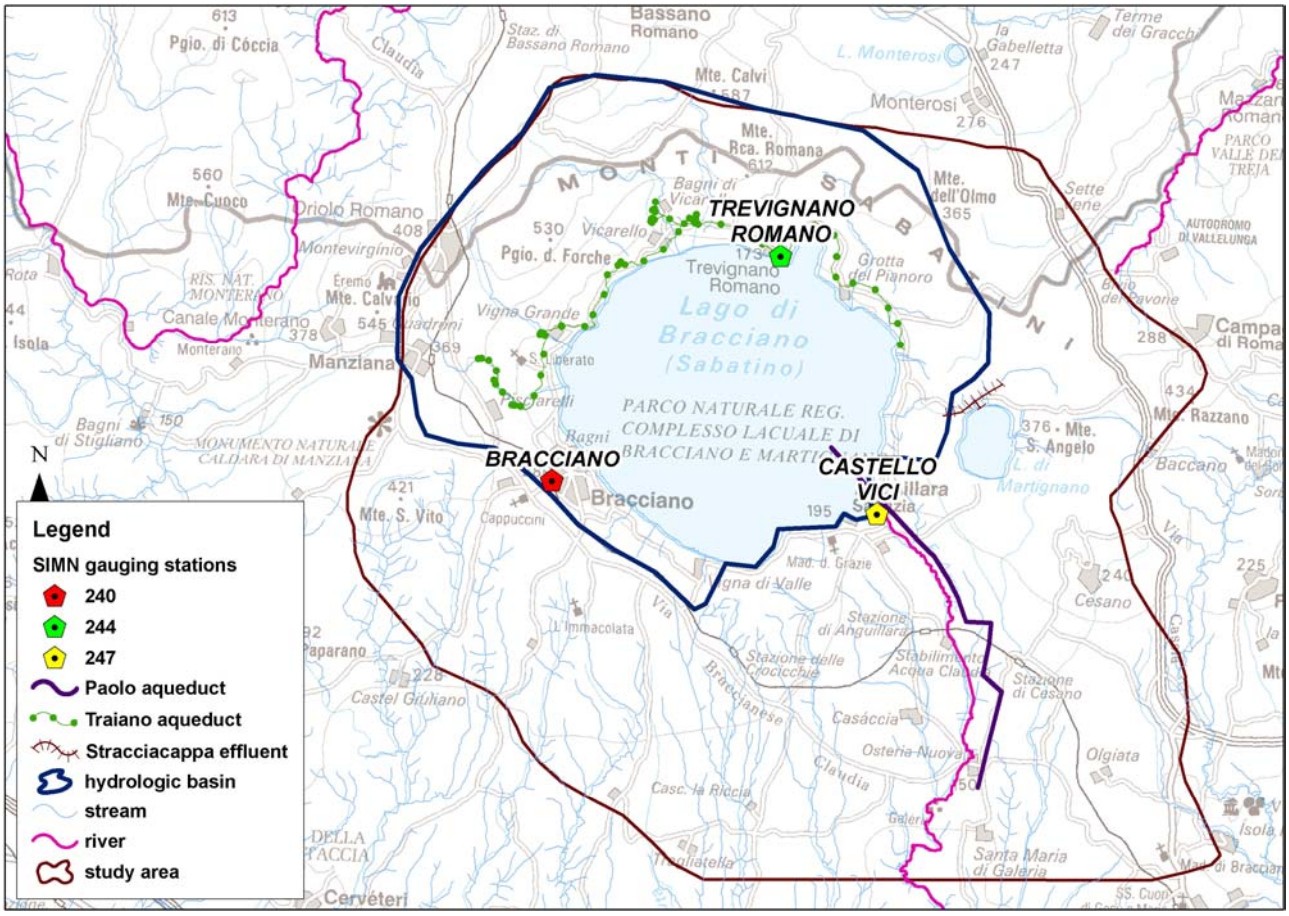

Figure 2.13: SIMN gauging stations around Bracciano Lake

Table 2.2: Annual cumulative rain, annual average evaporation and annual cumulative runoff at three SIMN gauging stations.

Station	Year	Cumulative Rain			Average Evaporation			Runoff into the lake		
		m	m^3/y	m^3/s	m	m^3/y	m^3/s	m	m^3/y	m^3/s
BRACCIANO	1997	1.058	60294600	1.912	1.268	72257972	2.291	0.087	8177310	0.2593
BRACCIANO	1998	1.139	64923000	2.059	1.268	72279319	2.292	0.087	8177310	0.2593
BRACCIANO	1999	1.018	58026000	1.840	1.248	71154692	2.256	0.087	8177310	0.2593
BRACCIANO	2000	0.861	49099800	1.557	1.278	72860537	2.310	0.087	8177310	0.2593
BRACCIANO	2001									
BRACCIANO	2002	1.019	58060200	1.841	1.268	72285400	2.292	0.105	9813709	0.311
BRACCIANO	2003	0.799	45565800	1.445	1.303	74294891	2.356	0.105	9813709	0.311
BRACCIANO	2004	1.288	73427400	2.328	1.240	70651764	2.240	0.105	9813709	0.311
BRACCIANO	2005	1.237	70497600	2.235	1.228	69996288	2.220	0.105	9813709	0.311
BRACCIANO	2006	0.764	43530900	1.380	1.277	72815514	2.309	0.105	9813709	0.311
BRACCIANO	2007	0.602	34291200	1.087	1.280	72985681	2.314	0.105	9813709	0.311
CASTELLO VICI	1997	0.832	47435400	1.504	1.104	62917242	1.995	0.087	8177310	0.259
CASTELLO VICI	1998	1.023	58299600	1.849	1.219	69481734	2.203	0.087	8177310	0.259
CASTELLO VICI	1999	0.808	46067400	1.461	1.217	69390244	2.200	0.087	8177310	0.259
CASTELLO VICI	2000									
CASTELLO VICI	2001	0.647	36867600	1.169	1.159	66067715	2.095	0.087	8177310	0.259
CASTELLO VICI	2003	0.789	44990100	1.427	1.109	63206042	2.004	0.105	9813709	0.311
CASTELLO VICI	2004									
CASTELLO VICI	2005	1.003	57193800	1.814	1.215	69242733	2.196	0.105	9813709	0.311
CASTELLO VICI	2006	0.548	31241700	0.991	1.238	70569901	2.238	0.105	9813709	0.311
TREVIGNANO ROMANO	1997	0.988	56327400	1.786	1.290	73530607	2.332	0.087	8177310	0.259
TREVIGNANO ROMANO	1998									
TREVIGNANO ROMANO	1999	0.758	43194600	1.370	1.281	73020790	2.315	0.087	8177310	0.259
TREVIGNANO ROMANO	2000									
TREVIGNANO ROMANO	2001									
TREVIGNANO ROMANO	2002									
TREVIGNANO ROMANO	2003									
TREVIGNANO ROMANO	2005									
TREVIGNANO ROMANO	2006	0.715	40777800	1.293	1.270	72414795	2.296	0.105	9813709	0.311

Lake Bracciano constituted an important water reservoir for the city of Roma, from the nineteenth century the Municipal Water Agency of Roma (ACEA) obtained the concession to withdrawal from Bracciano lake an amount of around 1000 l/s of water., that fed the Paolo aqueduct. The monthly average values of abstraction were transmitted by ACEA, for the last ten years; in Fig. 2.14 is possible to see the average annual trend plot from the year 1997 to 2007 (l/s).

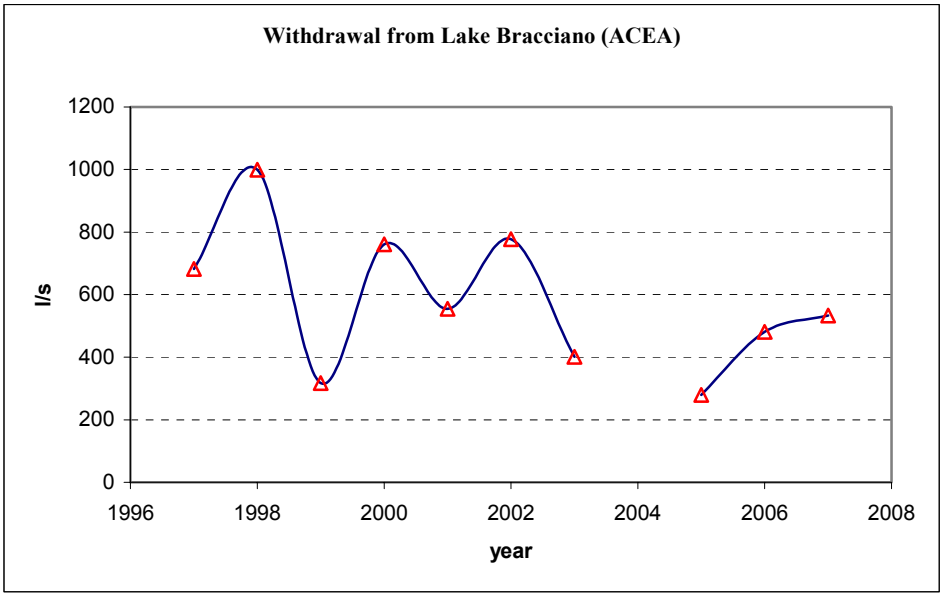

Figure 2.14: average year value of Lake Bracciano withdrawal

ii) Martignano Lake

Martignagno Lake is a shallow smaller lake located at 2 km to the east of Bracciano with an extension of 2.4 km2, water table elevation around 207 m a.s.l., maximum depth of 55 m, The lake consists in a close basin fed by rainfall without emissaries. During recent years the water table stood several meters (about 20) below the tunnel that fed the Roman Alsietino Aqueduct. There was an artificial outlet built in the IX century connecting the actual lake and former lake Stracciacappa (see Fig. 2.13), with Paolo aqueduct, but nowadays has been probably blocked by some collapse. Due to the absence of tributaries, the lake level has minor change and residence time is quite long, indicated as 29.6 years, with high risk for pollution. Martignano Lake is linked to a shallow aquifer, it was not consider in the groundwater model construction, where the focus went to the main volcanic aquifer.

2.2 GEOLOGICAL SETTING

2. 2.1 Pre.volcanic period

Below the volcanic products there are autochthonous Neogene sediments lying on allochthonous deposits belonging to "Flysch tolfetani" (Fazzini et al., 1972). The Neogene sediments are in contact with limestone and limestone-marl of Meso-Cenozoic sequence belonging to Umbria-Marche basin (Funiciello & Parotto, 1978). Just south east of Bracciano Lake, in the area of Baccano-Cesano, the Meso-Cenozoic substratum is raised to form a small median ridge (high structural Baccano-Cesano) (Funiciello et al., 1979; De Rita et al., 1983; Di Filippo & Toro 1993).

2.2.2 Volcanic period

Bracciano Lake is part of Sabatini Volcanic District, which started its activity over 600,000 and ends approximately 40,000 years ago (De Rita 1993), at the same time with the other alkaline potassic districts in the Latium region (Central Italy). The various explosive eruption centers in the District are in a vast area, more or less flat, largely occupied by clayey sediments of Plio-Pleistocene (Graben area of the principal Graben), limited to the west by the flysch hills of Monti della Tolfa Districts and the dominant Cerite-Manziana acid-Tolfetano with older activity. To the east the vast area is connected to the Meso-Cenozoic sedimentary hills of Mount Soratte and, further south, Monti Cornicolani. Highly explosive volcanic products, emitted from different vents in the area, have produced a very complex situation from west to east, in terms of nature, thickness and extent of volcanic deposits (see Fig. 2.15). In the western sector (Fig. 2.1) from Monti della Tolfa to Anguillara, the first volcanic deposits are related to local activities, cinder cones, lavas and pumice-ash scoriaceous fall deposits, associated with wind directions at the time of eruption at initial Sacrofano centre, located east of Martignano (Capelli et al., 2005).

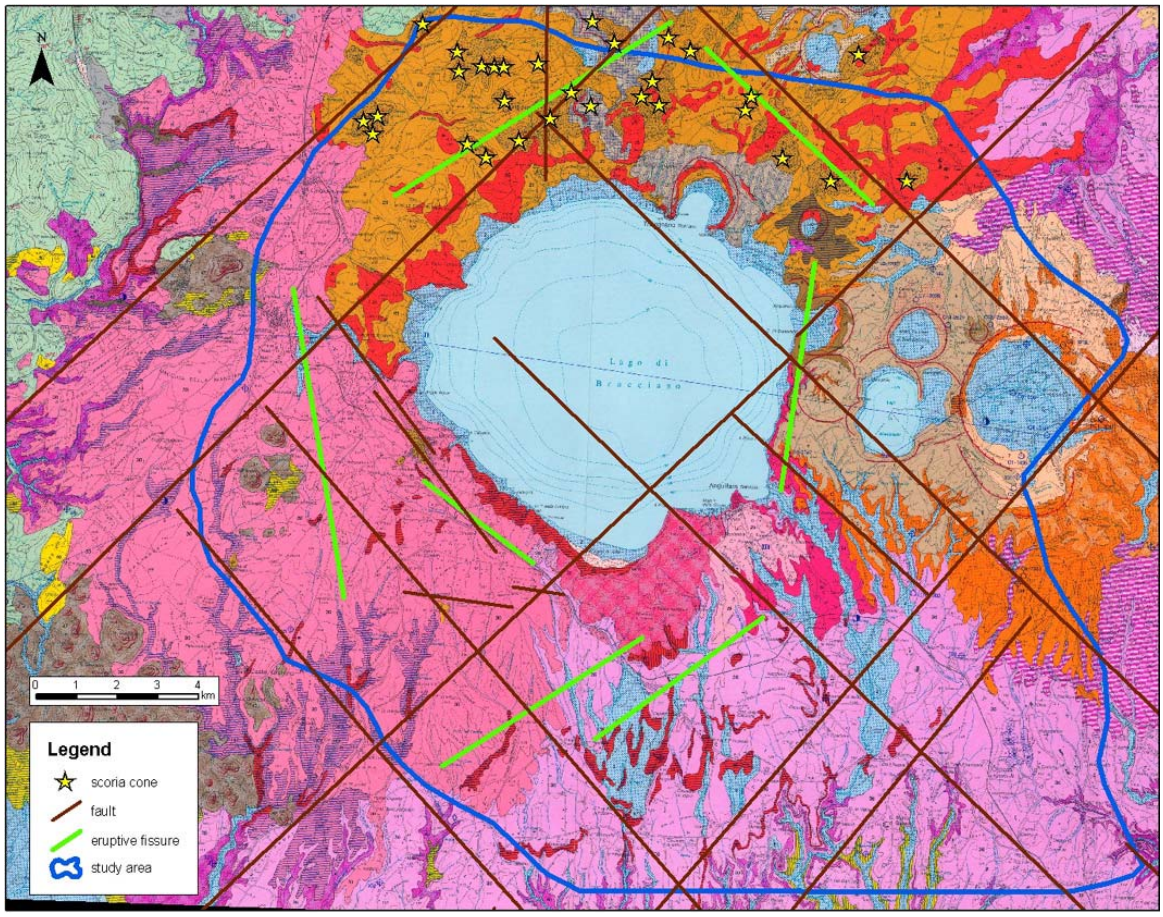

Figure 2.15: Geologic map of the area (De Rita, 1993)

The explosive volcanic activity begins (from the early stages of activity) in the eastern sector, near the hills of Mount Soratte. In this place it quickly built up the first volcano, called "Morlupo-

Castelnuovo di Porto", to which belong most of outcropping deposits in the eastern district of Sabatini area. The shape of this centre is no longer recognizable, since it was buried by more recent products.

During the construction of "Morlupo-Castelnuovo di Porto", the volcanic activity began even farther west, where Sacrofano volcano rose, just east of the ridge Baccano-Cesano, at that time still at high elevation (De Rita et al., 1993a). This volcano is perhaps the most important of the Sabatini District, both for its activity from 600,000 to 370,000 years ago, and the volume of material erupted. Around 400,000 years ago, the centre of Sacrofano had a paroxysmal phase of activity with emission of large volumes of fall deposits, both from the main building, from the principal vent and from peripheral and minor cinder cones. Also lava effusions were emitted. All products erupted during this stage, explosive and effusive, are chemically under-saturated and with a high potassium composition. During the same interval of time the volcanic activity was also present in all other sectors of the volcanic District. To the north and south of actual Bracciano Lake position, large lava flows, from tephritic-phonolitic to phonolitic-tephritic, were emplaced along regional faults and cinder cones located along the same fractures. In a very short time, estimated between 400,000 and 250,000 years, was deposited about 15% of the entire erupted material during the volcanic activity of Sabatini District.

The activity of regional faults and the massive depletion of the magma chambers caused the collapse of volcano-tectonic basin of Bracciano Lake and the subsidence of more than 200 meters of Baccano-Cesano high structural. The paroxysmal phase was accompanied by the emission (since the collapse of the hollow post and Bracciano) of pyroclastic flows from fractures centres around the area of collapse of Bracciano and was completed by intense episodes of explosive hydromagmatic centers located all around the collapsed area.

About 370,000 years ago, after the paroxysmal stage, the center of Sacrofano enters its final stage of activity. At the end of violent episodes hydromagmatic, happened the collapse of the terminal part of the volcano, with the formation of a large caldera surrounded by a low wall. Once Sacrofano centre was extinct, volcanic activity continued in Sabatini District only in the eastern sector, with a distinctly hydromagmatic characterization.

In quick succession were built up the tuff ring of Monte Razzano and Monte S. Angelo and the whole centre of Baccano, which activity ended around 40,000 years ago. The last eruptive episodes, were in the eastern sector from Martignano, Stracciacappa and Le Cese centres.

In the sketch of Fig. 2.16 are represented the main steps of the volcanic tectonic evolution of the Sabatini complex.

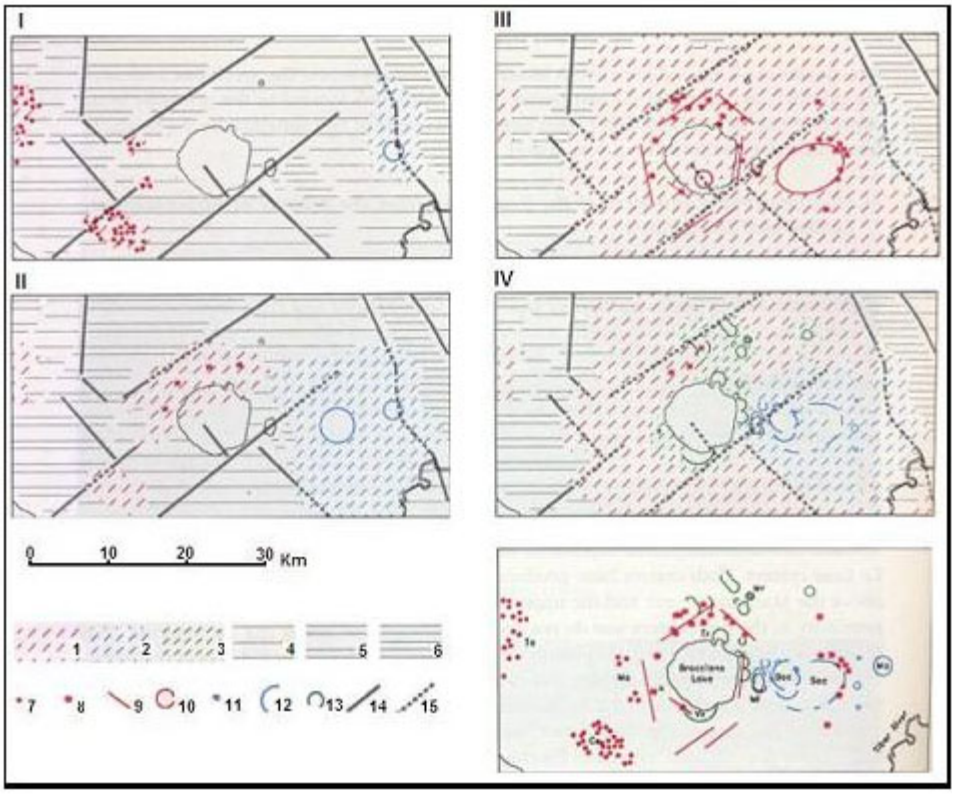

Figure 2.16: Sketch of Monti Sabatini volcanic complex activity (De Rita, 1993)

I) Pre-volcanic situation as reconstructed through drilling data. The main regional faults are indicated. The magmatic acidic activity of Tolfa-Cerite-Manziate area and the hydromagmatic activity of Morlupo-Castelnuovo di Porto center are indicated.

II) Sacrofano hydromagmatic activity began together with some magmatic activity in the northern sector.

III) Paroxismal stage of the magmatic activity in the Sabatini volcanic complex. Around 0.4-0.3 Myr magmatism with an unsaturated character was active all over the area.

IV) The final phase of Sabatini activity was mainly concentrated in the eastern sector and had hydromagmatic character.

1 = products with mainly magmatic character; 2 = products with mainly hydromagmatic character; 3 = products with mainly phreato-magmatic character; 4 = neoauthoctonous units (outcropping and covered by volcanic products); 5 = allochtonous units. They extended below the volcanic cover also when a reduced thickness of neoauthoctonous units was present; 6 = Meso-Cenozoic calcareous units, the same symbol indicate areas where these units were actually below volcanics but at shallow depth; 7 = acidic domes; 8 = scoria cones; 9 = emission fracture system; 10 = magmatic craters and caldera; 11 = hydromagmatic edifices; 12 = hydromagmatic craters and calderas; 13 = phreati-magmatic craters; 14 = main regional fault system; 15 =hypothetical regional faults systems. (De Rita et al., 1993)

Detailed geologic information about pre-volcanic and volcanic units are reported in Annex A

2.3 HYDROGEOLOGICAL SETTING - DEVELOPMENT OF THE CONCEPTUAL MODEL

A conceptual model of a ground-water flow and hydrologic system is an interpretation or working description of the characteristics and dynamics of the physical hydrogeologic system. The purpose of the conceptual model is to consolidate site and regional hydrogeologic and hydrologic data into a set of assumptions and concepts that can be evaluated quantitatively. Development of the conceptual model reuquires the collection and anlysis of hydrogeologic and hydrologic data pertinent to the aquifer system under investigation. (ASTM, D5447-04)

Reconstruction of a conceptual model is the first step in approaching groundwater models. In the present study, it was considered the aquifer present in volcanic deposits, as unique main aquifer, on the basis of the geologic and hydrogeologic understanding.
The aim of this study is to better understand the aquifer-Bracciano lake interactions, by developping an useful tool for the management of water resources with a special attention to the lake.
From a geologic point of view it was analyzed the hydraulic behavior of the different volcanic deposits with the aim to identify areas with a homogenous hydraulic behavior. It was also analyzed the presence of pre-volcanic low permeability sediments below volcanic deposits, which constitute the main surface of hydraulic discontinuity, with a function of base-floor for the conceptual model. The presence of low permeability sediments, located along the perimeter of the area, constitutes the boundary for the model.

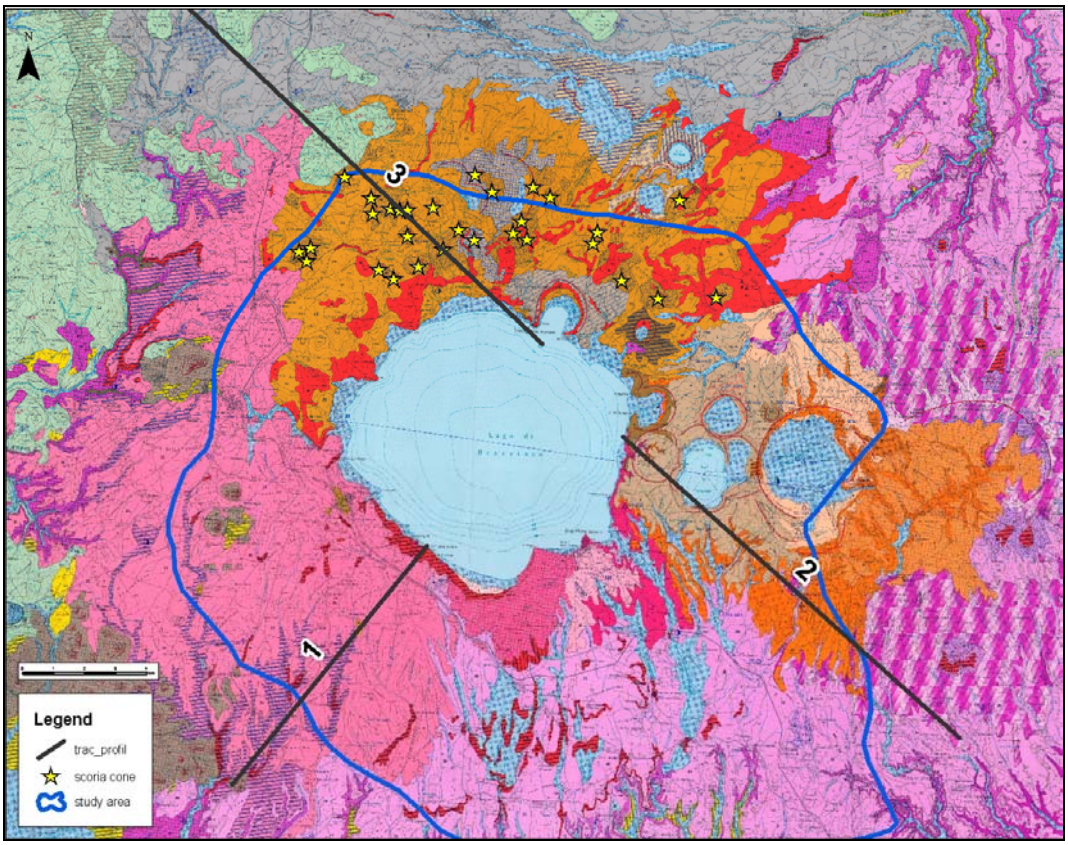
N
3
2
1
Legend
trac_profil
scoria cone
study area

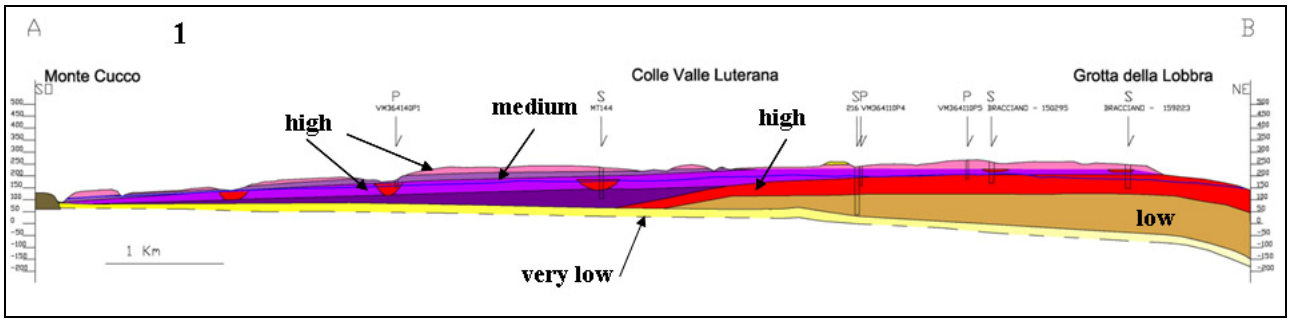
A
1
B
Monte Cucco
Colle Valle Luterana
Grotta della Lobbra
SO
NE
high
medium
high
low
very low
1 Km

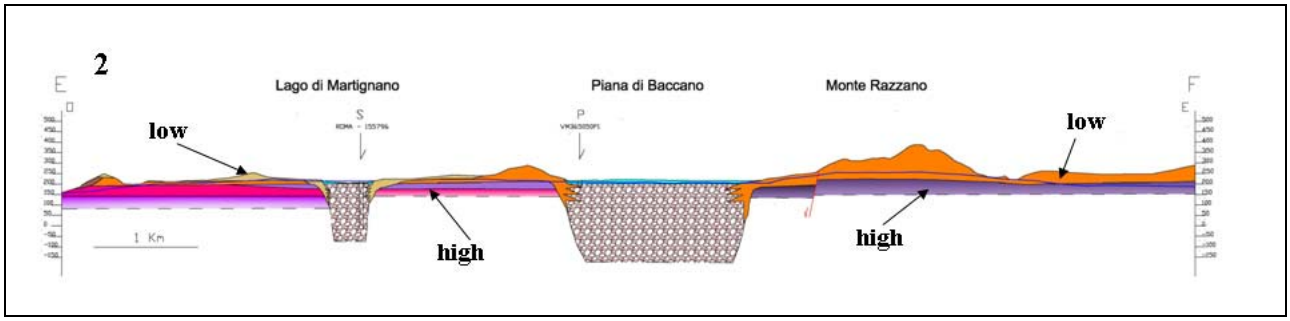
E
2
F
Lago di Martignano
Piana di Baccano
Monte Razzano
low
low
high
high
1 Km

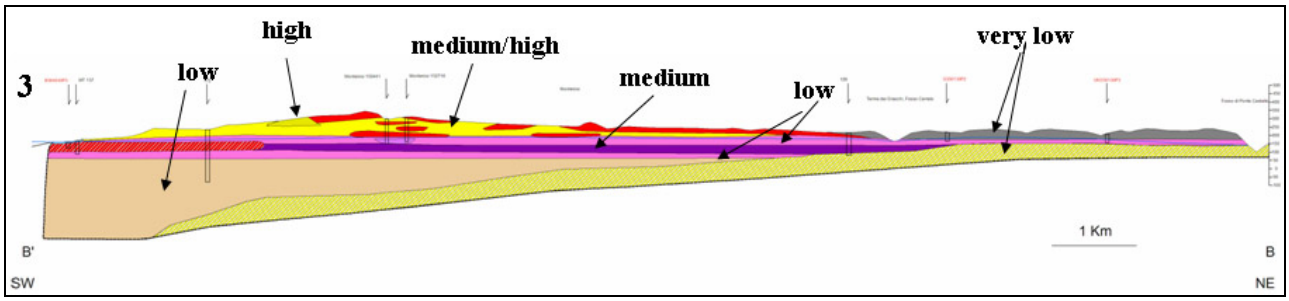

Figure 2.17: Geologic sections with a qualitative indication of permeability characteristics of different beds.

Sabatini volcanic district is constituted by a big number (hard to quantify) of vents. There are several strombolian centers of emission (scoria and tuff cones) and there are many fractures from which lavas and explosive volcanic products were erupted (Fig. 2.16 and 2.17). The volcanic activity is characterized by magmatic and hydromagmatic products. Emission centers are present in the east sector of Morlupo, Sacrofano and also in the edges of the volcanic tectonic depression of Bracciano. Alternating volcanic activity and interruption periods, the action of atmospheric agents and the variability of the volcanic materials, induced variable stratigraphic conditions not comparable to sedimentary context. Only in vents more marginal areas volcanic products assumed more uniform characteristics, from the view of water circulation, and could be assimilated to continuous sedimentary formation.

Hydraulic circulation has particular local conditions influenced by the upper part of the low permeability sediments, its thickness variations and lithological characteristics of the underlying formation. The permeability of volcanic deposits is very variable, it depends from volcanic activity products: hydromagmatic deposits can be consider to be generally low permeable, on the other side scoria cones porosity is predominantly permeable. Another factor conditioning the deposits permeability is if the cooling process was fast or slow.

The circulation of hydrothermal fluids tends to waterproof a porous and highly permeable deposit, with the deposition of zeolites mineral, as the case of the “tufo rosso a scorie nere” ignimbrite, with low permeability lithoid and zeolites local minerals inserted in a predominant pozzolana highly porous and permeable unit.

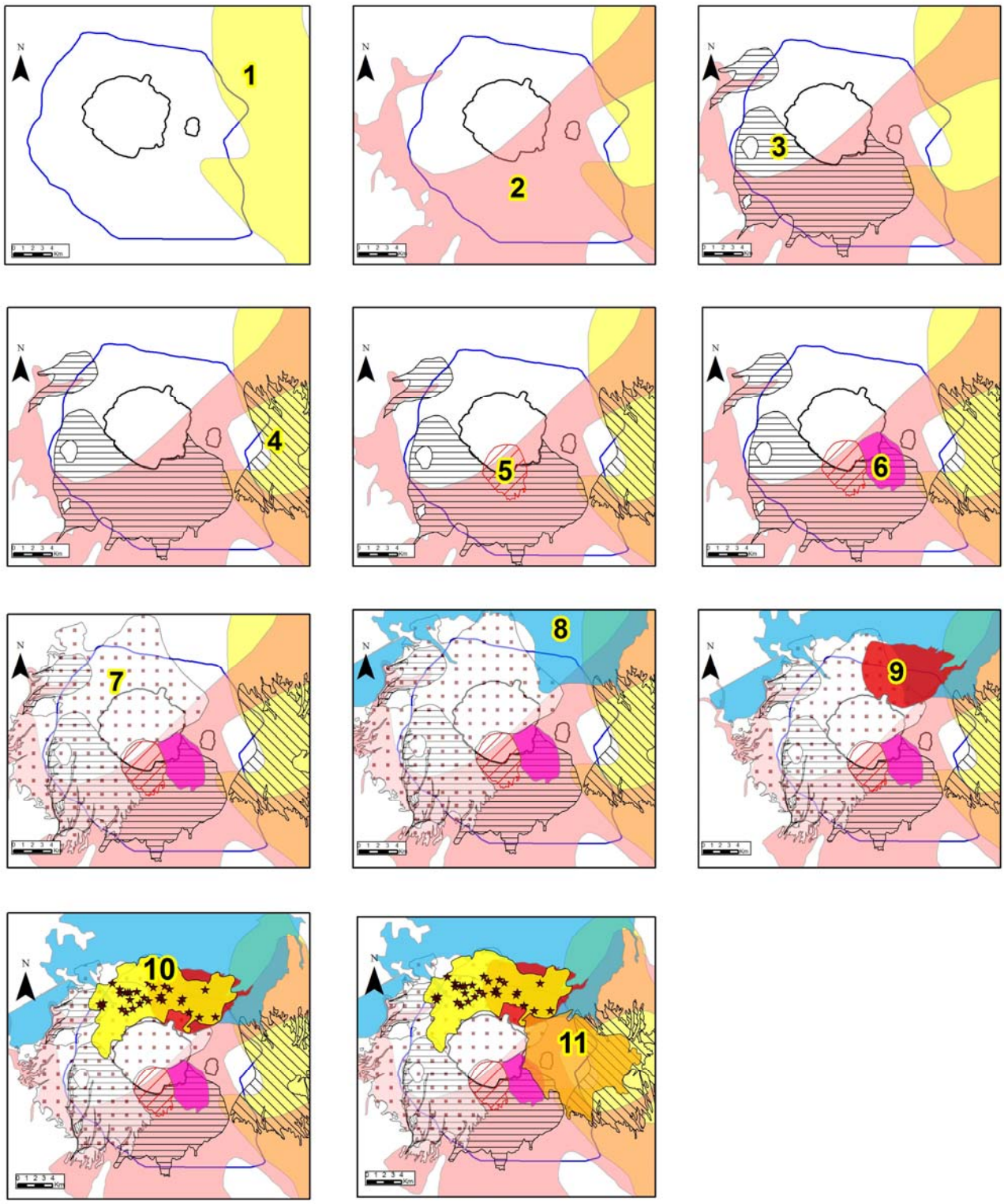

Figure 2.18: Extension of main volcanic deposits in the study area, following time scale from older to more recent units: 1.TGT (Yellow Tiberina Tuff); 2.TRSNS (Sabatini Red tuff with black scoria); 3.LP-TRSNS (lava post TRSNS); 4.TGS (Sacrofano yellow tuff);5. TVV (Vigna di Valle tuff); 6.TPP (Pizzo Prato tuff); 7.TBR (Bracciano tuff); 8. TRSNV (Vicano Red tuff with black scoria); 9. LP-TRSNV (lava post TRSNV); 10. SC-L(Scoria cones and North Bracciano lava); 11. HYDRO (Hydromagmatic products of Baccano, Stracciacappa East centers)

Fig 2.18 shows the deposition, step by step, of the main volcanic deposits in the study area. Within each volcanic deposit, the hydraulic properties have peculiar characteristics and may also vary greatly, as previously mentioned, according to deposition processes or subsequent alterations. Volcanic deposits affect water circulation not only within a single deposit but also at catchment scale by determining the hydraulic conductivity of the various deposits and their connections.

To this extent, after describing the hydraulic properties of volcanic rocks, the analysis of water circulation was performed through the observation of the reconstructed water table from 2009 field data in comparison with previously acquired piezometric maps. Starting from the ancient volcanic deposits emplaced in the eastern part (TGT, 1 in Fig. 2.18). The paroxysmal explosive eruption that produced the emplacement of the "tufo rosso a scorie nere" Sabatino (TRSNS, 2 in Fig. 2.18), changes strongly the paleo-morphology of this sector (as well as the eastern). Pyroclastic deposits 10 to 25 m thick were deposited. These deposits of TRSNS, having predominant pozzolana characteristic, highly permeable in depressed paleo-morphology, were transformed, with cooling and deposition of zeolites in tuff lithoid reddish, fractured permeability and modest porosity. For its permeability in pozzolana facies, its thickness, even higher than 20 meters, and extension across the area, TRSNS could be considered one of the main aquifer in Sabatini context. The unity of TRSN Sabatino emerges fairly continuous at the edge of the volcanic district. This unit is considered a good stratigraphic indicator: its distribution must have been influenced by topographical conditions existing prior to its emplacement and not present in the high structural of Baccano-Cesano (Cioni, 1993), still morphologically prominent at the time of deposition (De Rita et al., 1993).

After the deposition of TRSNS intense volcanic products, mainly Strombolian lava, a massive (170 km2) lava sequence, with overall thickness locally exceeding 30 meters was emplaced at south of Bracciano Lake (LP_TRSNS, 3 in Fig. 2.18). This layer of lava, with dispersed deposits of pumice-fallout ashes and scoria, is permeable due to fracturing and locally (in bed or on the roof of a single flow) along the scoriaceous facies debris related to the flow of lava.

In the western sector (study area) Bracciano tuff (erupted about 177,000 years BP, 7 in Fig. 2.18). also determines the groundwater circulation for its high porosity, its thickness and its extension. These aquifers are connected, at least locally, through their erosion and tectonic contacts.

In the eastern sector the TRSNS include the aquifer, in addition to fallout and pyroclastic deposits connected to the initial center of Sacrofano.

In the area including Vigna di Valle and the eruptive center of La Conca, two volcanic deposits older than Tufo di Bracciano are present: Tufo di Vigna di Valle (deposit phase 5 in Fig. 2.18) and the pyroclastic flow deposit of Pizzo Prato (deposit phase 6 in Fig. 2.18). These deposits would be emplaced in rapid succession (De Rita et al., 1993) in a phase of tectonic collapse of river Arrone

valley area between Anguillara and Martignano. Their permeability varies from porous to very porous with thickness higher than 10 m in Vigna di Valle and Pizzo Prato chaotic thick deposits with pumice. The southern part of the study area can be considered as a high permeability zone, considering the superimposed volcanic deposits (see later for further discussion).

In this area the presence of high structural pre-volcanic Meso-Cenozoic substrate, has conditioned by its collapse (common to many other volcanic districts) the emplacement of a powerful series of deposits associated with hydromagmatic centers of Baccano, Martignano Stracciacappa, Laguscello, Polline, Trevignano, La Conca, located in the eastern sector of the study area. These layers, mainly ash and of low permeability, previously determined the presence of former lakes, nowadays dried (as Baccano and Stracciacappa), the presence of shallow aquifer and constitute a vertical "barrier" to the main volcanic aquifer located in the more permeable volcanic deposits above desribed (TRSNS, TBR, LP-TRSNS). This situation is represented in Fig 2.17 section 2.

Deposits associated to hydromagmatic centers have mainly low permeability, even if they can be locally very permeable due to sandy scoriaceous layers, strongly influencing the groundwater movement in the eastern and north-east sector.

In the studied volcanic context, the presence of many surfaces of hydraulic discontinuities has to be considered together with possible presence of several local aquifers. To this extent it was performed the reconstruction of the main hydraulic discontinuities constituted by the pre-volcanic low permeability sediments, as the roof of one main volcanic aquifer, that well represent the situation at a basin scale.

2.3.1 Reconstruction of hydraulic discontinuity surface

The substrate on which volcanic vents formed was particularly complex and consisting of at least four geologic types, with complex mutual structural relations:

- Allochthonous pelitic-arenaceus, calcareous.marl and clay sediments;
- Limestone and limestone marl;
- Sediment cycle autochthonous Neogene, clay and sandy-clay;
- Acid volcanic deposits of Tolfa-Cerite-Manziana sector.

Therefore an important step consisted in the "review" of the volcanic basement surface.

These units, so heterogeneous in terms of permeability, are interconnected both vertically (direct contacts via faults or trust, depositional contacts) and horizontally (contacts via direct or reverse faults, intrusive contacts as the case of dominant acid complex of Tolfa and Cerite-Manziana district), thus increasing the complexity of the prevolcanic substrate.

The bottom of the aquifer is constituted of the low permeability sediments belonging to volcanic substrate.

It was possible to start from the base volcanic surface produced by the project Joint venture ENEL-VDAG-URM (1994). In this previous work the pre-volcanic sediments were not subdivided according to their hydraulic properties, hence in the present study this aspect was investigated to differentiate between low-permeability and permeable pre-volcanic sediments.

A first challenging step was gathering geologic information useful to individuate modifications to the basement surface: geologic maps, sections and stratigraphic logs.

Collected information were a total of 729 stratigraphic logs from different sources:

431 stratigraphic logs retrieved from ISPRA (Istituto Superiore per la Protezione e la Ricerca Ambientale) database. These data were collected in accordance with the regulation of private well (L. 464/84);

74 stratigraphic logs relative to the Regional Administration database;

103 stratigraphic logs from the Hydrogeology laboratory of Roma Tre University;

111 stratigraphic logs relative to ENEL databases, built in the 70's as part of ENEL geothermal research projects.

Data quality was very variable and affected by drilling techniques, competence of report author, etc. In Fig. 2.19 are shown all the points with stratigraphic log that have been considered and analyzed. Only 123 points, inside and around the area, could be used to the low permeability surface reconstruction, because they cross all volcanic deposits and reach pre-volcanic sediments, having information on the hydraulic properties of the pre-volcanic sediments. In Fig 2.19 are also reported five tables relative to the stratigraphic logs of the corresponding red points indicated in the map. These

tables provide an example on what which kind of information was possible to gather. The surface reconstructed from the Enel project was included in a GIS environment as isobaths. The elevations of the low permeability pre-volcanic sediments, taken from stratigraphic logs, were selected. A TIN (Triangulated Irregular Network) was constructed from isobaths (mass points) and point data related to the stratigraphic logs (points) and then converted into a GRID.

Tectonics was also used to reconstruct the abovementioned surface. All the faults affecting the pre-volcanic basement were selected and included in the reconstruction process, as elements of discontinuity (polylines barrier). The output GRID and isobaths from GIS elaboration were then checked, and inserted as bottom information in the model, as described in Chapter 4.

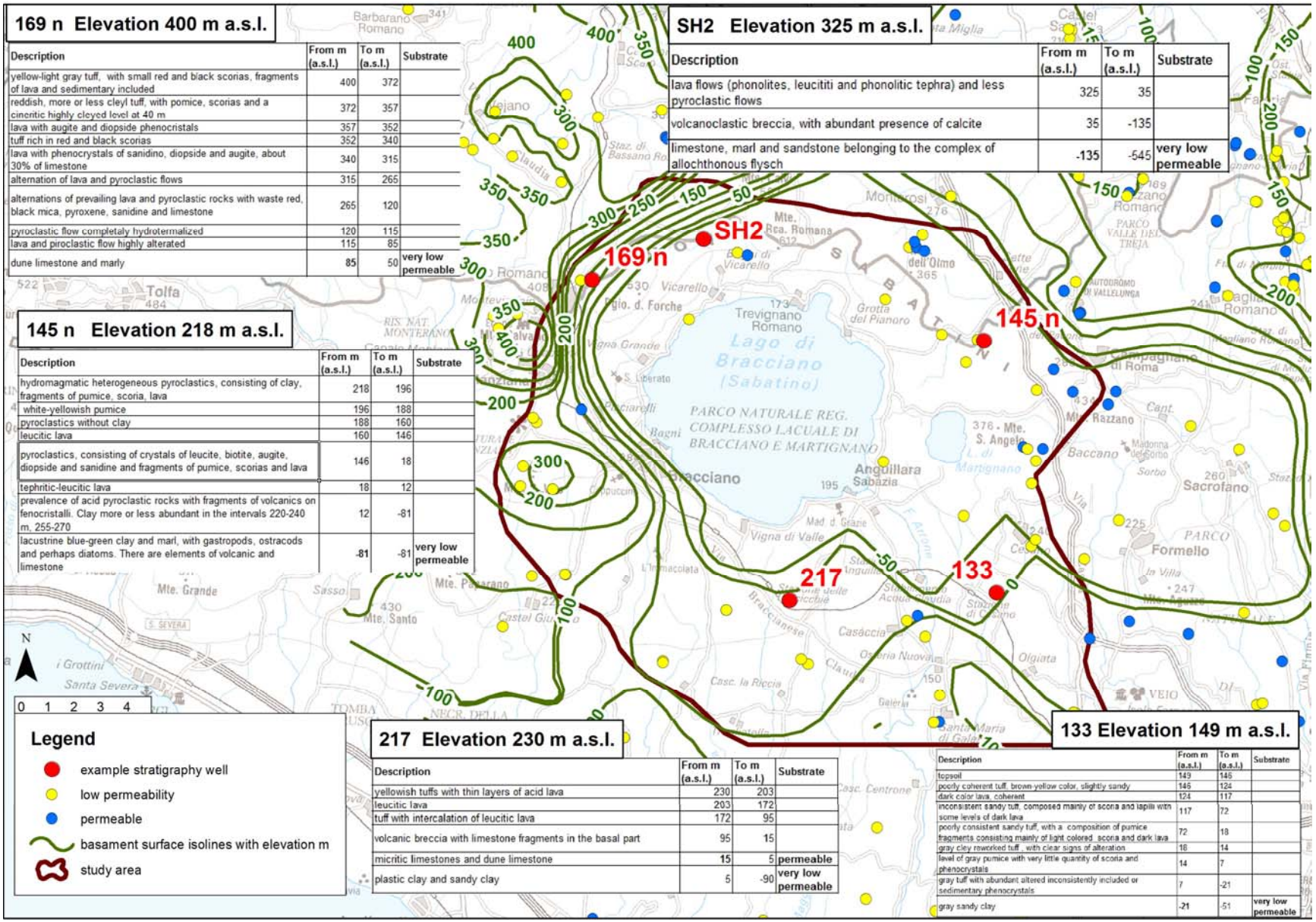

Figure 2.19: Main hydraulic discontinuity surface map and location of the stratigraphy logs analyzed. Five example tables are reported

The trend of the main hydraulic discontinuity surface, is very articulated. In the western part of the study area the volcanic deposits decrease in thickness and the pre-volcanic sediments outcrops, exerting a role of hydraulic barrier to groundwater flow. In the southern part there is an increase of the pre-volcanic sediments (isobaths 100 m a.s.l. in the Santa M. Galeria area), which acting as a barrier to the groundwater flow, divide it into two fluxes (with southeast and southwest direction). In the southern part the outcrops of pre-volcanic sediments appear inside valleys, producing springs aligned with the streams. In the eastern part the thickness of volcanic rocks reaches the higher values of the area (around 500-600 m of volcanic deposits). Fig. 2.20 represents the topography surface and pre-volcanic low permeability top surface, consider as the bottom of the aquifer.

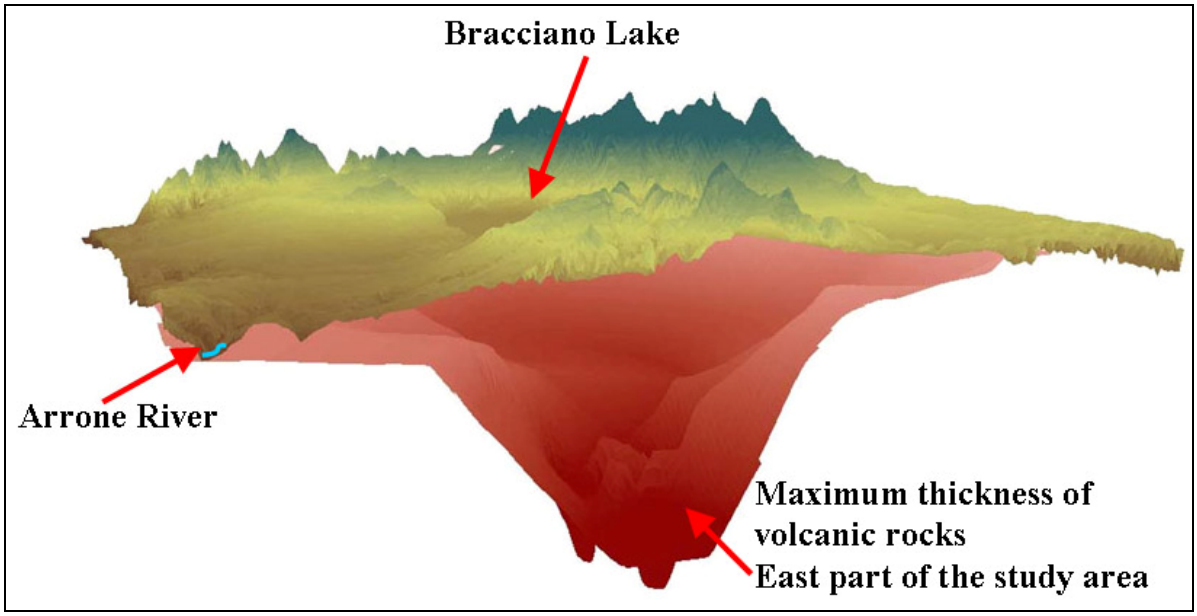

Figure 2.20: View of the volcanic aquifer

2.3.2 Water table reconstruction and groundwater flow analysis

Once analyzed the hydraulic behavior of the main volcanic deposits and the trend of substrate surface, now will be presented the results of a measurement campaign performed in 2009, during this work of study.

The survey campaign was carried out during spring and summer 2009 static water level was measured in 238 wells, 15 springs distributed all over the area and its surroundings. Flow measurement of the principal streams in the study area was also performed (Fig. 2.21 and Fig. 2.22).

Data collected were elaborated and a piezometric surface was man-drown (Fig. 2.21) to better elucidate the aquifer-lake and stream-aquifer connections and exchanges. The idea was also to obtain a "photography" of the actual situation to compare with previous representations of the piezometric surface made by Camponeschi & Lombardi, 1968 and by the Hydrogeology laboratory of Roma Tre University, in which this work od study has been elaborated in 2002 (Capelli et al., 2005).

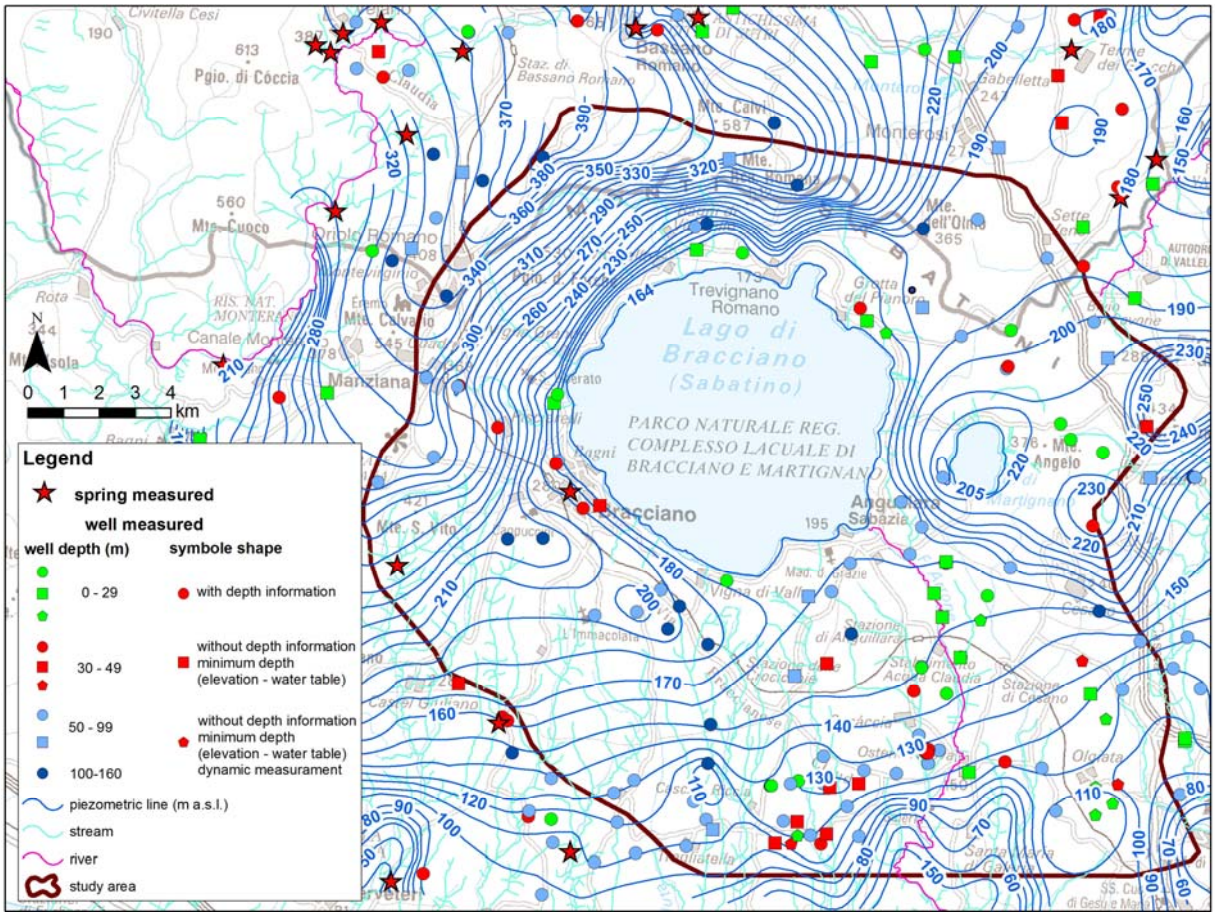

Figure 2.21 – Piezometric map (survey campaign 2009)

In Fig. 2.21 measured wells have been divided in several classes of different depth, considering real depth if data avaiable and considering the "minimum well depth", calculated from the difference between quota elevation and measured water table, in case of missing data. Another factor that has

been taken into account were conditions measurement was taken (static water table or dynamic water table).

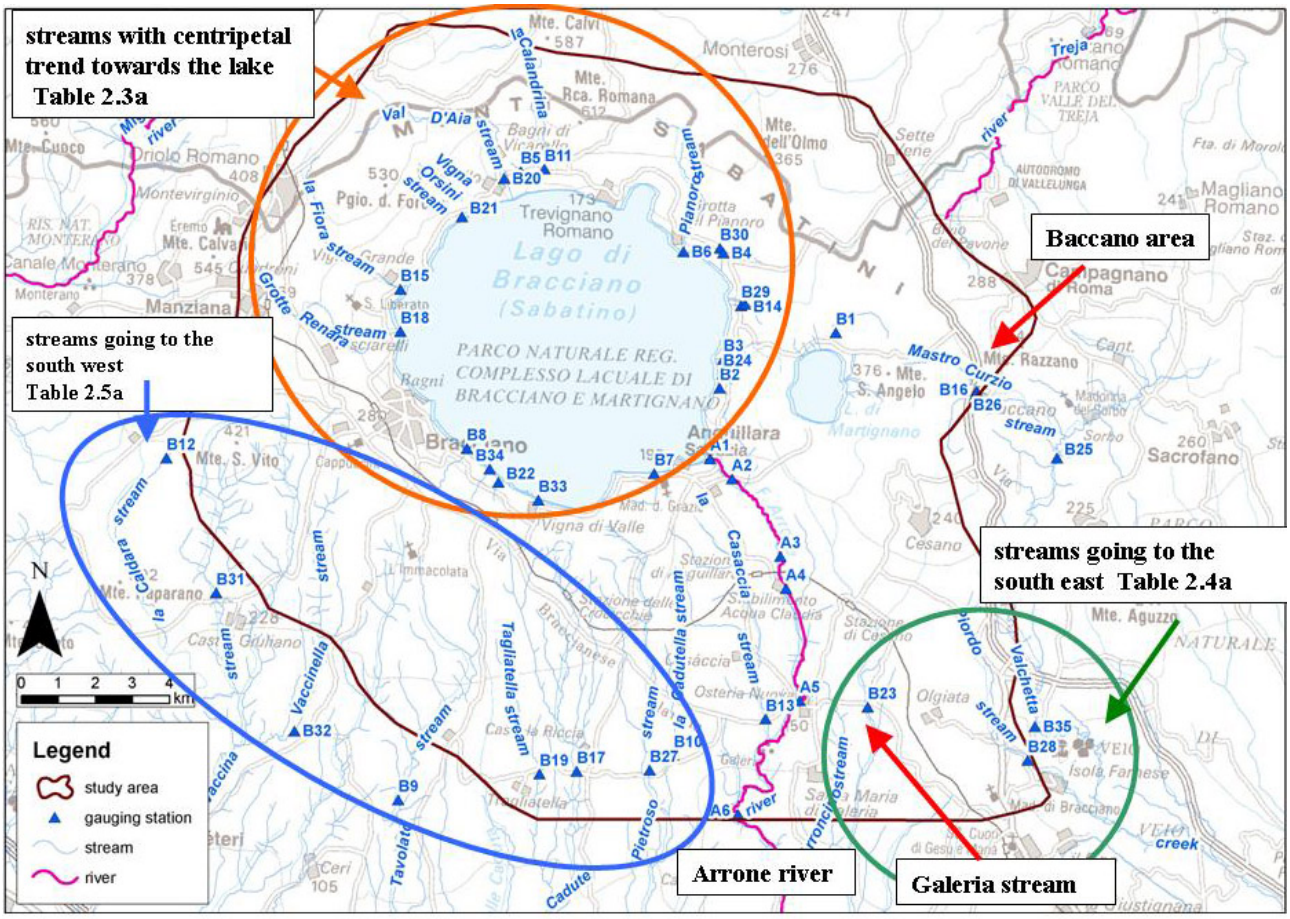

Figure 2.22 – Gauging stations in the area

The quantification of the flow in different sectors is needed to perform water budget calculation, important component to build the groundwater model.

Several stream flow measurements were conducted in Bracciano area, in 1981/1982, in 1999 and in 2002: survey campaigns conducted by the Hydrogeology Laboratory of University of Roma Tre. A survey campaign in 1968 conducted by Lombardi and Giannotti, one in 1992 (Boni et al., unpublished 1992), another in 1995 (Aquaital S.R.L., 1997).

All the before mentioned survey campaign did not cover the whole study area, so the comparison could not be generalized to all the sampled streams in 2009. Analyzing discharges with centripetal direction towards the lake, it is possible to observe a flow decrease from the flow measured in 1992 (Boni et al., unpublished 1992). In winter 1992 the discharge was 150 l/s (considering only the northern streams), while in summer 2009 total amount of water drained to the lake was only 30 l/s.

In the Table 2.3.b (Annex B) all streams measurement are reported and in the Table 2.3.a, the seasonal total amount of water drained to the lake is calculated in different years.

The streams located in the northwest side of the lake (Grotte Renara , Fiora , Vicarello and Val D'Aia) have several springs that feed Traiano aqueduct, active since roman period. The water company ACEA declared that the average water drained by the Traiano aqueduct drainage varies from 50 to 200 l/s. This water has to be considered as outflow of hydrogeological basin.

Table 2.3.a: Total contribution of the streams with a centripetal direction towards the lake

Total lake inflow		
Season	***Year***	***l/s***
winter	**1992**	**151.0**
summer	**1995**	**50.7**
winter	**1995**	**60.7**
summer	**2009**	**32.4**

In the southeast area Valchetta creek drains water from the hydrogeologic basin of Bracciano (Fig 2.21). In Table 2.4.b (Annex B) measured values, from different survey campaigns, are reported and in Table 2.4.a the seasonal total amount of water drained by the southeast area of the basin, computed for different years. The value of 341.7 l/s included both contribution of B28 and B35 stations (code in Fig. 2.22), in the estimation of study area drain water, it has to be consider only the B28 station contribute (115.6 l/s).

Table 2.4.b: Total contribution of the streams draining the southeast side

Total water drained the southeast side		
Season	***Year***	***l/s***
winter	**1999**	**294.4**
summer	**1999**	**14.0**
winter	**1981-1982**	**101.0**
summer	**1981-1982**	**500.0**
summer	**2009**	**341.7**

In the southern part of the area streams are located draining from southwest side of the basin. In the Table 2.5.b (Annex B) all values are reported and a Table 2.5.a, the total seasonal amount of drained water by streams is computed for different years.

Table 2.5.a: Total contribution of the streams draining southwest side

Total water drained		
Season	***Year***	***l/s***
winter	**1981**	**109.0**
summer	**1981**	**49.0**
summer	**2002**	**37.0**
summer	**2009**	**87.3**

Arrone River, effluent of Bracciano Lake, flows near Fregene (Tyrrenian coast) after running about 37 km, the collection area of surface water (river basin considering also Bracciano Lake) covers an area about 200 km2. In 1700 a dam was built near the beginning of Arrone River. On this artificial spillway some jets have been positioned at a height of 163.4 m a.s.l.. These jets enter into use during phases of exceptional floods when the lake level exceeds safe altitude. According to data provided by the water agency ACEA (Lombardi & Giannotti, 1969), in the period 1943-1963, only six years the lake has overflowed naturally, with a complessive flow about 5.106 m3/year. During this period Arrone flow rates were solely linked to the groundwater supply, not being recharged by the lake.

Table 2.6:Arrone river discharge in 1968 (a), in 1981 (b); in 1995 (c) and in 2009 (d)

Map code	*Stream*	*Elevation (m a.s.l.)*	*Year*	*Season*	*FLOW m^3/s*
A1	*Arrone river*	*167.3*	*1968*	*summer*	*0.000*
A2	*Arrone river*	*165.0*	*1968*	*summer*	*1.010*
A3	*Arrone river*	*158.0*	*1968*	*summer*	*0.906*
A5	*Arrone river*	*136.0*	*1968*	*summer*	*0.993*
A6	*Arrone river*	*44.0*	*1968*	*summer*	*1.266*

b.

Map code	*Stream*	*Elevation (m a.s.l.)*	*Year*	*Season*	*FLOW m^3/s*
A1	*Arrone river*	*167.0*	*1981*	*winter*	*0.010*
A1	*Arrone river*	*167.0*	*1981*	*summer*	*0.010*
A5	*Arrone river*	*136.0*	*1981*	*winter*	*0.020*
A5	*Arrone river*	*136.0*	*1981*	*summer*	*0.010*

c.

Map code	*Stream*	*Elevation (m a.s.l.)*	*Year*	*Season*	*FLOW m^3/s*
A3	*Arrone river*	*158.0*	*1995*	*summer*	*0.000*
A3	*Arrone river*	*158.0*	*1995*	*winter*	*0.004*
A5	*Arrone river*	*136.0*	*1995*	*summer*	*0.075*
A5	*Arrone river*	*136.0*	*1995*	*winter*	*0.124*

d.

Map code	Stream	Elevation (m a.s.l.)	Year	Season	FLOW m^3/s
A1	Arrone river	167.0	2009	summer	0.000
A3	Arrone river	158.0	2009	summer	0.000
A4	Arrone river	142.0	2009	summer	0.030
A5	Arrone river	136.0	2009	summer	0.188

These Tables show a quite variable flows with time. In some points, where Lombardi and Giannotti in 1968 measured flow of 1000 l/s, the river bed is now dry.

Comparing the data reported by Lombardi and Giannotti with those acquired during the field campaign carried out in summer 1995 and in July 2009, it can be drawn a completely different situation in terms of flow rates. In both campaigns the flow at the Lake effluent of Bracciano Lake (first measurement) is zero because of the artificial barrier that isolated the lake. As reported by Lombardi and Giannotti (1969), it beginning to have a sustained flow in Mola Vecchia (1010 l/s), a few hundred meters downstream from Lake effluent.

A second measurement was made at Valle Trave bridge, where the comparison between the two campaigns apparently explains the changes occurred in the last 30 years. Lombardi and Giannotti measured flow slightly less than the previous section (906 l/s), assuming a section of the river in which the water was drained by the aquifer. In 2009 a dry riverbed was observed in this point.

Marked difference was also registered in the flow at Osteria Nuova (Fig. 2.22, code A5): 993 l/s in 1967, and 187 l/s in 2009.

From the data listed above this decrease in flow could be attributed to the change of the piezometric surface elevation, with a general reduction that led the river to be dry for a few sections or sensibly reduce its flow. The lack of recharge may be attributed to a change in the level of Bracciano Lake as suggested by Lombardi and Giannotti (1969). The average level of the lake in April 1967 is 1.32 (± 0.02 m, ACEA data) compared to 0 hydrometric set at 161.74 m (163.06 m), this data confirms that in that time the lake did not exceed the bulkhead in Anguillara (the overflow is 30 cm higher). Lombardi and Giannotti hypothesized a direct water supply from the lake to the alluvial Arrone deposits, because, despite they had not project design, considering the age of the construction of the bulkhead, they guessed that the river was not isolated only at the surface but also through at deeper strata. The water of the lake, then infiltrated among the river sediments, re-emerges a little further downstream, approximately near Mola Vecchia, where the terrain elevation is almost the same of the lake level (163 m). At this point the first measure of flow in the river bed with considerable flow was performed. In July 2009, the Bracciano Lake level was 0.66 m on the 0 hydrometric (162.4 m a.s.l.), and below the level preciously recorded. It means that the water flowing through the alluvial deposits can not come out directly in a short distance from the Lake effluent, but probably further

downstream. During 2009 measurements, there were no larger flows than 1967, so probably by lowering the lake level has also changed the way of recharge to Arrone River. Now the river drains the regional aquifer and does not receive a direct recharge from the lake through river sediments.
The observed Arrone flux of 0.157 m3/s was measured in a gauge station (A5 in Fig. 2.22) placed some kilometres upstream of the edge of the model domain. It has to be consider the amount of 0.1 m3/s water discharged by the depurator point two kilometres upstream from the A5 measured station (Fig. 2.28). All things considered, a value of 0.240 m3/s for the whole outflow of the Arrone inside the study area was judged reasonable.
In the study area during summer 2009 total drain outflow measured was around 0.5 m3/s, in addition to a variable volume of 0.05 - 0.2 m3/s. of water drained by Traiano aqueduct from the streams located in the northwest side of Lake Bracciano. Other contribution of 0.1 m3/s has to be considered in the Baccano area, where an artificial drainage system (built to dry the former wetland) collects water discharged downstream (code B25, Fig. 2.22). Galeria stream (measured in location code B23 with absent flow) drains around 0.05 in the last tract. Considering all contributions, a total amount of drain outflow from study area can be estimated to be around 0.75 m3. In Table 2.7 above mentioned information are listed and each contribution location could be see in Fig. 2.22.

Table 2.7: Total contribution of the streams draining the study area

Total water drained in the study area (2009)	
	m3/s
contribution of the streams with a centripetal direction towards the lake	0.0324
contribution of the streams draining the southeast side	0.1156
contribution of the streams draining southwest side	0.0873
Arrone river drainage	0.24
Galeria stream drainage, last tract	0.05
Baccano area drainage contribution	0.1
northwest drainage contribution, captured by Traiano aqueduct	0.12
TOTAL	**0.7453**

In last 40 years several piezometric maps have been designed for the Bracciano area, in this work will be considered the piezometric map relative to 1967-1978 survey campaign made by Camponeschi and Lombardi (1968) and the piezometric map relative to 2002 survey campaign carried out by Hydrogeology Laboratory of the University Roma Tre (Capelli et al, 2005). Both maps consider the existence of one main aquifer inside volcanic deposits. In the present study the same approach was kept in the reconstruction of piezometric surface. Analyzing three piezometric surfaces (Fig. 2.21; Fig. 2.23; Fig. 2.24) it is possible to observe the presence of a high gradient area located in the north

west of the lake (in 1968, 2002 and 2009). In piezometric map from 1969, the strong effect of the drains on the piezometric lines in the North West zone is clearly visible, this drainage "disappears" in the following representation of the piezometric surface. It indicates the lowering of the water table.

In the southern sector piezometric lines trend matches in all three reconstructions, with a visible lowering of water table from 1967-68 to 2002 and 2009.

The hydraulic behavior of the volcanic deposits, hosting the aquifer, could be derived by the reconstructed piezometric maps.

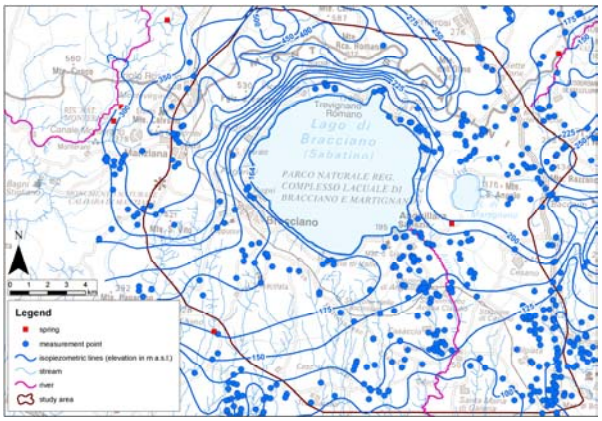

Figure 2.23: Piezometric map (Camponeschi and Lombardi, 1968)

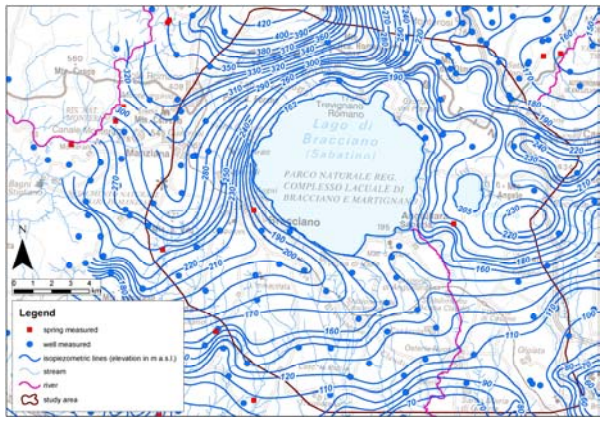

Figure 2.24: Piezometric map 2002 (Capelli et al., 2005)

To improve the understanding of hydraulic behavior of the volcanic deposits, were studied also pumping test results. The available information about hydraulic conductivity in the study area from pumping tests results are only 12 (Fig 2.25), there are some data coming from pumping tests, made by the local potable water company or by owners of the wells. Unfortunately none of these pumping tests have the information about the influence of the withdrawal observed in some nearby piezometres. Only few of these pumping tests could be related to a stratigraphic log, so most of the data could not be used.

It is necessary to reflect on which observations are representing the scale that the model study has and the discretization of the numerical groundwater model. A short term pumping tests represent an area near the pumping well, eventually not representing the model grid scale that will be used in this study (100 m). It can be problematic to use measured values of hydraulic conductivity directly in the model, since the hydraulic conductivity has a local "meaning" and is scale dependent (Sonnenborg & Henriksen, 2005). The following type model has been proposed to describe K's dependence on scale (Neuman, 1994; Shculze-Makuch et al., 1999)

$K = cVm, \quad V \leq Vm$ [m/s] Eq. 2.2

where V is the volume of geologic material that is included in the measurement; m is a scaling exponent and c is a constant which theoretically describes the hydraulic conductivity of the V=0.

When a heterogeneous aquifer is modelled as a homogeneous entity, there will necessarily be a mistake, while some sites will be simulated with a too high head level and elsewhere will be simulated with too low head levels. One criterion can be to consider if the mean of the head residuals between observed and simulated head is near zero, it will generally be considered an acceptable approach.

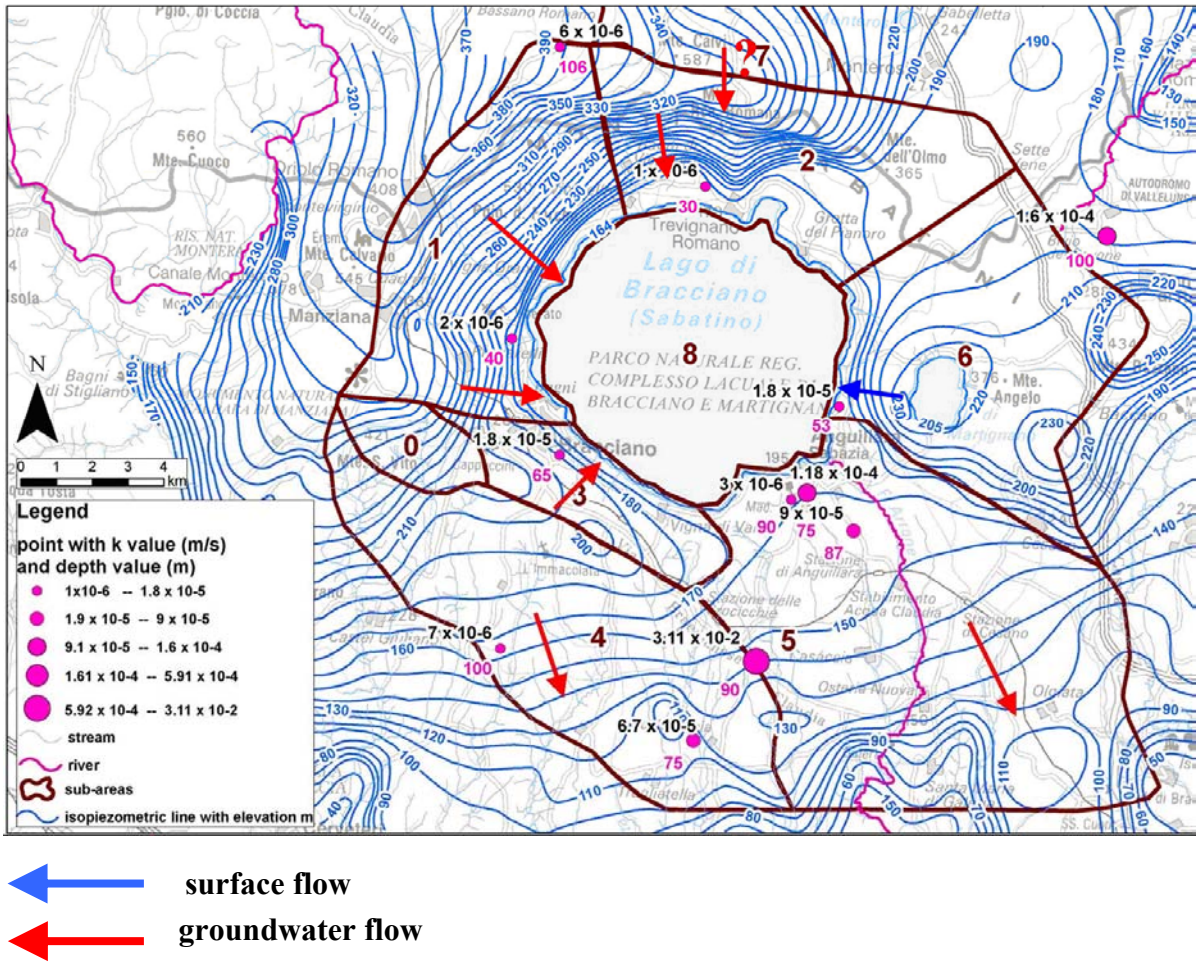

Figure 2.25: Wells hydraulic conductivity information (labels: in pink the well depth and in black the K values)

Considering the hydrogeological basin of Bracciano, to describe water circulation, the area was subdivided in the sub-basins indicated in Fig. 2.25, taking into consideration the following characteristics:

- thickness of the aquifer (calculated from the difference between the elevation of the piezometric surface related to 2009 campaign survey and the elevation of the pre-volcanic basement)
- piezometric trend
- the presence of areas of hydraulic closure, where low permeability deposits outcrops

- hydraulic characterization of volcanic deposits.

Sub-basin 1. The North-West Sector

At the north-west and west of Lake Bracciano were found prevolcanic sediments in outcrops. These sediments are characterized as clay and flysch and they represent a support above lake level. No groundwater inflow enters the sub-basin 1 from outside, due to the presence of clay and flysch structural border. From here the clay and the flysch dip to east-south direction. The lowering of the contact surface between flysch and volcanic deposits is connected to the presence of volcanic tectonic discontinuities with a concentric distribution (Fig. 2.15). These faults are related to the tectonic collapse of Lake Bracciano. In the higher relief the thickness of the permeable volcanic deposits is smaller due to the presence of low permeability prevolcanic sediments at high elevations, going toward the lake the thickness rapidly increases. In this basin the aquifer is limited in the upper part by umpermeable deposits and it is drained by the lava and other high permeability sediments. In Fig. 2.17, in the geologic section number 3, it is represented the above mentioned situation. Heterogeneous volcanic rocks have here a quite low equivalent hydraulic conductivity (linked to eruptive fissure fractures or faults presence).

In the piezometric map made by Camponeschi e Lombardi (1968), the piezometric lines appear strongly conditioned from the draining streams Fiora, Vicarello and Val d'Aia. In the following piezometric maps (2002 and 2009), the lines have a trend much more regular, the elevation of the water table is lower and so the water table intercepts streams at lower elevations. Due to the few anchor points present in this sub-basin, the subjective interpretation affects the reconstruction of the piezometric surface, that strongly indicate a steep trend. The sub-basin 1 (together with the sub-basin 2) gives the higher contribution to lake groundwater inflow.

Sub-basin 2. The Northern Sector

In this area the aquifer thickness has values around 100 and 200 m. The hydraulic connection with the Vicani volcanic aquifer is dynamic and there is no structural closure. It could be hypothesized a groundwater contribution from the Vicani aquifer to this sub-basin and more in general to Bracciano hydrogeological basin. From piezometric maps it is possible to observe a dynamic seepage, but it can be that below the water surface a component of the flux direct to the south exists (from north where water table elevation is generally higher, to the south where its elevation is lower). If there was a contribution to groundwater coming from another hydrogeological basin, it should be considered in the global hydrogeological balance. It seems likely an external contribution and the mathematical model could help to evaluate the correctness of this hypothesis.

Sub-basin 3. The South West lake

This sub-basin is located next to a high of clay (sub-basin 0). The sub basin 0 conditions the direction of water flow into different directions: to the lake, to the south and to the east. The direction of water table in the sub-basin 3 is toward the lake. The presence of a piezometric ridge, identifying a portion of a basin with a groundwater flow directed toward the lake (sub-basin 3) and another portion toward south-west (sub-basin 4, towards the Tavolato stream, to the Sanguinara and Vaccinella streams), is indicated in the reconstruction of the piezometric in 1968 by Camponeschi and Lombardi, in 2005 by Capelli et al., and finally in this work. The presence of faults located approximately parallel to the ridge and the presence of a suspected eruptive fissure, would lead to assume the presence of a kind of hydrogeological "barrier".

Sub-basin 4. External

This sub-basin is almost "external" to the Bracciano Lake catchments area, it was added with the idea of expanding the area of investigation, since the closure appeared to be too "close" to the lake. In addition to the zenith, there is a component of recharge from the lake (in the area to the south). This basin has a dynamic connection with the sub-basin 3, as was explained before.

Sub-basin 5. The Southern Sector

In this area the thickness of volcanic aquifer deposits is variable. In some zones reach high values, for example in the south east part, where the tectonic has lowered the pre-volcanic deposits. It represents the southern sub-basin and in south, south-east it is fed (in addition to the zenith), by the groundwater flow from Bracciano Lake.

The volcanic deposits are positioned mainly on Quaternary terrain characterized by a variable permeability, but generally lower than the permeability of volcanic units presented in this sub-basin. In the valleys, where outcrops the contact between volcanic deposits and prevolcanic sediments, there are numerous springs draining the basin. In this area, in the sandy and gravel layers of the Quaternary sedimentary series, a groundwater deeper circulation is present. This deeper groundwater system could be supplied by an seepage from upper layers and also from the Bracciano Lake, being its bottom part some meters higher. The volcanic sediments have here high permeability (Fig. 2.17 section number 1). This sub-basin is characterized by the presence of Arrone River, effluent of Bracciano lake .

Sub-basin 6. The Eastern Sector

In this sector the thickness of volcanic rocks reaches the highest values of the entire catchments area (up to about 900 m). The volcanic rocks outcrops are the most superficial part and are related to hydromagmatic events. They are characterized by very low permeability. The presence of Martignano Lake (as well as the area of Baccano and Stracciacappe, former lakes dried up in the ancient period), can be attributed to the presence of a surface circulation, and therefore it is assumed the presence of a shallow aquifer, in lateral connection with Lake Bracciano and with the main aquifer Lake Bracciano belongs, but vertically "isolated". In the reconstruction of the piezometric lines, it was decided to maintain continuity with regard to Martignano (where the aquifer is considered superficial) and the context of Bracciano. The idea is to emphasize the presence of a lateral exchange from Martignano to Bracciano. The measures of the water table level available for this area, are related to shallow wells, for this reason it was not possible to identify the presence of multi layer aquifer.

Sub-basin7. The external Northern Sector

This sector could be considered as “link” of possible hydraulic connection between the Vico context and the Sabatini one, as supported by Boni et al. (unpublished 1992), but it was never quantified.
In relation to the reconstruction of the surface of low permeability sediments and of water table, a groundwater inflow from this area could supply water to the catchment area of Bracciano Lake.

On the basis of previous information, here listed:
comparison of several historical piezometric heads;

- geology;
- basement surface reconstruction;
- analysis of results from pumping wells
- it was possible to define areas considered to have an homogeneous hydraulic behavior.

In Fig. 2.26 is shown the distribution of the areas. To every area it was assigned an “equivalent” homogeneous hydraulic conductivity, in the groundwater model. The areas are defined as follows:

- Kxyz1: area characterized by hydromagmatic products, low permeability;
- Kxyz2: fractured lava and course tuff, area characterized by a high permeability;
- Kxyz3: clay and sandy clay sediments, very low permeability;
- Kxyz4: different kinds of volcanic deposits, wide extension of tuff units, characterized by a mean permeability;
- Kxyz6: different kinds of pyroclastic products, scoria cones and lava cones. Low permeability;
- Kxyz8: different kinds of deposits: volcanic and, fluvial - alluvial, variable permeability.

- Kxyz12: stratified lava (dip into the lake), quite low permeability,

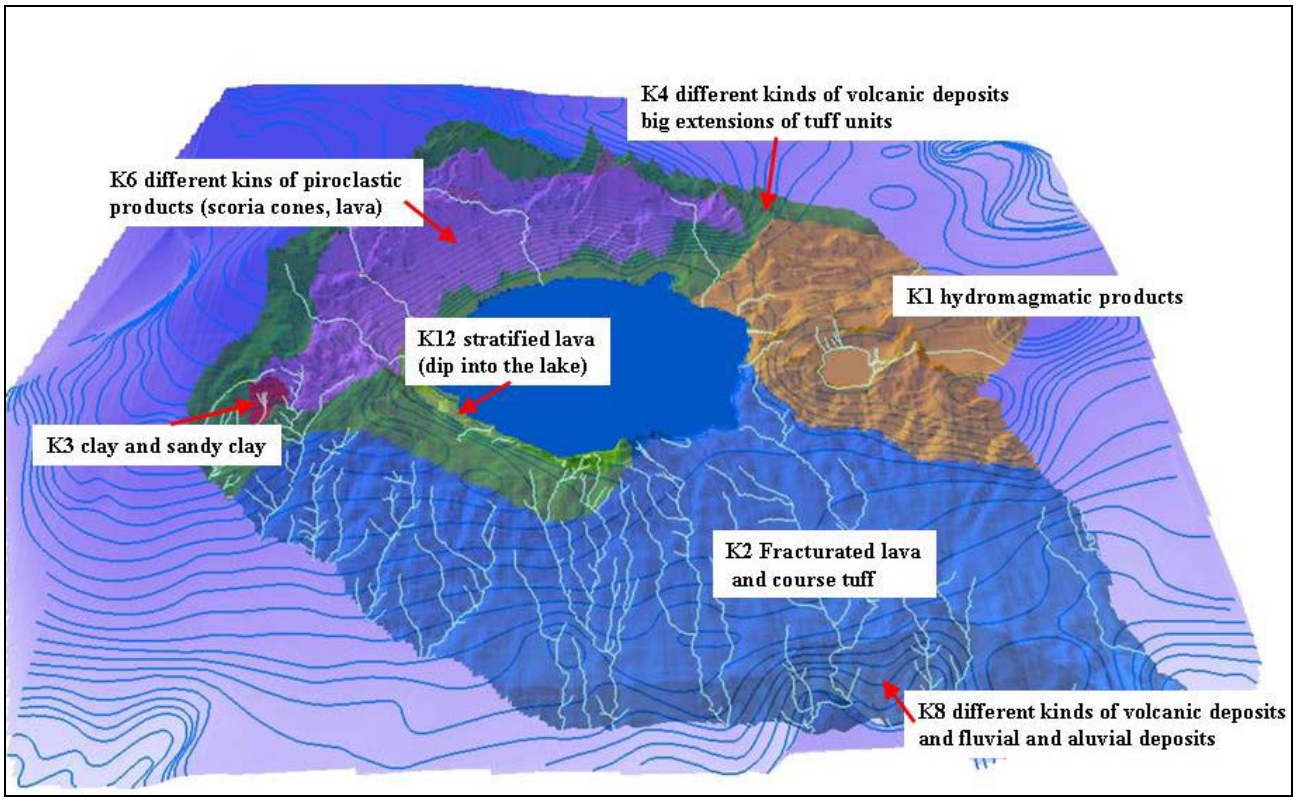

Figure 2.26 – Identified areas with a "homogeneous" hydraulic behavior. Piezometric surface and piezometric lines are shown and areas with a homogeneous hydraulic behavior are represented with different colors

The hydrogeologic balance was calculated for a selected area (Fig 2.27), in order to estimate the southward outflow from the study area. It was necessary to make an estimation of this value in order to achieve all the information useful to building the conceptual model.

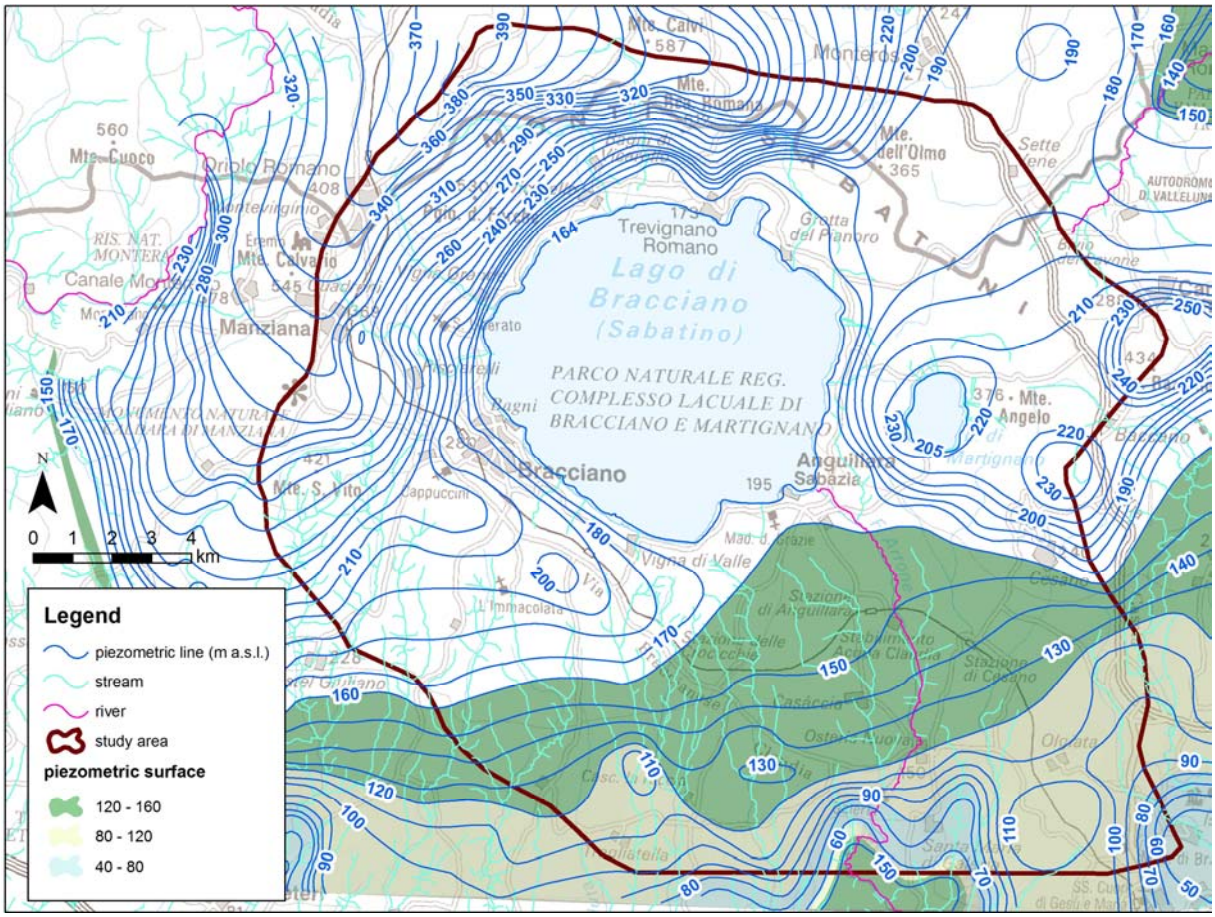

Figure 2.27: selected area for the hydrogeologic balance calculation

The hydrogeologic balance was determined by considering a line parallel to the isopiezometric line of 130 m a.s.l. and supposing hydraulic trasmissivity to be constant:

$$Q = L * T * i \qquad [m3/s] \qquad \text{Eq. 2.3}$$

where

L = length of the line in m = 17000

i = mean hydraulic gradient = 0.01126 (calculated between the isopiezometric line of 150 m and the one of 130 m)

T = hydraulic trasmissivity in m2/s = 8.5 * 10-3 (from experimental data, Lombardi & Giannotti, 1969). The total flow rate is:

Q = 17000 m x 0.01126 x 0.0085 m2/s = 1,627 m3/s

Considering that the system outflow piezometric elevation is from 100 to 60 m a.s.l. and that at those elevation an amount of the calculated outflow is drained by Arrone river and Galeria (approx.

0.100 m3/s in total), the net southward outflow could be consider as 1.627 m3/s- 0.1 m3/s = 1.527 m3/s.

2.3.3 Withdrawal

The volume of withdrawal and its distribution of the withdrawal in the area are essential to evaluate the water balance of a basin. Total amount of abstraction was estimated in different ways depending on kinds of withdrawal:

- Water supply for potable use was estimated by the PRGA document (Regional water management plan);
- Value of monthly average withdrawal from Lake Bracciano, was transmitted by ACEA, for the last ten years; ACEA provided also values of the Traiano aqueduct withdrawal.
- Water supply for industrial and irrigation use was estimated by an evaluation of the water requirement.
- Water supply for domestic uses was evaluated considering the official database provided by Regional and Provincial Administration (Fig. 2.29)

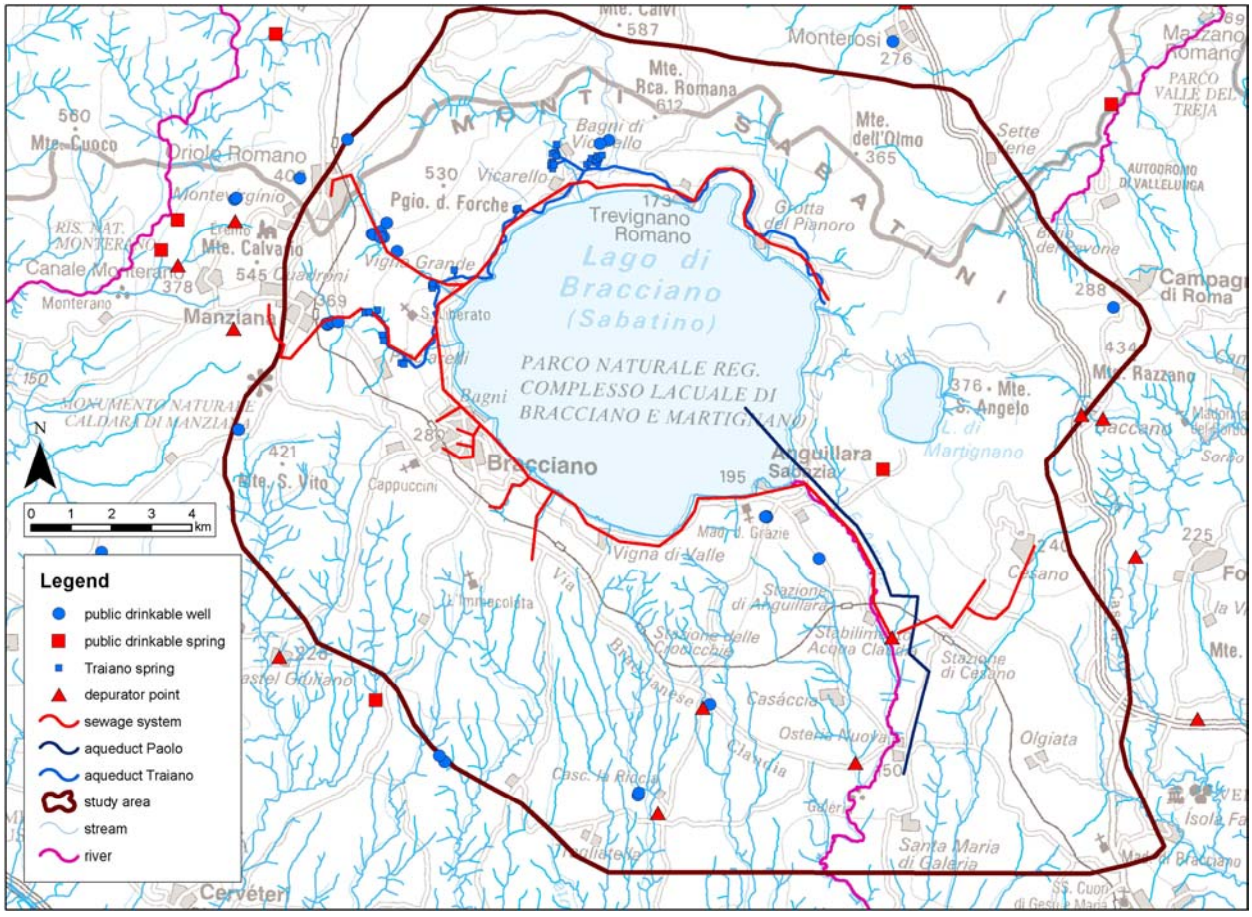

Figure 2.28: potable public withdrawal, aqueducts, sewage system and depurator sites.

In the case of PRGA, it was possible to consider the amount of withdrawal for several wells distributed in the study area (reported in Fig. 2.28) and feeding public aqueducts of the towns around Bracciano Lake. A problem concerning PRGA is the reliability of data since no official version of this plan exists and all the information are as not validated version provided by Regional Administrator.

The estimation of industrial and agriculture abstraction was made by the evaluation of water requirement. This evaluation was made according to a distributed grid (considering a cell value of 100 m) based on different information, as land use, climate and information on population and on the economical activities as given by the National Statistic Institute (ISTAT)

The estimation procedure assesses the amount of water requirements by applying the appropriate coefficients (specific values of water requirement) from ISTAT census categories and classes of landuse. The identification of UTW_1 (Unit of Territory Water Requirement) is necessary to distribute the quantities of water requirement on the territory in relation to the location of different water requirements. The water requirement was assessed for each of the UTW, by comparison of estimated needs from ISTAT census2 with the categories of the map of the UTW, for instance all the areas (polygons in the shape) defined as industrial are connected to the ISTAT information about number of employee. The determination of abstraction from water bodies, once the needs are known, (in a given area) can be considered as the difference between water needs and water supplied from outside sources. More information on this procedure are reported in Capelli et al., 2005.

Once the procedure of water requirement estimation was completed it was compared with locations of industrial and agricultural withdrawals, stored in the regional database (Fig. 2.27). While the information on pumping rate inside regional database are not reliable, data location were useful to cross this information with hydro-exigency estimation. For the domestic withdrawal it was made the assumption that the domestic withdrawal could be equal to 350 m3/year for a garden (1000 m2), more 300 m3/year for 3 resident persons (274 l/day/resident-person).

Abstraction data calculated for the area of Lake Bracciano basin (380 km2) are shown in Table 2.8.

[1]UTW were drawn from aerial photo survey of the year 2001

[2] ***ISTAT census of 2001 (population and industry) and census 2000 (agriculture)

Table 2.8: Lake Bracciano basin abstraction

use	*source of information*	*number of wells/point of abstraction present in regional and province official database*	*m^3/s*	*note*
Industrial and other use	Regional Database	9	0.032	unreliable
	water requirement estimation		0.074	
Irrigation	Regional Database	785	2.306	unreliable
	water requirement estimation		0.214	
Private-Potable and domestic use	Regional Database	73	0.175	unreliable
	water requirement estimation		0.020	
Public-Potable	PRGA	21	0.190	
Potable and other	ACEA from Lake (Paolo aqueduct)	1	0.518	period 2002-2008 (0.613 m^3/s in 1997-2001)
Gardens and fountains	ACEA (Traiano aqueduct)	1	0.200	
TOTAL ABSTRACTIONS IN THE STUDY AREA		**2982**	**1.216**	

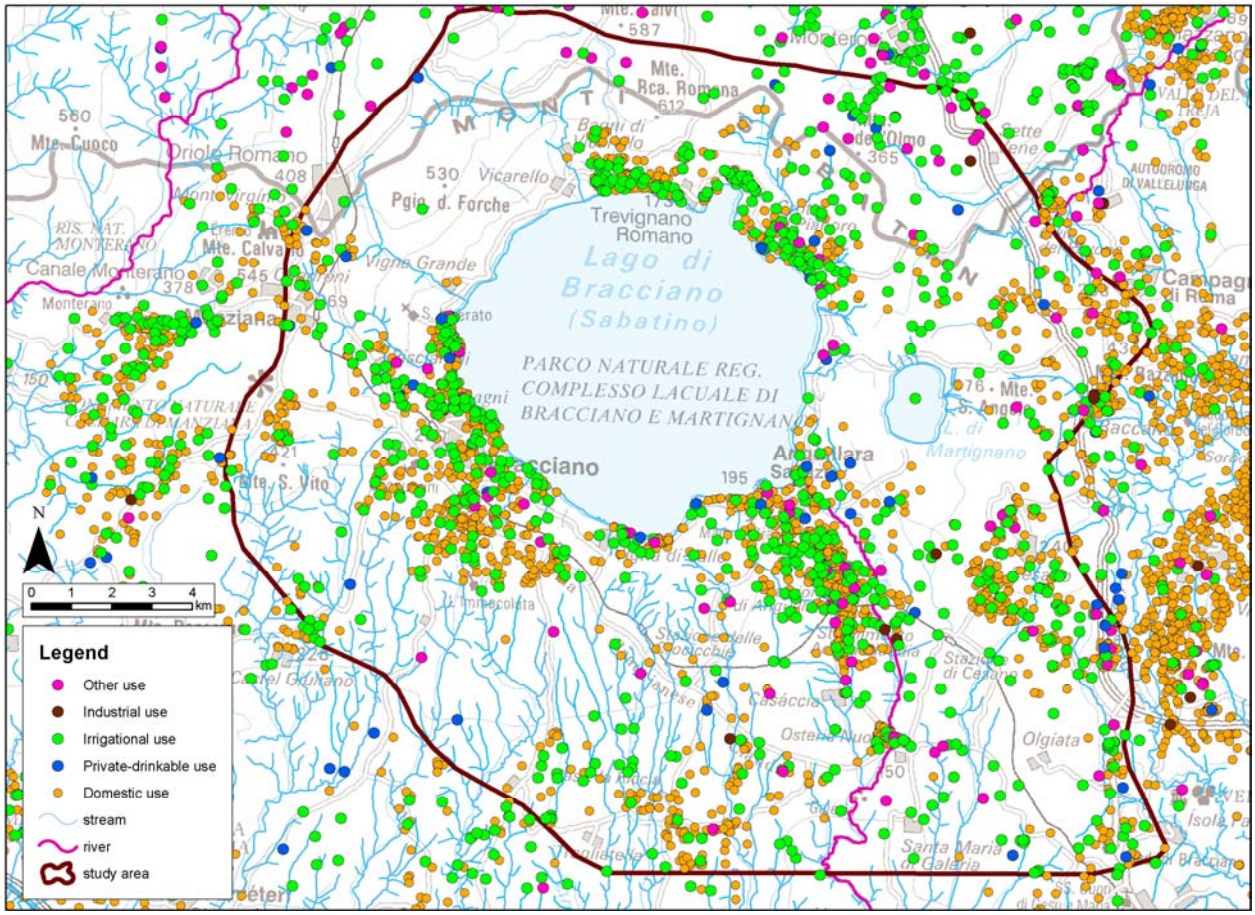

Figure 2.29: withdrawal on the study area (from official database provided by Regional and Provincial Administration)

2.3.4 Water budget

Water budget was calculated from the mean values of different components, represented in the scheme of Fig. 2.30 (listed in the Tab. 2.9 and 2.10, for the periods 1997-2001 and 2002-2008). These periods were selected considering that they could be related to the piezometric maps drawn with 2002 and 2009 survey campaign measuraments.

Some observations should be made on the calculated water budget. First of all it has not been considered an amount of uncertainty. It could be argued that a more or less 10% of error has to be taken into account in the evaluation of the Net Precipitation and also in the evaluation of withdrawal from the water requirement.

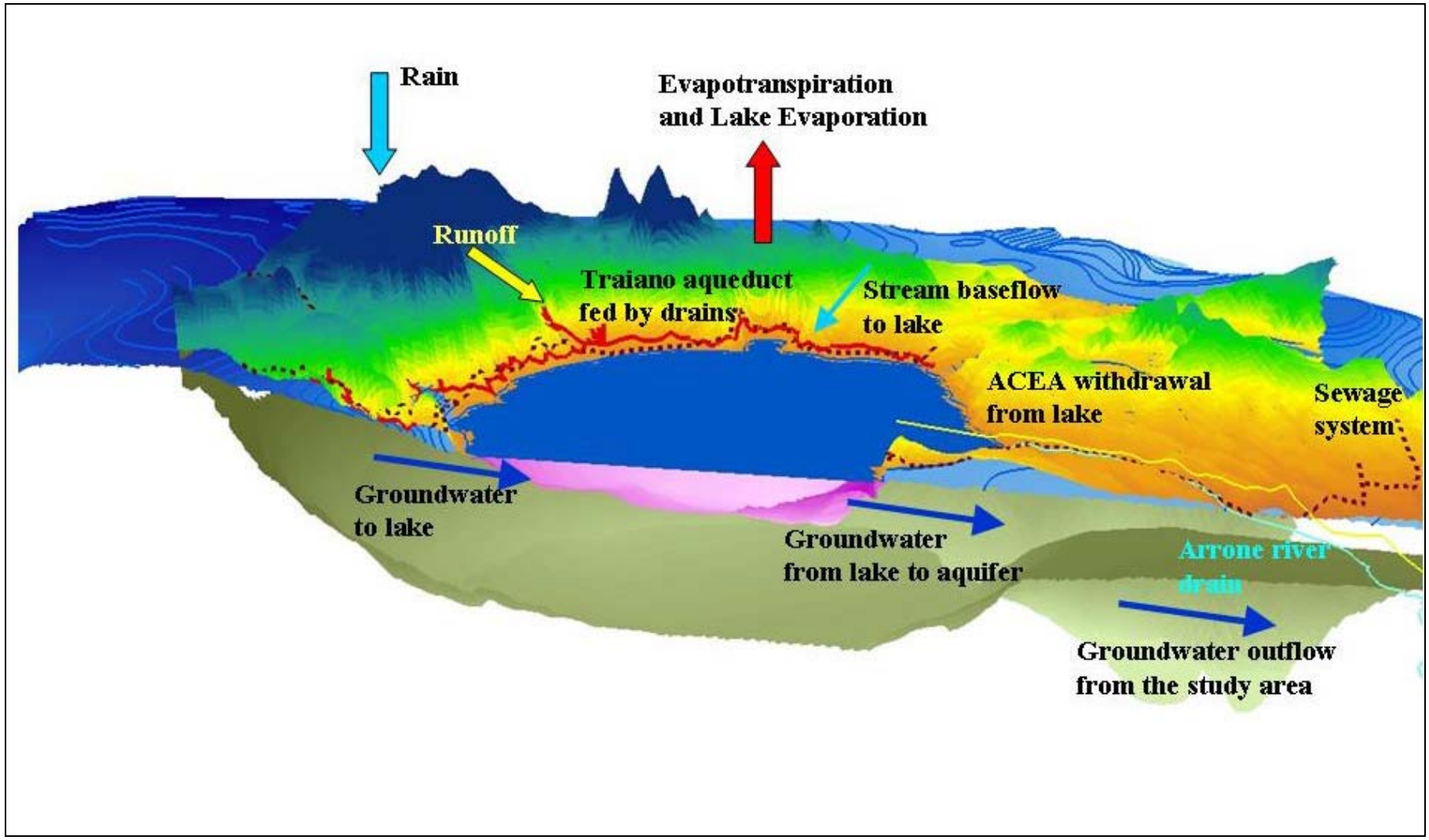

Figure 2.30:schematic representation of study area inflow and outflow

Table 2.9: Water budget (1997-2001)

Water Budget (mean values of the years 1997-2001) used for model 2002 simulation					
	Surface of the basin 380 km^2	**mm/year**	**Mm^3/year**	**m^3/s**	**notes**
BASIN INFLOW	Rain	713.00	235.65	7.472	
	Evapotraspiration	346.00	114.35	3.626	
	Runoff	84.00	27.76	0.880	a percent of runoff goes to the lake (is an INFLOW to the lake)
	Recharge	268.00	88.57	**2.809**	
	sewage discharge inside the basin				water drained by sewage in the north of Bracciano Lake, is returned to the basin in the southern part (Cesano)
ASIN OUTFLOW	Water going out from the system, in the southern area	145.70	48.16	1.527	Estimation
	Total abstraction (Table 2.8)	121.67	46.29	1.468	Estimation
	Drain outflow			?	No survey campaign
	water drained by sewage system				Estimation

Table 2.10: Water budget (2002-2008)

Water Budget (mean values of the years 2002-2008) used for model 2009 simulation					
	Surface of the basin 380 km^2	**mm/year**	**Mm^3/year**	**m3/s**	**notes**
BASIN INFLOW	Rain	863.00	285.2	9.044	
	Evapotraspiration	373.00	123.3	3.909	
	Runoff	112.00	37.0	1.174	a percent of runoff goes to the lake (is an INFLOW to the lake)
	Recharge	330.00	109.1	**3.458**	
	sewage discharge inside the basin				water drained by sewage in the north of Bracciano Lake, is returned to the basin in the southern part (Cesano)
BASIN OUTFLOW	Water going out from the system, in the southern area	145.70	48.2	1.527	Estimation
	Total abstraction (Table 2.8)	109.65	41.7	1.323	Estimation
	Drain outflow			0.750	0.033 m3/s into Lake Bracciano, 0.1 m3/s feed Traiano aqueduct
	water drained by sewage system				Estimation
	TOTAL BASIN OUTFLOW	298.37	113.5	**3.600**	

The water captured by the sewage system from runoff (quantify in Table 2.11), after to collect wastewater, is discharged by the depurator point located in the Arrone river (Fig. 2.28), as was mentioned above.

In Table 2.11 is reported the lake budget, calculated considering the specific inflows and outflows. Values listed in the Tables 2.9, 2.10 and 2,11 relative to general water budget and to the lake budget, need to be compared with the values generated by the mathematical model.

The conceptual model is to consolidate local and regional hydrogeological and hydrologic data into a set of assumptions and concepts that can be quantitatively evaluated.

The overall aim of Chapter 2 is to prepare all the information needed for the mathematical model building, i.e. geometry reconstruction, understanding of the fluxes, understanding of the amount of water that enter and that goes out from the study area.

Table 2.11: Lake budget (2002-2008)

LAKE BRACCIANO		mm/year	Mm^3/year	m^3/s	notes
INTO THE LAKE	**Rain**	951.0	542.07	**1.719**	
INTO THE LAKE	**Runoff from hydrologic basin**		98.08	**0.311**	
	Runoff from hydrologic basin, without the water capted from sewage system		86.02	**0.273**	
INTO THE LAKE	**stream baseflow to the lake**		15.77	**0.050**	
TOTAL INFLOW			**643.862**	**2.042**	
OUTFLOW FROM THE LAKE	**Evaporation from the lake**	1266.0	721.62	**2.288**	
OUTFLOW FROM THE LAKE	**Withdrawal from lake**		163.36	**0.518**	
OUTFLOW FROM THE LAKE	**water captured by the sewage system from runoff (from hydrologic basin)**		8.81	**0.030**	during 340 d/y
			3.24	**0.150**	during 25 d/y
TOTAL OUTFLOW			**884.976**	**2.806**	

3. HYDROGEOLOGICAL MODEL

3.1 GOVERNING EQUATIONS

3.1.1 Darcy's Law

In fluid dynamics and hydrology, Darcy's law is a phenomenological derived constitutive equation that describes the flow of a fluid through a porous medium. The law was formulated by Henry Darcy based on the results of experiments on the flow of water through beds of sand. It also forms the scientific basis of fluid permeability used in the earth sciences.

Although Darcy's law (an expression of conservation of momentum) was originally determined experimentally by Darcy, it has since been derived from the Navier-Stokes equations via homogenization.

One application of Darcy's law is to water flow through an aquifer. Darcy's law, along with the equation of conservation of mass, is equivalent to the groundwater flow equation, one of the basic relationships of hydrogeology.

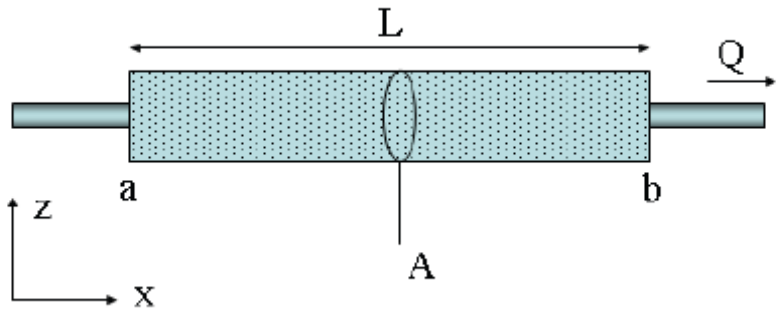

Figure 3.1 – Diagram showing definitions and directions for Darcy's law

Darcy's law is a simple proportional relationship between the instantaneous discharge rate through a porous medium, the viscosity of the fluid and the pressure drop over a given distance.

$$Q = \frac{\kappa A(P_b - P_a)}{\mu L} \qquad [m^3/s] \qquad \text{Eq. 3.1}$$

The total discharge, Q [m^3/s] is equal to the product of the permeability κ [m^2] of the medium, the cross-sectional area A [m^2] to flow, and the pressure drop ($P_b - P_a$) [$kg/m*s^{-2}$ or Pa], all divided by the dynamic viscosity μ [kg/m*s) or Pa*s], and the length L [m] the pressure drop is taking place over. The negative sign is needed because fluids flow from higher to lower pressure. So if the change in pressure is negative (in the x-direction) then the flow will be positive (in the x-direction). Dividing both sides of the equation by the area and using more general notation leads to:

$$q = \frac{-\kappa \nabla P}{\mu L} \qquad \text{[m/s]} \qquad \text{Eq. 3.2}$$

where q is the filtration velocity or Darcy flux (discharge per unit area [m/s]) and ∇P is the pressure gradient vector. This value of the filtration velocity (Darcy flux), is not the velocity which the water traveling through the pores is experiencing (Darcy, 1856).

The pore (interstitial) velocity (v) is related to the Darcy flux (q) by the porosity (φ). The flux is divided by porosity to account for the fact that only a fraction of the total formation volume is available for flow. The pore velocity would be the velocity that a conservative tracer would experience if carried by the fluid through the formation.

$$\upsilon = \frac{q}{\varphi} \qquad \text{[m/s]} \qquad \text{Eq. 3.3}$$

Darcy's law is only valid for slow, viscous flow; fortunately, most groundwater flow cases fall in this category. Typically any flow with a Reynolds number (based on pore size length scale) less than one is clearly laminar (R_e<1), and it would be valid to apply Darcy's law. Experimental tests have shown that flow regimes with values of Reynolds number up to 10 may still be Darcian. Reynolds number for porous media flow is typically expressed as

$$\mathrm{Re} = \frac{\rho e d_{30}}{\mu} \qquad \text{[dimensionless]} \qquad \text{Eq. 3.4}$$

Where ρ is the density of the fluid [kg/m^3], e is the specific discharge (not the pore velocity, [m/s]), d_{30} is a representative grain diameter [m] for the porous medium (often taken as the 30% passing size from a grain size analysis using sieves), and μ is the dynamic viscosity of the fluid [kg/m*s].

3.1.2 Groundwater flow equation

The groundwater flow equation, in its most general form, describes the movement of groundwater in a porous medium (aquifers and aquitards). It is known in mathematics as the diffusion equation, and has many analogues in other fields. It is often derived from a physical basis using Darcy's law and a conservation of mass for a small control volume. Many solutions for groundwater flow problems were borrowed or adapted from existing heat transfer solutions.

Mass balance

A mass balance must be performed, and used along with Darcy's law, to arrive at the transient groundwater flow equation. It is simply a statement of accounting, that for a given control volume, aside from sources or sinks, mass cannot be created or destroyed. The conservation of mass states that for a given increment of time (Δt) the difference between the mass flowing in across the boundaries, the mass flowing out across the boundaries, and the sources within the volume, is the change in storage.

$$\frac{\Delta M_{stor}}{\Delta t} = \frac{M_{in}}{\Delta t} - \frac{M_{out}}{\Delta t} - \frac{M_{gen}}{\Delta t} \qquad [\text{kg/s}] \qquad \text{Eq. 3.5}$$

Diffusion equation (transient flow)

Mass can be represented as density times volume, and under most conditions, water can be considered incompressible (density does not depend on pressure). The mass fluxes across the boundaries then become volume fluxes (as are found in Darcy's law). Using Taylor series to represent the in and out flux terms across the boundaries of the control volume, and using the divergence theorem to turn the flux across the boundary into a flux over the entire volume, the final form of the groundwater flow equation (in differential form) is:

$$S_s \frac{\partial h}{\partial t} = -\nabla \cdot q - G \qquad [\text{s}^{-1}] \qquad \text{Eq. 3.6}$$

where S_s [m^{-1}] represents specific storage, q [m/s] the flux and G[s^{-1}] represents the source terms. This is known in other fields as the diffusion equation or heat equation, it is a parabolic partial differential equation (PDE). This mathematical statement indicates that the change in hydraulic head

with time (left hand side) equals the negative divergence of the flux and the source terms. This equation has both head and flux as unknowns, but Darcy's law relates flux to hydraulic heads, so substituting it in for the flux leads to

$$S_s \frac{\partial h}{\partial t} = -\nabla \cdot \left(- K \nabla h\right) - G \qquad [s^{-1}] \qquad \text{Eq. 3.7}$$

Now if hydraulic conductivity (*K,* [m/s]) is spatially uniform and isotropic (rather than a tensor), it can be taken out of the spatial derivative, simplifying them to the Laplacian, this makes the equation

$$S_s \frac{\partial h}{\partial t} = K \nabla^2 h - G \qquad [s^{-1}] \qquad \text{Eq. 3.8}$$

dividing through by the specific storage (S_s), puts hydraulic diffusivity ($\alpha = K/S_s$ or equivalently, $\alpha = T/S$) on the right hand side. The hydraulic diffusivity is proportional to the speed at which a finite pressure pulse will propagate through the system (large values of α lead to fast propagation of signals). The groundwater flow equation then becomes

$$\frac{\partial h}{\partial t} = a \nabla^2 h - q \qquad [m/s] \qquad \text{Eq. 3.9}$$

Where the sink/source term, now has the same units but is divided by the appropriate storage term (as defined by the hydraulic diffusivity substitution).

3.1.3 Solving groundwater flow equation

The partial differential equation (PDE) must be solved to use the groundwater flow equation to estimate the distribution of hydraulic heads, or the direction and rate of groundwater flow. The most common means of analytically solving the diffusion equation in the hydrogeology literature are:

- *Laplace, Hankel and Fourier transforms* (to reduce the number of dimensions of the PDE);
- *Similarity transform* (also called the Boltzmann transform) is commonly how the Theis solution is derived;
- *Separation of variables*, which is more useful for non-Cartesian coordinates;

• *Green's functions*, which is another common method for deriving the Theis solution from the fundamental solution to the diffusion equation in free space.

No matter which method it is used to solve the groundwater flow equation, initial conditions (heads at time $t = 0$) are needed in the transient simulations and boundary conditions in steady state simulations, as the case of Bracciano model. The latter will be presented in next chapter, (representing either the physical boundaries of the domain, or an approximation of the domain beyond that point). Often the initial conditions are supplied to a transient simulation, by a corresponding steady-state simulation (where the time derivative in the groundwater flow equation is set equal to 0).
There are two broad categories of how the (PDE) would be solved; either analytical methods or numerical methods, or something possibly in between. Typically, analytical methods solve the groundwater flow equation under a simplified set of conditions *exactly*, while numerical methods solve it under more general conditions to an *approximation*.

Analytical methods

Analytical methods typically use the structure of mathematics to arrive at a simple, elegant solution. The required derivation for all with the simplest domain geometries can be quite complex (involving non-standard coordinates, conformal mapping, etc.). Typically analytical solutions are simply an equation that can give a quick answer based on a few basic parameters. The Theis equation is a very simple (yet still very useful) analytic solution to the groundwater flow equation, commonly used to analyze the results of an aquifer test or slug test.

Numerical methods

The topic of numerical methods is quite large, being of use to most fields of engineering and science. Numerical methods have been around much longer than computers have (in the 1920s Richardson developed some of the finite difference schemes still in use today, but they were calculated by hand, using paper and pencil, by human "calculators"), but they have become very important through the availability of fast and cheap personal computers. A quick survey of the main numerical methods used in hydrogeology, and some of the most basic principles is shown in Section 3.2 and further discussed.

3.2 GROUNDWATER MODELS

Groundwater models are computer models of groundwater flow systems, and are used by hydrogeologists to simulate and predict aquifer conditions.

Usually a groundwater model is meant to be a (computer) program for the calculation of groundwater flow and level. Some groundwater models include (chemical) quality aspects of the groundwater. Groundwater models may be used to predict the effects of hydrological changes (like groundwater abstraction or irrigation developments) on the behaviour of the aquifer and are often named groundwater simulation models.

As the computations in mathematical groundwater models are based on groundwater flow equations, which are differential equations that can often be solved only by approximate methods using a numerical analysis, these models are also called mathematical, numerical, or computational groundwater models (Rushton, 2003). Various types of numerical solutions like the finite difference method and the finite element method are discussed below.

Groundwater models can be one dimensional, two dimensional, three dimensional and semi three dimensional. Two and three-dimensional models can take into account the anisotropy of the aquifer with respect to the hydraulic conductivity, *i.e.* the non homogenous variation of this property along different directions.

1. One-dimensional models can be used for the vertical flow in a system of parallel horizontal layers.
2. Two-dimensional models could be applied to a vertical plane by assumption that groundwater characteristics repeat themselves in other parallel vertical planes (Fig. 3.2). Spacing equations of subsurface drains and the groundwater energy balance applied to drainage equations (Oosterbaan R.J. et al., 1996) are examples of two-dimensional groundwater models.

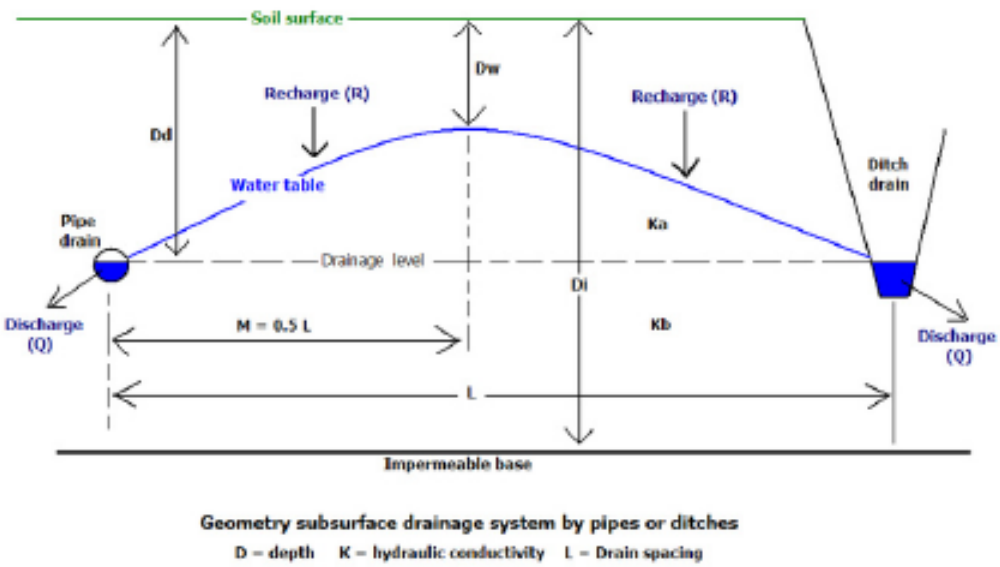

Figure 3.2 – Two-dimensional model of subsurface drainage in a vertical plane

3. Three-dimensional models like MODFLOW (MODFLOW, 2000) require discretization of the entire flow domain. To that end the flow region must be subdivided into smaller elements (or cells), in both horizontal and vertical sense. Within each cell the parameters are maintained constant, but they may vary between the cells (Fig. 3.3).

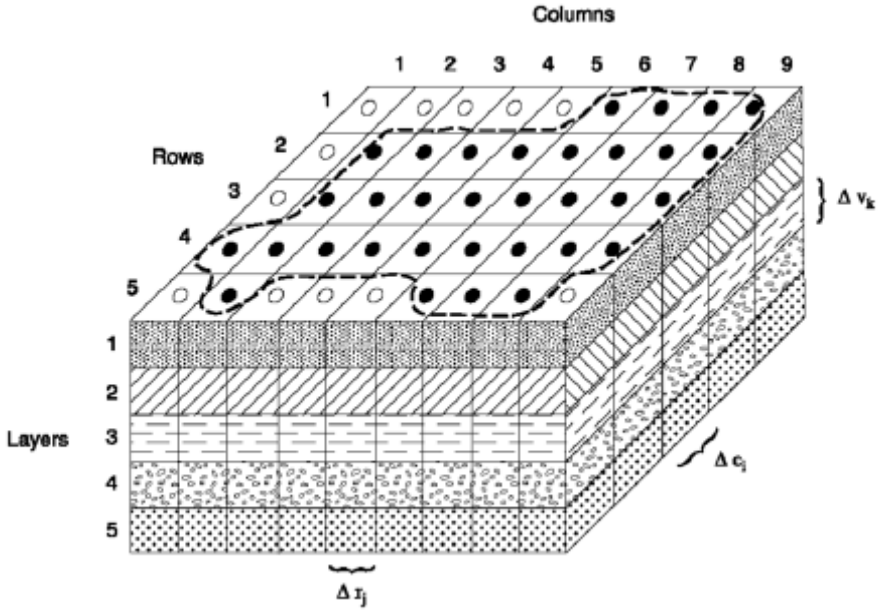

Figure 3.3 – Tree-dimensional grid, Modflow

4. In semi 3-dimensional models the horizontal flow is described by 2-dimensional flow equations (*i.e.* in horizontal x and y direction). Vertical flows (in z direction) are described (a) with 1-dimensional flow equation, or (b) derived from a water balance of horizontal flows converting the excess of horizontally incoming over the horizontally outgoing groundwater into vertical flow under the assumption that water is incompressible. Using numerical solutions of groundwater flow equations, the flow of groundwater may be found as horizontal, vertical and, more often, as **intermediate**.

There are two broad categories of numerical methods: gridded or discretized methods and non-gridded or mesh-free methods. In the common finite difference method and finite element method (FEM) the domain is completely gridded ("cut" into a grid or mesh of small elements). The analytic element method (AEM) and the boundary integral equation method (BIEM sometimes also called BEM, or Boundary Element Method) are only discretized at boundaries or along flow elements (line sinks, area sources, etc.), the majority of the domain is mesh-free.

3.2.1 General properties of gridded methods

Gridded methods like finite difference and finite element methods solve the groundwater flow equation by breaking the problem area (domain) into many small elements (squares, rectangles, triangles, blocks, tetrahedron, etc.) and solving the flow equation for each element (all material properties are assumed constant or possibly linearly variable within an element), then linking together all the elements using conservation of mass across the boundaries between the elements (similar to the divergence theorem). This results in a system which overall approximates the groundwater flow equation, but exactly matches the boundary conditions (the head or flux is specified in the elements which intersect the boundaries).

Finite differences are a way of representing continuous differential operators using discrete intervals (Δx and Δt), and the finite difference methods are based on these (they are derived from a Taylor series). For example the first-order time derivative is often approximated using the following forward finite difference, where the subscripts indicate a discrete time location,

$$\frac{\partial h}{\partial t} = h'\left(t_i\right) \approx \frac{h_i - h_{i-1}}{\Delta t} \qquad \text{[m/s]} \qquad \text{Eq. 3.10}$$

The forward finite difference approximation is unconditionally stable, but leads to an implicit set of equations (that must be solved using matrix methods). The similar backwards difference is only conditionally stable, but it is explicit and can be used to "march" forward in the time direction, solving one grid node at a time (or possibly in parallel, since one node depends only on its immediate neighbours). Rather than the finite difference method, sometimes the Galerkin FEM approximation is used in space with finite differences still used in time.

Application of finite difference models

MODFLOW is a well-known example of a general finite difference groundwater flow model. It is developed by the US Geological Survey as a modular and extensible simulation tool for modelling groundwater flow. Many commercial products have grown up around it, providing graphical user interfaces to its input file based interface, and typically incorporating pre - and post-processing of user data. Many other models have been developed to work with MODFLOW input and output, making linked models which simulate several hydrologic processes possible (flow and transport models, surface water and groundwater models and chemical reaction models), because of the simple, well documented and free nature of MODFLOW.

Application of finite element models

Finite element programs are more flexible in design (triangular elements vs. the block elements most finite difference models use) and there are some programs available for subsurface flow, solute and heat transport processes, but unless they are gaining in importance they are still not as popular in with practicing hydrogeologists as MODFLOW is. Finite element models are more popular in university and laboratory environments, where specialized models solve non-standard forms of the flow equation (unsaturated flow, density dependent flow, coupled heat and groundwater flow, etc.)

Application of finite volume models

Finite volume method is a method for representing and evaluating partial differential equations as algebraic equations (Le Veque, 2002; Toro, 1999). Similar to the finite difference method, values are calculated at discrete places on a meshed geometry. "Finite volume" refers to the small volume surrounding each node point on a mesh. In the finite volume method, volume integrals in a partial differential equation that contain a divergence term are converted to surface integrals, using the di-

vergence theorem. These terms are then evaluated as fluxes at the surfaces of each finite volume. Because the flux entering a given volume is identical to that leaving the adjacent volume, these methods are conservative. Another advantage of finite volume method is that it is easily formulated to allow for unstructured meshes. The method is used in many computational fluid dynamics packages.

3.2.2 Modelling protocol

When it has been determined that a numerical model is necessary and the purpose of the modelling effort has been clearly defined, the task of model design and application begins. A protocol for modelling includes code selection and verification, model design, calibration, validation, sensitivity analysis, and finally the prediction.

The protocol described below is a translation of the general terminology and methodology defined above into the field of distributed hydrological modelling. It is furthermore inspired by the modelling protocol suggested by Anderson and Woessner (1992), but modified concerning certain steps. The protocol is illustrated in Fig. 3.4 and described step by step in the following text.

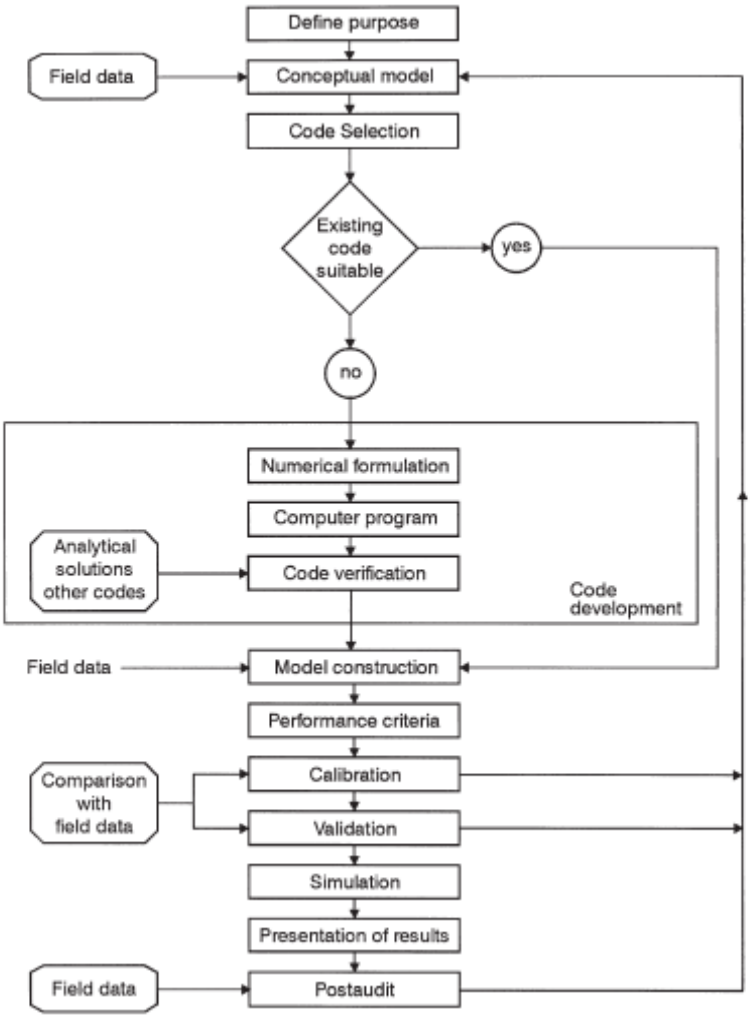

Figure 3.4 - Logical framework in a hydrological model application – a modelling protocol. (Refsgaard, 1997)

Step 1: The first step in a modelling protocol is to define the purpose of the model application. An important element in this step is to give a first assessment of the desired accuracy of the model output.

Step 2: Based on the purpose of the specific problem and an analysis of the available data, the user must establish a conceptual model.

Step 3: After having defined the conceptual model, a suitable computer program has to be selected. In principle, the computer program can be prepared specifically for the particular purpose. In practice, a code is often selected among existing generic modelling systems. In this case it is important to ensure that the selected code has been successfully verified for the particular type of application in question.

Step 4: In case no existing code is considered suitable for the given conceptual model a code development has to take place. In order to substantiate that the code solves the equations in the conceptual model within acceptable limits of accuracy, code verification is required. In practice, code verification involves comparison of the numerical solution generated by the code with one or more analytical solutions or with other numerical solutions.

Step 5: After having selected the code and compiled the necessary data, a model construction has to be made. This involves designing the model with regard to the spatial and temporal discretization, setting boundary and initial conditions and making a preliminary selection of parameter values from the field data. In the case of distributed modelling, the model construction generally involves reducing the number of parameters to calibrate, e.g. by using representative parameter values for different soil types.

Step 6: The next step is to define performance criteria that should be achieved during the subsequent calibration and validation steps. When establishing performance criteria, due consideration should be given to the accuracy desired for the specific problem (as assessed under step 1) and to the realistic limit of accuracy determined by the field situation and the available data (as assessed in connection with step 5). If unrealistically high performance criteria are specified, it will either be necessary to modify the criteria or to obtain more and possibly quite different field data.

Step 7: Model calibration involves adjustment of parameter values of a specific model to reproduce the observed response of the catchment within the range of accuracy specified in the performance criteria. It is important in this connection to assess the uncertainty in the estimation of model parameters, for example from sensitivity analyses.

Step 8: Model validation involves conduction of tests which document that the given site-specific model is capable of making sufficiently accurate predictions. This requires using the calibrated model, without changing the parameter values, to simulate the response for a period other than the calibration period. The model is said to be validated if its accuracy and predictive capability in the validation period have been proven to lie within acceptable limits or to provide acceptable errors. Validation schemes for different purposes are outlined below.

Step 9: Model simulation for prediction purposes is often the explicit aim of the model application. In view of the uncertainties in parameter values and, possibly, in future catchment conditions, it is advisable to carry out a predictive sensitivity analysis to test the effects of these uncertainties on the predicted results.

Step 10: Results are usually presented in reports or electronically, e.g. in terms of animations. Furthermore, in certain cases, the final model is transferred to the end user for subsequent day-to-day operational use.

Step 11: An extra possibility of validation of a site-specific model is a so-called *postaudit*. A *postaudit* is carried out several years after the modelling study is completed and the model predictions can be evaluated against new field data.

Step 12: Model redesign. Typically the *postaudit* will lead to new insights into system behaviour which may lead to changes in the conceptual model or changes in model parameters.

Although few modelling studies follow all steps in the above protocol, it represents the ideal against which the completeness of a modelling study should be measured. All modelling studies should proceed through step 7. Typically, generic and interpretive studies will not proceed beyond this. If a second set of field data does not exist, model validation (step 8) necessarily will be skipped. Model *postaudit* (step 11) has not been considered a normal part of a modelling protocol, but in view of the important information gained from the few *postaudits* it is clear that should be part of modelling protocol.

3.2.3 Conceptual model

The first step in modelling protocol discussed is to establish the purpose of the model; the second is to formulate a conceptual model of the system. A conceptual model is *an interpretation or working description of the characteristics and dynamics of the physical system* (D 5718-95(2006). Conceptual model can be a pictorial representation of the groundwater flow system, frequently in the form of a block diagram or a cross section (Fig. 3.4). The nature of the conceptual model will determine the dimensions of the numerical model and the design of the grid.

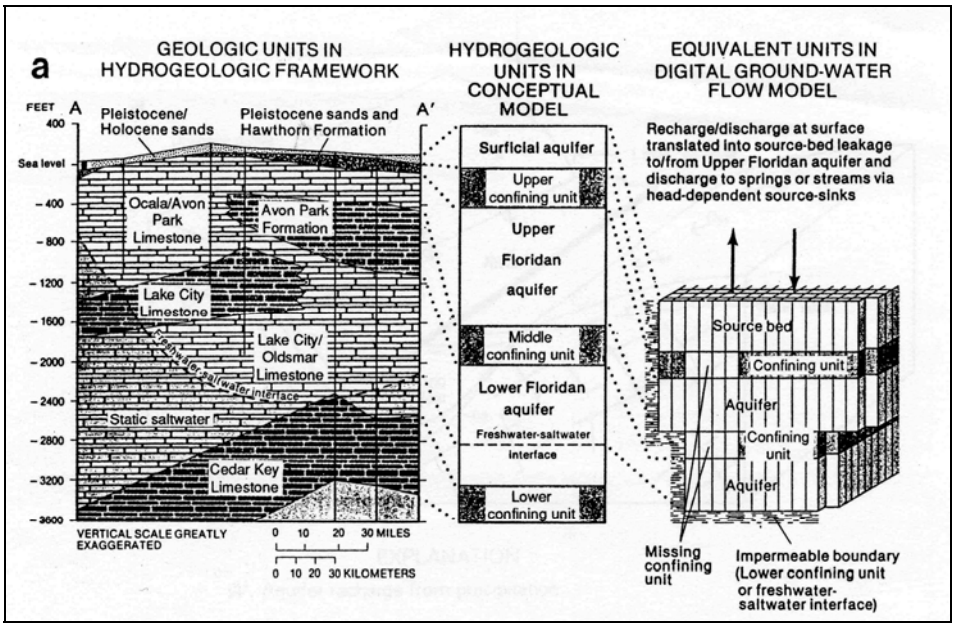

Figure 3.5: Translation of geologic information into a conceptual model suitable for numerical modelling (Anderson & Woessner, 1992).

The purpose of building a conceptual model is to simplify the field problem and organize the associated field data so that the system can be analyzed more readily. Simplification is necessary because a complete reconstruction of the field system is not feasible. The data requirements for a groundwater flow model are listed in Table 3.1. These data should be assembled when formulating the conceptual model. In theory, the closer the conceptual model approximates the field situation, the more accurate is the numerical model. However, in practice it is desirable to strive for parsimony, by which it is implied that the conceptual model has been simplified as much as possible yet retains enough complexity so that it adequately reproduces system behaviour. It is critical that the conceptual model be a valid representation of the important hydrogeologic conditions; failure of numerical models to make accurate prediction can often be attributed to errors in the conceptual model.

Table 3.1: Data requirements for groundwater flow model

Data requirements for Groundwater Flow Model	
A. Physical framework	
	1. Geologic map and cross sections showing the areal and vertical extent and boundaries of the system
	2. Topographic map showing surface water bodies and divides
	3. Contour maps showing the elevation of the base of the aquifers and confining beds.
	4. Isopach maps showing the thickness of the aquifer and confining beds
	5. Maps showing the extent and thikness of stream and lake sediments
B. Hydrogeologic framework	
	1. Water table and potentiometric maps for the aquifers
	2. Hydrographs of groundwater head and surface water levels and discharge rates
	3. Maps and cross sections showing the hydraulic conductivity and/or trasmissivity distribution
	4. Maps and cross sections showing the storage properties of the aquifers and confining beds
	5. Hydraulic conductivity values and their distribution for stream and lake sediments
	6. Spatial and temporal distribution of rates of evapotranspiration, groundwater recharge, surface water-groundwater interaction, groundwater pumping and natural groundwater discharge

The first in formulating the conceptual model is to define the area on interest, i.e. identify the boundaries of the model. Numerical models require boundary conditions, such that the head or flux must be specified along the boundaries of the system. Whenever possible the natural hydrogeologic boundaries of the system should be used as boundaries of the model. However, for some problems it may be necessary to restrict the problem domain to less than that encompassed by natural aquifer boundaries. In either case, the true hydrogeologic boundaries of the system should be identified when formulating the conceptual model.

There are tree steps in building a conceptual model:

i) Defining hydrostratigraphic units

Geologic information including geologic maps and cross sections, well logs, and borings, are combined with information on hydrogeologic properties to define hydrostratigraphic units for the conceptual model. In modelling a regional flow system, aquifers and confining beds are defined using the concept of the hydrostratigraphic unit, which was introduced by Maxey (1964) and reassessed by Seaber (1988). Simply stated, hydrostratigraphic units comprise geologic units of similar hydrogeologic properties. Several geologic formations may be combined into a single hydrostratigraphic unit or geological formation may be subdivided into aquifer and confining units.

ii) Preparing the water budget

The sources of water to the system as well as the expected flow direction and exit points should be part of the conceptual model. The field-estimated inflow may include groundwater recharge from

precipitation, overland flow, or recharge from surface water bodies. Outflow may include spring flow, base flow to streams, evapotranspiration, and pumping. Underflow may occur either inflow or outflow. A water budget should be prepared from the field data to summarize the magnitudes of these flows and changes in storage. During model calibration in field-estimated water budget will be compared with the water budget computed by the model

iii) Defining the flow system

Hydrologic information is used in conceptualize the movement of groundwater trough the system. Hydrologic information on precipitation, evaporation, and surface water runoff, as well as head data and geochemical information are used in this analysis. Water level measurements are used to estimate the general direction of groundwater flow, the location of recharge and discharge areas, and the connection between aquifers and surface water systems. Definition of the flow system may be based solely on physical hydrologic data, but it is advisable to use geochemical data whenever possible to strengthen the conceptual model.

3.2.4 Boundary Conditions

Boundary conditions are mathematical statements specifying the dependent variable (head) or the derivative of the dependent variable (flux) at the boundaries of the problem domain, which constrains the equation of the mathematical model.

Hydrogeologic boundaries are represented by the following three types of mathematical conditions:

- Specific head boundaries (Dirichlet conditions) for which head is given;
- Specified flow boundaries (Neumann conditions) for which the derivative of head (flux) across the boundary is given. A no-flow boundary condition is set by specifying flux to be zero;
- Head-dependent flow boundaries (Chauchy or mixed boundary conditions) for which flux across the boundary is calculated given a boundary head value. This type of boundary condition is sometimes called mixed boundary condition because it relates boundary heads to boundary flows. There are several types of head-dependent flow boundaries.

3.2.5 Modelling lake systems, Lake-aquifer interaction

Heads and flow patterns in surficial aquifers can be strongly influenced by the presence of stationary surface-water bodies (lakes) that are in direct contact, vertically and laterally, with the aquifer. Conversely, lake stages can be significantly affected by the volume of water that seeps through the lakebed that separates the lake from the aquifer.

An approach to the simulation of lakes that does not require the use of any modular package is simply to represent parts of the model grid as having the hydraulic characteristics of a lake by specifying a high hydraulic conductivity for lake-volume grid cells, the “high k” technique. The lake stage is computed for lake-volume grid cells with the same equations used to compute aquifer heads. Because the hydraulic conductivity is high, little or no spatial variation in head (stage) will occur in the lake-volume grid cells. The principal difficulty in using the “high K” technique is that stream-lake connections are difficult to represent accurately. Also, the representation of lake-bed leakance requires some effort. Generally, the “high K” technique is most useful for simple application problems.

In the Lake Package (Merritt and Konikow, 2000), a lake is represented as a volume of space within the model grid which consists of inactive cells extending downward from the upper surface of the grid. Active model grid cells bordering this space, representing the adjacent aquifer, exchange water with the lake at a rate determined by the relative heads and by conductances that are based on grid cell dimensions, hydraulic conductivities of the aquifer material, and user-specified leakance distributions that represent the resistance to flow through the material of the lakebed.

When MODFLOW is used for steady-state calculations, water fluxes to and from the lake must be known or estimated in performing the Newton’s Method calculations for equilibrium lake stages.

Seepage between Lake and Aquifer

The direction and magnitude of seepage between a lake and the adjacent aquifer system depends on the relation between the lake stage and the hydraulic head in the ground-water system, both can vary substantially in time and space. Seepage from a lake into the surficial aquifer that surrounds it, where the lake acts as a source of recharge to the aquifer, occurs when and where the lake stage is higher than the altitude of the water table in the adjacent part of the aquifer. Typical situations in which substantial recharge to the aquifer occurs are those where a lake receives surface inflows in excess of outflows, perhaps from a stream discharging into the lake, or where the water level in the aquifer is drawn down by pumping from wells. Seepage from the surficial aquifer into a lake usually occurs where the water-table altitude is normally higher than that of the lake. Such cases are found in regions with karstic topography where lakes commonly have no substantial surficial inflows or outflows. In these environments, the rate of evaporation from the open lake surface is greater than groundwater evapotranspiration, so more water is removed per unit area from the lake than from the surficial aquifer. Because less water per unit volume is stored in the aquifer than in the lake, periods of rainfall cause the water table to rise higher than the lake stage, thus increasing the rate of seepage from the aquifer into the lake. In this manner, the lake can act as a hydraulic sink

for the ground-water system. In other hydrologic environments, a lake can represent a mixed or "flow-through" condition where, in some areas of the lake-bed, seepage is into the lake and in other areas, seepage is out of the lake. For all of these conceptual cases, quantification of the rate of seepage between the lake and the aquifer is by an application of Darcy's Law:

$$q = K\frac{h_l - h_a}{\Delta l} \qquad \text{[m/s]} \qquad \text{Eq. 3.11}$$

where

q is the specific discharge (seepage rate)

K is the hydraulic conductivity [m/s] of materials between the lake and a location within the aquifer below the water table;

h_l is the stage of the lake [m];

h_a is the aquifer head [m];

Δl *is* the distance [m] between the points at which *hl* and *ha* are measured.

As written, the seepage rate in Eq. 3.11 is positively signed when seepage is from the lake into the aquifer ($h_l > h_a$).

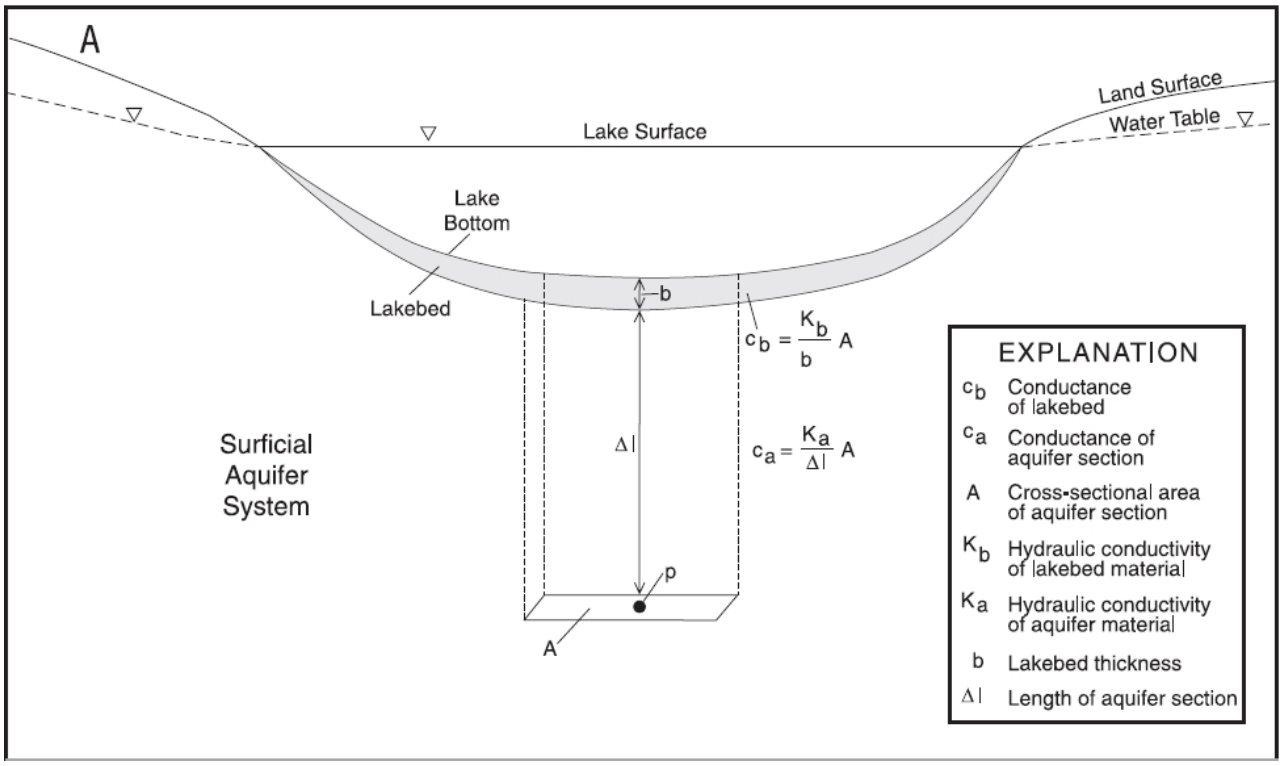

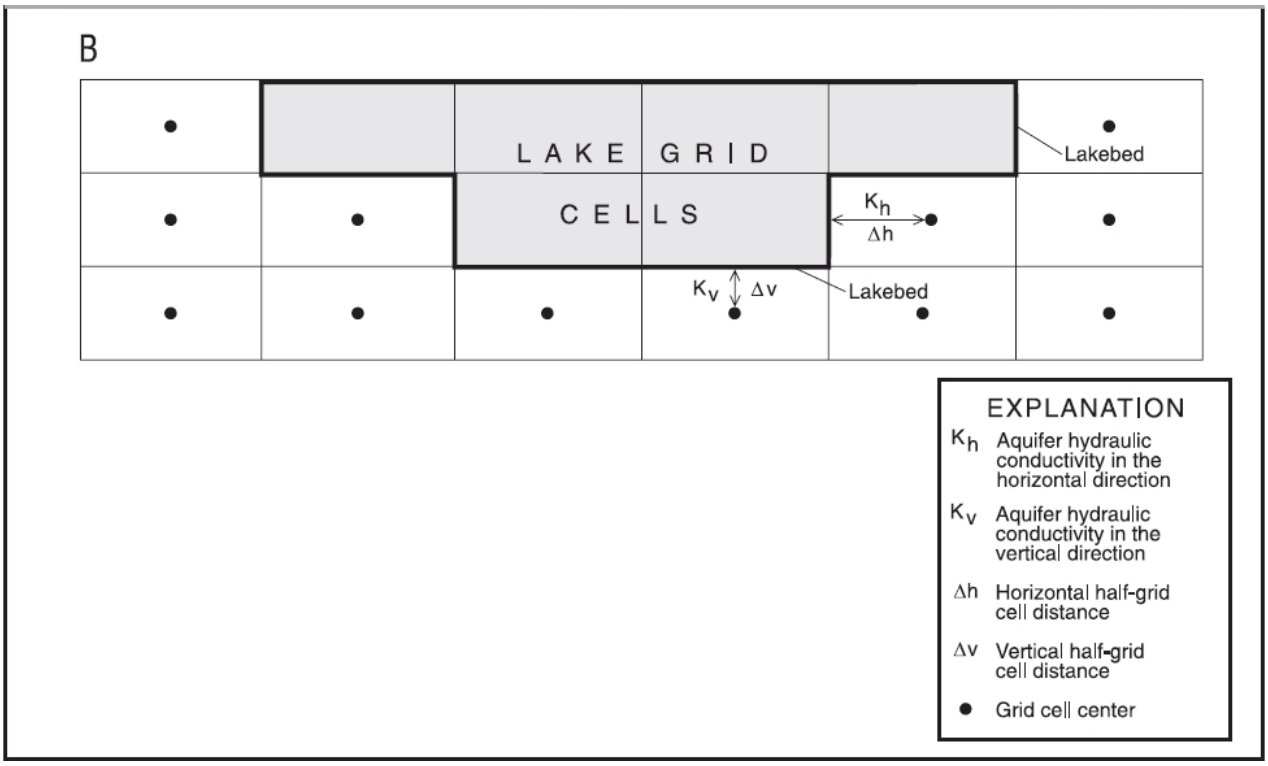

Figure 3.6: A and B: Lake-Aquifer interaction parameters (Merritt and Konikov, 2000)

Using a common cross-sectional area, A, the conductance of the lakebed is expressed as $c_b = K_b*A/b$, where K_b is the hydraulic conductivity of the lakebed material, A the cross section area and b is the lakebed thickness (Fig. 3.6 A). The conductance of the aquifer segment is expressed as $c_a = K_a*A/\Delta l$, where K_a is the aquifer hydraulic conductivity and Δl is the length of the travel path in the aquifer to the point where the aquifer head h_a is measured. The equivalent conductance, c [m^2/s], of the entire path between the points in the lake and aquifer where the heads are measured is found by treating the conductances of the lakebed and aquifer as if they were in series (McDonald and Harbaugh, 1988):

$$\frac{1}{c} = \frac{1}{c_b} + \frac{1}{c_a} \text{ or} \qquad [s/m^2] \qquad \text{Eq. 3.12}$$

$$c = \frac{A}{\frac{b}{K_b} + \frac{\Delta l}{K_a}} \qquad [m^2/s] \qquad \text{Eq. 3.13}$$

In the numerical modelling context, Δl is half the grid cell dimension in the appropriate coordinate direction (Fig. 3.6 B), the distance between the edge of the aquifer grid cell that is the interface with

the lakebed and the aquifer grid cell center), A is the cross-sectional area of the grid cell in a plane perpendicular to the travel distance Δl, and K_a is the aquifer hydraulic conductivity in the direction of Δl (either horizontal, K_h, or vertical, K_v). The procedure described above and automated in the Lake Package provides a mathematically correct estimate of the conductance of flow between the lake and the aquifer, the accuracy of which is primarily limited by the accuracy with which the parameters in the formula can be quantified from field data. Either of the terms in the denominator of the right side of equation 4 may or may not dominate quantitatively, depending on the properties of the natural system being investigated.

Lake water budget

The water budget procedure incorporated in the Lake Package is implied by the equation used to update the lake stage. The explicit form of this equation is:

$$h_l^n = h_l^{n-1} + \Delta t \frac{p - e + rnf - w - sp + Q_{si} - Q_{so}}{A_s} \qquad \text{[m]} \qquad \text{Eq. 3.14}$$

Where, used in the steady state simulations:

h_l^n is the lake stages [m] from the present time steps;

h_l^{n-1} is the lake stages [m] from the previous time steps, not present in the steady state;

Δt is the time step length [s], that is 1 for a steady state case;

p is the rate of precipitation [m^3/s] on the lake during the time step;

e is the rate of evaporation [m^3/s] from the lake surface during the time step;

rnf is the rate of surface runoff to the lake [m^3/s] during the time step;

w is the rate of water withdrawal from the lake [m^3/s] during the time step (a negative value is used to specify a rate of augmentation);

Q_{si} is the rate of inflow from streams [m^3/s] during the time step;

Q_{so} is the rate of outflow to streams [m^3/s] during the time step;

A_s is the surface area of the lake [m^2] at the beginning of the time step; and

sp is the net rate of seepage between the lake and the aquifer [m^3/s] during the time step (a positive value indicates seepage from the lake into the aquifer), and is computed as the sum of individual seepage terms for all M lake/aquifer cell interfaces:

$$sp = \sum_{m}^{M} c_m \left(h_l - h_{am} \right) \qquad \text{[m}^3\text{/s]} \qquad \text{Eq. 3.15}$$

where

h_{am} is the head in the aquifer cell across the m^{th} interface [m];

c_m is the conductance across the m^{th} interface [m^2/s]. (Fig. 3.6A)

3.2.5 Code selection

MODFLOW (McDonald and Harbaugh, 1988) is a three-dimensional finite-difference groundwater model.

The Visual MODFLOW® 2009.1 software product (Schlumberger Water Service, licence of Hydrogeology Laboratory of Roma Tre) implements the MODFLOW 1996, MODFLOW 2000 and MODFLOW 2005 code. It has a modular structure that allows it to be easily modified to adapt the code for a particular application.

The Groundwater Vistas®5.41 software product (ESI, licence of the Hydrogeologic Laboratory of Roma Tre) implements MODFLOW 2000, MODFLOW 2005 codes…

MODFLOW-2005 simulates steady and transient flow in an irregularly shaped flow system in which aquifer layers can be confined, unconfined, or a combination of confined and unconfined. Flow from external stresses, such as flow to wells, areal recharge, evapotranspiration, flow to drains, and flow through river beds, can be simulated. Hydraulic conductivities or transmissivities for any layer may differ spatially and be anisotropic (restricted to have the principal directions aligned with the grid axes), and the storage coefficient may be heterogeneous. Specified head and specified flux boundaries can be simulated, or a head dependent flux across the model's outer boundary, that allows water to be supplied by a boundary block in the modelled area at a rate proportional to the head difference between a "source" of water outside the modelled area and the boundary block.

In addition to simulating ground-water flow, the scope of MODFLOW-2005 has been expanded to incorporate related capabilities such as Lake package, solute transport and ground-water management; however, the present study incorporates only the ground-water flow parts of MODFLOW. The ground-water flow equation is solved using the finite-difference approximation. The flow region is subdivided into blocks in which the medium properties are assumed to be uniform. In plan view the blocks are made from a grid of mutually perpendicular lines that may be variably spaced. Model layers can have varying thickness. A flow equation is written for each block, called a cell. Several solvers are provided for solving the resulting matrix problem; the user can choose the best solver for the particular problem. Flow-rate and cumulative-volume balances from each type of inflow and outflow are computed for each time step.

The flow equations are:

1) Steady state

$$\frac{(T_1+T_0)}{2}(H_1-H_0)+\frac{(T_2+T_0)}{2}(H_2-H_0)+\frac{(T_3+T_0)}{2}(H_3-H_0)+\frac{(T_4+T_0)}{2}(H_4-H_0)+q=0$$

Eq. 3.16

2) Transient

$$\frac{(T_1+T_0)}{2}(H_1-H_0)+\frac{(T_2+T_0)}{2}(H_2-H_0)+\frac{(T_3+T_0)}{2}(H_3-H_0)+\frac{(T_4+T_0)}{2}(H_4-H_0)+q=$$
$$S\frac{H^{t+\Delta t}-H^t}{\Delta t}$$

Eq. 3.17

where the term on the left represents the balance of flows into and out of the cell boundary:

- the hydrodynamic characteristics of the aquifer (mean transmissivity and differences in hydraulic head H between the central cell and each of the four adjacent cells);
- volumes of water entering or leaving the cell due to artificial stresses (recharge and pumping) and/or interaction with other natural or artificial, both surficial and underground, represented by source terms Q

In order to use MODFLOW, initial conditions have to be specified in transient conditions and boundary conditions in steady state conditions. Hydraulic properties and stresses must be specified for every model cell in the finite-difference grid. Input data are read from files.

3.2.6 Calibration process

Both qualitative and quantitative calibration criteria can be considered. The qualitative calibration criteria should include:

- The general characteristics of the model (groundwater head distributions)
- The general flow characteristics (water balance)
- Flow paths of contour line
- Simulated “plume” directions

- Evaluated hydrological conditions used to calibrate the model
- Analyze the "soundness" of the hydraulic properties of the aquifer (ASTM D5490, 2008) when compared to a-priori assessments based on literature and observations

The quantitative calibration criteria consists of the comparison between the results of a simulation and the head observations. Eventually, flow observations can also be included.
Groundwater flow models are calibrated by comparing calculated (predicted) values (H, Q) in the aquifer with observed values (field measurements). The idea is to make adjustments in the parameters to better match model predictions with known conditions in the field.
Calibration of a flow model allows the model to accurately predict field heads and flows. Calibration is accomplished by finding a set of parameters, boundary conditions and stresses that produce simulated heads and fluxes that match field-measured values within a defined uncertainty. The quantification of these values is known as the *inverse* problem.
In an *inverse* problem the objective is to determine values of the parameters and hydrogeologic stresses from information about heads, whereas in the forward problem system parameters such as hydraulic conductivity, specific storage and hydrologic stresses such as recharge rate are specified and the model calculates heads.
Calibration parameters are the hydraulic properties or boundary conditions (more conceptual) that are changed during the calibration process. In the case of flow models, the flow properties are: hydraulic conductivity, infiltration from aquitard, amount of storage etc. Boundary conditions are: rate of recharge, evapotranspiration rate, conductance of the river.
The Visual Modflow calibration statistics and GWV calibration statistics provide information on:

- Number of data points: number of observations selected for a particular "snapshot" in time.
- Calibration residuals defined by the difference between the calculated results (X_{cal}) and the observed results (X_{obs}) at selected data points (as shown in the following equation)

$$R_i = X_{cal} - X_{obs} \qquad \text{[m]} \qquad \text{Eq. 3.18}$$

Max Residual ($\overline{R}$) and Minimum Residual are reported, together with:

- Residual Mean is the mean Residual value defined by the equation:

$$\overline{R} = {}^{1}\!/_{n} \sum_{i=1}^{n} R_i \qquad \text{[m]} \qquad \text{Eq. 3.19}$$

- The Absolute Residual Mean $|\overline{R}|$ is similar to the Residual Mean except that it is a measure of the average absolute Residual value defined by the equation:

$$\left|\overline{R}\right| = 1/n \sum_{i=1}^{n} \left|\overline{R}_i\right| \qquad \text{[m]} \qquad \text{Eq. 3.20}$$

The absolute Residual Mean measures the average magnitude of the Residuals and therefore provides a better indication of calibration than the Residual Mean.

- Standard Error of the Estimate (SEE) is a measure of the variability of the residuals around the expected residual value, and is expressed by the following equation:

$$SEE = \sqrt{\frac{\frac{1}{n-1}\sum_{i=1}^{n}\left(R_i - \overline{R}\right)^2}{n}} \qquad \text{[m]} \qquad \text{Eq. 3.21}$$

- Root Mean Squared (RMS) is defined by the following equation:

$$RMS = \sqrt{\frac{1}{n}\sum_{i=1}^{n}(Q_{cal} - Q_{obs})^2} \qquad \text{[m]} \qquad \text{Eq. 3.22}$$

- Normalized Root Mean Squared is the RMS divided by the maximum difference in the observed head values, and is expressed by the following equation:

$$NormalizedRMS = \frac{RMS}{(X_{obs})_{\max} - (X_{obs})_{\min}} \qquad \text{[dimensionless]} \qquad \text{Eq. 3.23}$$

The Normalized RMS is expressed as a percentage, and is a more representative measure of the fit than the standard RMS, since it accounts for the scale of the potential range of data values.

- The Correlation Coefficent (Cor) is calculated as the covariance (Cov) between the calculated results (X_{cal}) and the observed results (X_{obs}) at selected data points divided by the product of their standard deviations. The correlation is calculated using the following equation:

$$Cor(X_{cal}, X_{obs}) = \frac{Cov(X_{cal}, X_{obs})}{S_{cal} \times S_{obs}} \qquad \text{[dimensionless]} \qquad \text{Eq. 3.24}$$

The covariance is calculated using the following equation:

$$Cov(X_{cal}, X_{obs}) = \frac{1}{n}\sum_{i=1}^{n}(X_i - m_{cal}) \times (X_i - m_{obs}) \quad [\text{m}] \qquad \text{Eq. 3.25}$$

where m_{cal} and m_{obs} are the mean values of calculated and observed results, respectively

$$m_{cal} = \frac{1}{n}\sum_{i=1}^{n} X_{cal} \qquad [\text{m}] \qquad \text{Eq. 3.26}$$

$$m_{obs} = \frac{1}{n}\sum_{i=1}^{n} X_{obs} \qquad [\text{m}] \qquad \text{Eq. 3.27}$$

the standard deviations are calculated by the equations:

$$S_{cal} = \sqrt{\frac{1}{n}\sum_{i=1}^{n}(X_{cal} - m_{cal})^2} \qquad [\text{m}] \qquad \text{Eq. 3.28}$$

$$S_{obs} = \sqrt{\frac{1}{n}\sum_{i=1}^{n}(X_{obs} - m_{obs})^2} \qquad [\text{m}] \qquad \text{Eq. 3.29}$$

Correlation coefficients range in value from -1 to 1. The correlation coefficient determines whether two ranges of data move together –ie. whether large values of the other data set are associated with large values of the other data set (positive correlation), whether small values of one data set are associated with large values of the other data set (negative correlation), or whether values in both sets are unrelated (correlation near zero).

3.2.6.1 Parameter ESTimation (PEST)

PEST implements a nonlinear least-squares regression method to estimate model parameters by minimizing the sum of squared weighted residuals. The sum of squared weighted residuals, Φ, also is known as the objective function. Natural or man-made system can be described by the linear equation

$$\mathbf{Xb = c} \qquad \text{Eq. 3.30}$$

X is a *m* x *n* matrix. The elements of **X** are constant and hence independent of the elements of **b**, a vector of order *n* which, by assumption holds the system parameters. **c** is a vector of order *m* containing numbers which describe the system response to a set of excitations embodied in the matrix **X**, and for which we can obtain corresponding field or laboratory measurements used to infer the system parameters including **b**[3].

This "trustworthiness" is based on the consistency with which the *m* experimental measurements satisfy the *m* equations expressed by equation 2.1 when the *n* optimal parameter values are substituted for the elements of **b**.

Optimal parameters set is defined as the one with minimized sum of squared deviations between calculated and observed values; the smaller is this number (referred to as the "objective function") the greater is the consistency between model and observations and the greater is our confidence that the parameter has been correctly determined on the basis of field observations. Expressing this mathematically, we introduce Φ, defined as following:

$$\Phi = (c - Xb)^t (c - Xb_{est}) \qquad \text{Eq. 3.31}$$

where **c** now contains the set of laboratory or field measurements, the "t" superscript indicates the matrix transpose operation. The aim is to minimise Φ and the vector **b,** which minimises Φ, is

$$b_{theoretical} = (X_t X)^{-1} X^t c \qquad \text{Eq. 3.32}$$

Provided that the number of observations *m* equals or exceeds the number of parameters *n*, the matrix equation 2.4 provides a unique solution to the parameter estimation problem. Furthermore, as the matrix ($\mathbf{X}^t\mathbf{X}$) is defined as positive under these conditions, the solution is relatively easy to obtain numerically.

The vector $\mathbf{b}_{\mathbf{theoretical}}$ expressed by Eq. 3.32 differs from $\mathbf{b}_{\mathbf{est}}$ **(estmation)** of Eq. 3.31 (the equation which defines the system) in that the former is actually an estimate of the latter because **c** now contains measured data. In fact, $\mathbf{b}_{\mathbf{theoretical}}$ of equation 3.32 is the "best linear unbiased" estimator of the set of true system parameters appearing in equation 3.30. As an estimator, it is one particular realisation of the *n*-dimensional random vector **b** calculated, through equation 3.32.4, from the *m*-dimensional random vector **c** of experimental observations, of which the actual observations are but

[3] Note that for many problems to which PEST is amenable, the system parameters may be contained in **X** and the excitations may comprise the elements of **b**. Nevertheless, in the discussion which follows, it will be assumed, for the sake of simplicity, that **b** holds the system parameters.

one particular realisation**.** If σ^2 represents the variance of each of the elements of **c**, assumed to be independent, then σ2 can be estimated as

$$\sigma^2 = \Phi /(m - n) \qquad \text{Eq. 3.33}$$

where (m - n), the difference between the number of observations and the number of parameters to be estimated, represents the number of "degrees of freedom" of the parameter estimation problem. Equation 3.33 shows that σ^2 is directly proportional to the objective function and thus varies inversely with the goodness of fit between measured and calculated values.

Observation Weights

So far in the parameter estimation process all observations were assumed having same weight. However this will not always be the case, as some measurements may be more affect by experimental error than others.

Another problem arises where observations are diverse. However the units for these two quantities are different (kg/ha and dimensionless respectively); hence the numbers used to represent them may be of vastly different magnitude. Under these circumstances the quantity represented by the larger numbers will take undue precedence in the estimation process if the objective function is defined by equation 2.3; this will be especially unfortunate if the quantity represented by the smaller numbers is, in fact, measured with greater reliability than that represented by the larger numbers.

This problem can be overcome if a weight is supplied with each observation; the larger the weight pertaining to a particular observation the greater the contribution that the observation makes to the objective function. If the observation weights are housed in an m-dimensional, square, diagonal matrix **Q** whose i^{th} diagonal element q_{ii} is the square of the weight w_i attached to the i^{th} observation, equation 3.31 defining the objective function is modified as follows:

$$\Phi = (c - Xb)^t Q(c - Xb) \qquad \text{Eq. 3.34}$$

otherwise expressed as

$$\Phi = \sum_{i=1}^{m} (w_i r_i)^2 \qquad \text{Eq. 3.35}$$

where r_i (the i^{th} residual) expresses the difference between calculated and observed values for the i^{th} observation.

3.2.6.2 Sensitivity analysis

The purpose of sensitivity analysis is to quantify the uncertainty in the calibrated model caused by uncertainty in the estimates of aquifer parameters, stresses and boundary conditions. A sensitivity analysis is an essential step in all modelling applications.

During a sensitivity analysis, calibrated values for hydraulic conductivity, storage parameters, recharge and boundary conditions are systematically changed within the previously established plausible range. The magnitude of change in heads from the calibrated solution is a measure of the sensitivity of the solution to that particular parameter. The results of the sensitivity analysis are reported as the effects of the parameter change on the average measure of error selected as the calibration criterion. Ideally, the effect on the spatial distribution of head residuals is also examined.

Sensitivity analysis is typically performed by changing one parameter value at time. The effects of changing two or more parameters also might be examined to determine the widest range of plausible solutions. For example, hydraulic conductivity and recharge rate might be changed together so that low hydraulic conductivities are used with a high recharge rate and high hydraulic conductivities are used with a low recharge rate.

3.2.7 Model verification

Owing to uncertainties in the calibration, the set of parameters value used in the calibrated model may not accurately represent field values. Consequently, the calibrated parameters may not accurately represent the system under a different set of boundary conditions or hydrogeologic stresses.

Model verification will help establish greater confidence in the calibration. According to Konikow (1978), a model is verified “if its accuracy and predictive capability have been proven to lie within acceptable limits of error by tests independent of the calibration data”. In a typical verification exercise, values of parameters and hydrogeologic stresses determined during the calibration are used to simulate a transient response for which a set of field data exists.

4. CONSTRUCTION OF BRACCIANO MODEL

Groundwater flow model construction is the process of transforming the conceptual model into a mathematical form.

In order to perform this, the construction of a one layer mathematical model, using Visual Modflow software, was needed. The one layer model represents the groundwater flow in 2 dimensions. Bracciano Lake area together with the underlying aquifer are represented as a whole aquifer with a higher hydraulic conductivity compared to the surrounding areas.

A further step was to calibrate the result of the model (as presented in Chapter 5) and verify their closeness to reality/observations. In case of unsatisfactory results, the model structure was reviewed and changes introduced. The two models will be defined as VMF Bracciano model and GWV Bracciano model, or simply VMF model and GWV model from here on. All performed simulations are in steady state conditions.

Define the model domain, Define the model domain. Define initial conditions, boundary conditions, and hydraulic conditions, and the validity of their selection. Discuss any simplifying assumptions made to the conceptual model. Discussion should reference how the conceptual model is compatible with the modelling objectives and function. D 5718-2006 (ASTM).

4.1 MODEL GRID

The total study area is about 380 km^2.

The VMF Bracciano model is one-layer model, with 38000 active cells, 100 m grid size. The use of such grid is a reasonable approximation at a basin scale and is much more detailed scale considering the scale of the information held (topography, geology, recharge, withdrawal) for the study area. As reported in Refsgaard et al., 2010, for testing geological models are prescribed as 200-500 m, but for evaluation impacts from groundwater abstraction on water levels in wetlands and lakes 50-200 m is prescribed, using steady state models. The GWV Bracciano model is two-layer model, with 76024 active cells, 100 m grid size (as VMF Bracciano model).

4.2 HYDRAULIC PARAMETERS

Starting values of hydraulic conductivities were assigned to 8 areas of the VMF model, with an "homogeneous equivalent conductivity" identify in Section 2.3 (Fig. 2.25). These values took into account bibliographic values for volcanic deposits similar to Bracciano volcanic deposits and moreover they were compared to hydraulic conductivities resulting from the pumping tests.

The VMF Bracciano model initial best estimates of hydraulic parameter values and expected ranges are reported in Table 4.1. Once the hydraulic inputs were inserted, the VMF Bracciano model was calibrated and the resulting values were used as initial best estimates for hydraulic conductivities in GWV Bracciano model.

Table 4.1: Initial values of hydraulic conductivity and expected ranges.

Hydraulic conductivity m/s	***Description***	***Starting value***	***Range***
Kx1-Ky1 Kz1 $1*10^{-6}$	hydromagmatic products	$1* 10^{-5}$	$1*10^{-4}$ - $1*10^{-6}$
Kx2-Ky2 Kz2 $1*10^{-5}$	fractured lava and course tuff	$1*10^{-4}$	$1*10^{-3}$ - $1*10^{-5}$
Kx3-Ky3 Kz3 $1*10^{-8}$	clay and sandy clay sediments	$1*10^{-7}$	$1*10^{-6}$ - $1*10^{-8}$
Kx4-Ky4 Kz4 $1*10^{-6}$	different kinds of volcanic deposits, wide extension of tuff units	$1*10^{-5}$	$1*10^{-4}$ - $1*10^{-6}$
Kx5-Ky5 Kz5 $1*10^{-4}$	lake	$1*10^{-3}$	$1*10^{-2}$ - $1*10^{-4}$
Kx6-Ky6 Kz6 $1*10^{-7}$	different kinds of pyroclastic products, scoria cones and lava cones	$1*10^{-6}$	$1*10^{-5}$ - $1*10^{-7}$
Kx8-Ky8 Kz8 $1*10^{-7}$	different kinds of deposits: volcanic and fluvial - alluvial	$1*10^{-6}$	$1*10^{-5}$ - $1*10^{-7}$
Kx12-Ky12 Kz12 $1*10^{-7}$	stratified lava (dip into the lake)	$1*10^{-6}$	$1*10^{-5}$ - $1*10^{-7}$

4.3 MODEL BOUNDARY CONDITIONS

The model boundary conditions, as assigned in Bracciano model shown in Fig. 4.1, are:

1- Specific head or Dirichlet:
   a. in VMF Bracciano model, constant head at south was assigned along the 100 m a.s.l. piezometric line (elaborated from survey campaign of 2009).
   b. in GWV Bracciano model, constant head was assigned along the southern boundary of the model, each cell assumes a value extrapolated from piezometric surface (elaborated from survey campaign of 2009).

2- Specific flux or Neumann:
   a. NO FLUX all around the model border (except the southern part for GWV Bracciano model). The modelled area corresponds to an hydrogeologic basin, so it was

decided to consider it as a no flux boundary along all its perimeter, except in the southern part, where the volcanic aquifer feeds the sedimentary aquifer. There is an amount of water discharging from the Bracciano basin to south, hence in the southern part a specific head was assigned, as explained above.

3- Mixed or Chauchy:

a. assigned as DRAIN in correspondence of the model streams. In VMF Bracciano model identical conductance, assigned to all drains, was $2.11*10^{-4}$ m^2/s (considered as an acceptable value in the studied geologic context). In GWV Bracciano model the streams were divided initially in five "drain reach" groups, depending on their location and depending on their contribution to groundwater drainage. In this way it would be possible to compare the outflow from each drain reach to the observed flow, in the subsequent calibration step. An initial value of $2.11*10^{-4}m^2/s$ was assigned to the conductance of the five drain reach:

   i. *drain reach 0*: all streams eastward
   ii. *drain reach 9* streams with a centripetal direction, towards the lake (only in the northwest sector)
   iii. *drain reach 1*: streams with a centripetal direction, towards the lake
   iv. *drain reach 3*: streams toward southwest.
   v. *drain reach 2*: Arrone river and affluent streams

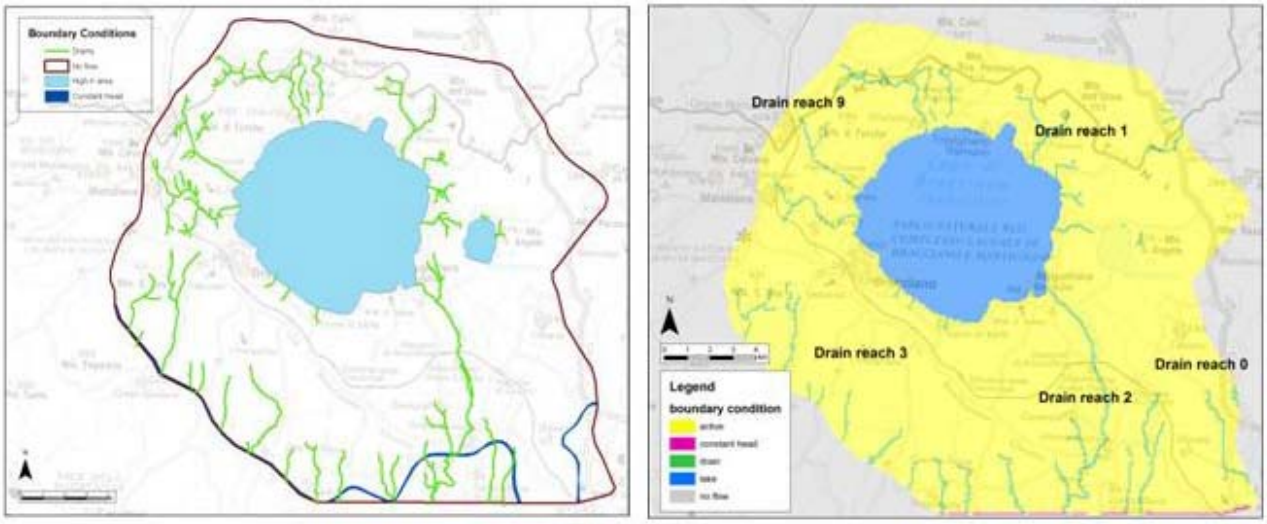

A **B**

Figure 4.1: **A**: VMF model boundary conditions; **B** GWV model boundary conditions

4.4 BRACCIANO LAKE

In VMF Bracciano model, the area occupied by Bracciano was represented as cells with higher hydraulic conductivity compared to other areas. Considering that VMF model is one-layer model the value of hydraulic conductivity was "composed" by the lake upper part and the volcanic underlying aquifer. Lake area has been represented as an aquifer characterized by a very high permeability (initial hydraulic conductivity value of 10^{-3} m^2/s). The representation of a lake as cells with a high hydraulic conductivity was reported in literature (Hunt et al., 2003; Hill et al., 1998), although in these studies, the presented models were composed by several layers.

In GWV Bracciano model, it was implemented the Lake Package. To all the cells within the Lake Bracciano perimeter were assigned a m a.s.l. value of Initial Lake Stage, Minimum and Maximum Stage; a m^2/s value of Hydraulic conductivity and a lakebed thickness (m). In the Fig. 4.2 there are all the initial inputs. The lake budget calculation, using Lake Package, starts from values that could be inserted in a spreadsheet:

- lake inflow: rain, runoff and stream baseflow,
- lake outflow: evaporation and withdrawal.

These volumes were taken from data exposed in Section 2.1.2.2 i.

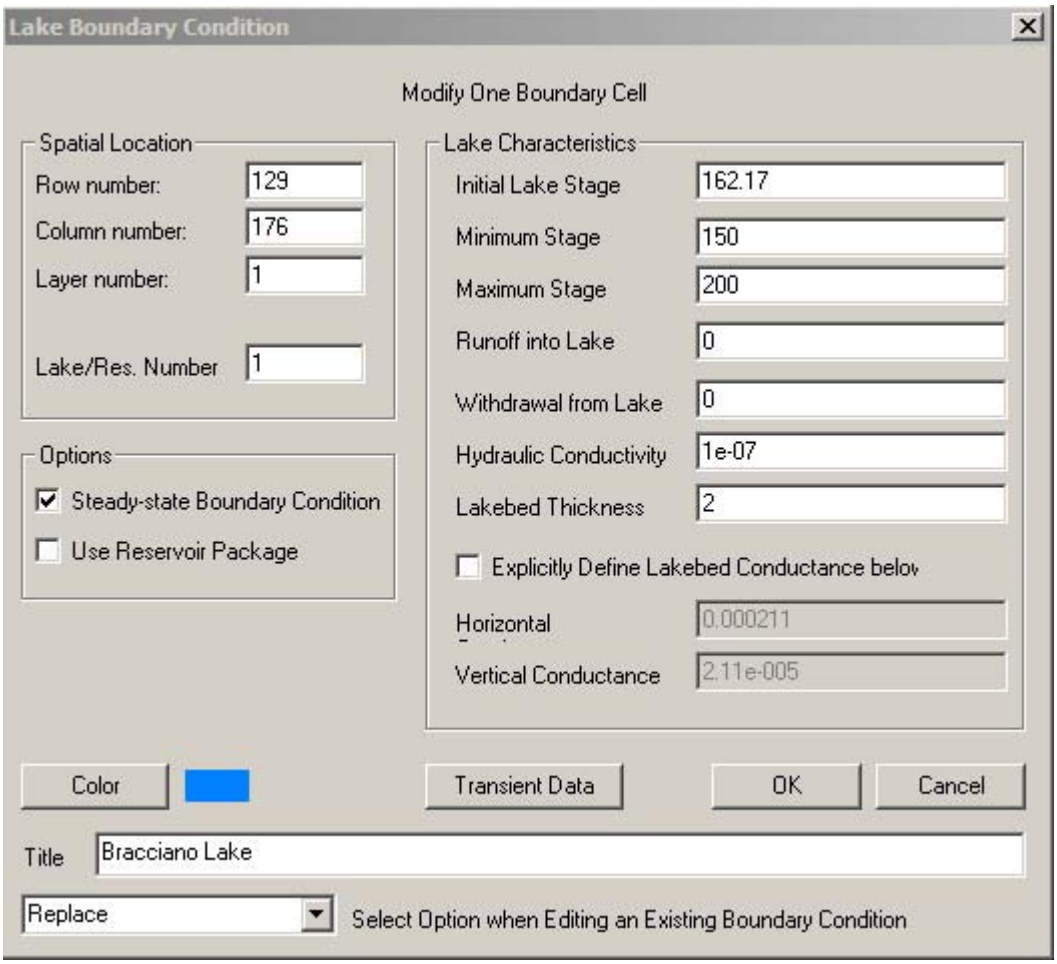

Figure 4.2: Lake boundary condition in Groundwater Vistas

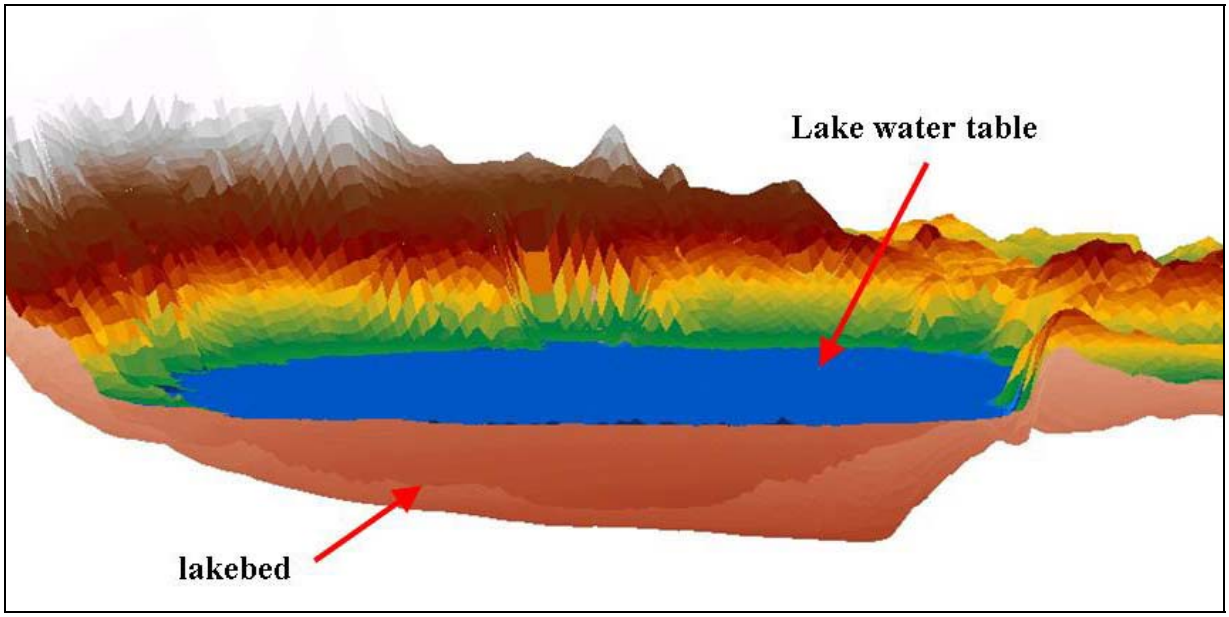

Figure 4.3 Lake view

An initial value of $1*10^{-7}$ m^2/s of lakebed hydraulic conductivity was inserted. Bottom sediments are very fine grained; therefore a reduced conductivity was attributed. In this study, it was not con-

sider “zonation” of the lakebed properties, suggesting higher K value along the shoreline, due to the presence of less finer sediments. The role played by the surface bottom break of slope to the aquifer-lake interaction requires a deeper investigation.

4.5 RECHARGE

The distributed recharge, calculated as reported in Section 2.1.2.1, was introduced in VMF model and GVW model. A different approach was then used by dividing the study area into 9 sub-basins (see Section 2.3.2) and for each area, an average recharge value was calculated (Table 4.2 and Fig. 4.4). For the Lake area see Section 4.3. This division was made to introduce these areas in the calibration process.

Table 4.2: Initial recharge values for the areas from 1 to 8

Zone	Recharge value (m/s)	Recharge value (m^3/s)
1	1.23E-08	4.51E-01
2	1.09E-08	4.90E-01
3	1.34E-08	1.63E-01
4	1.31E-08	2.14E-01
5	1.23E-08	7.48E-01
6	9.40E-09	9.14E-01
7	9.35E-09	4.94E-01
8	1.21E-08	9.07E-02
	TOTAL	3.56

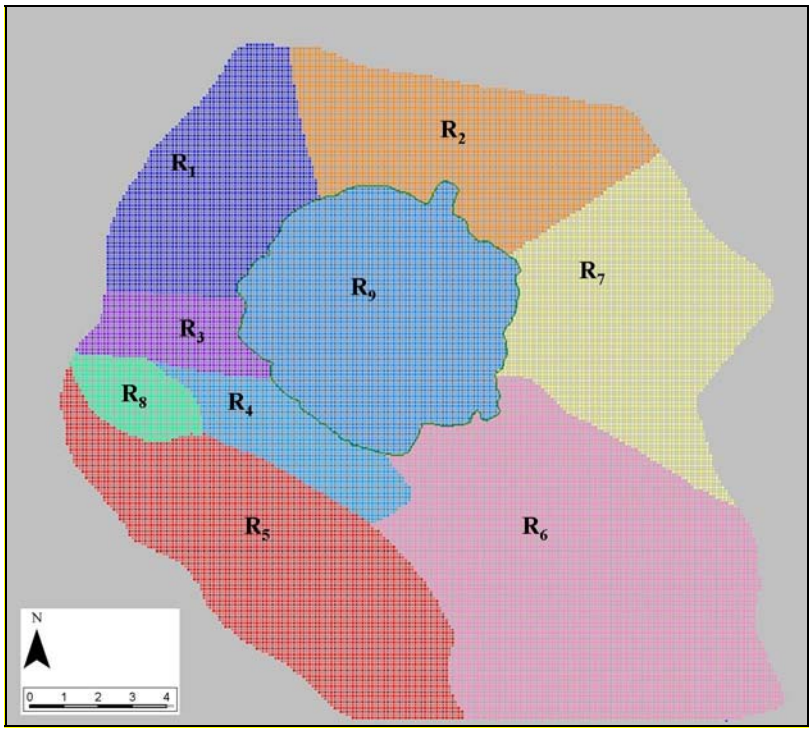

Figure 4.4: areas of calculated average recharge

4.6 WITHDRAWAL

All the information about abstraction on the study area where elaborated, as explained in Section 2.3.3 and were introduced in VMF and GWV model.

It should be pointed that withdrawal rate is negative in both VMF e GWV model, coherently with the modelling protocol in which every outflow from the system is indicated with negative values and every inflow to the system is indicated with positive values.

In the model should be entered all the necessary information, as screen top and bottom elevation, pumping rates, time (set as 1, in this steady state case), in Fig. 4.5 and 4.6 the screen shot relative to VMF and GWV model.

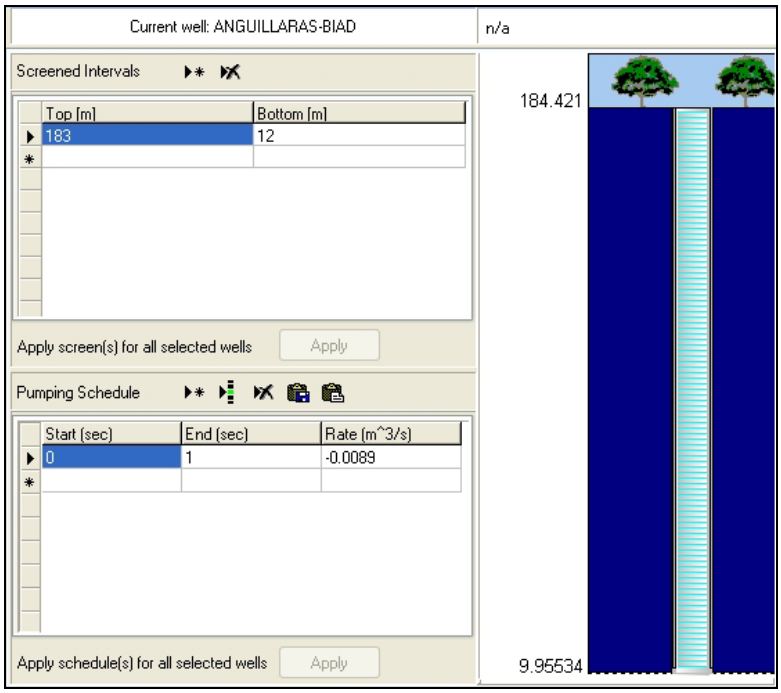

Figure 4.5: VMF pumping well screen shot

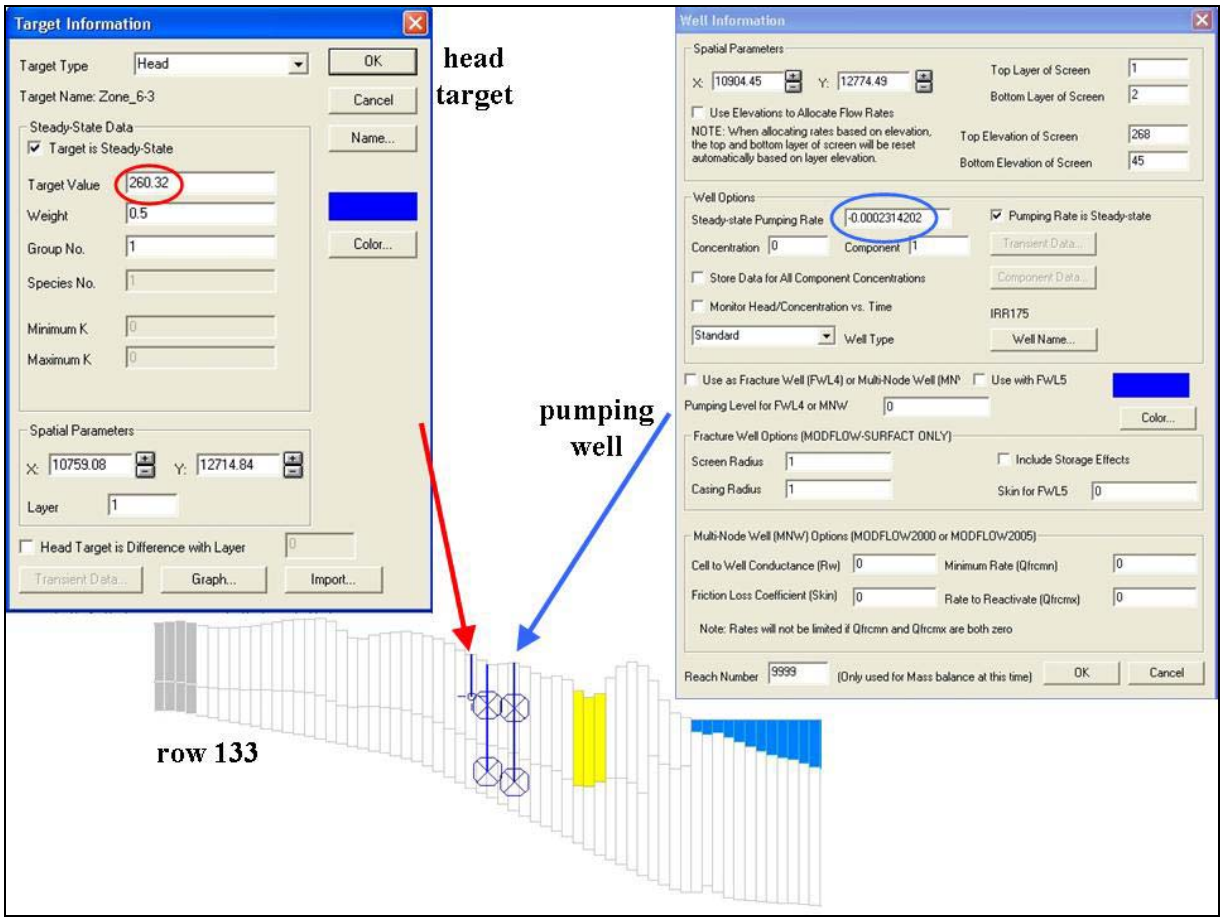

Figure 4.6: GWV section and screen shots

4.7 SELECTION OF CALIBRATION TARGETS

Wells, measured in 2009 survey campaign (see Fig. 2.20), were used as head targets in VMF model and in GWV model, in the latter the targets were distributed in both layers. Streams baseflow, measured in 2009 survey campaign (see Fig. 2.21), were used as flux targets in GWV model. Wells, measured in 2002 survey campaign (see Fig. 2.23), were used as head targets in VMF model, in the process of attempt a validation of the model.

The selected calibration targets for groundwater level, in VMF model, are shown in Tab. 4.3. In the zones 3 and 8 there are not calibration head target. In the case of zone 3, this is an “island” area of low sediments outcrop, so there are no wells known in that area. In the zone 8 unfortunately no information was achieved. Due to this lack of information, less importance was attribute to them during the calibration process.

Table 4.3: Number of targets used for the model calibration and their percentages

Hydrostratigraphic unit	K denomination	Group name	Number of head targets selected for calibration	Distribution of targets by sub-area (%)	Distribution of targets by unit (%)
Hydromagmatic products	K1	U1	18	14.2	14.2
Fractured lava and course tuff	K2	U2	22	17.3	
	K2	U3	34	26.8	44.1
Clay and sandy clay sediments	K3		0	0.0	0.0
Different volcanic deposits, wide extension of tuff units	K4	U8	4	3.1	
	K4	U9	5	3.9	
	K4	U10	5	3.9	
	K4	U5	7	5.5	16.5
Lake	K5	U11	22	17.3	17.3
Different pyroclastic products, scoria cones and lava cones	K6	U7	7	5.5	5.5
Different deposits: volcanic, fluvial and alluvial	K8		0	0.0	0.0
Stratified lava (dip into the lake)	K12	U6	3	2.4	2.4
TOTAL NUMBER OF HEAD TARGET			127	100.0	100.0

4.7.1 Uncertainty Determination

The methodology suggested by Sonnenborg & Henriksen (2005) was applied to determine the uncertainty of observational data, the purpose of quantifying the uncertainty of observational data (σ_{obs}) is to achieve a measure of how accurately the model reproduce the data. This may in principle be an objective criterion for how data weighted approximation and more importantly, how data of different types must be relatively weighted (important when using objective functions).

In Table 4.8 the sources of uncertainty in the head level observations are reported and also the relative values calculated for Lake Bracciano basin. It was chosen to consider the amount of uncertainty for the entire basin, as a "general situation" and then two different areas of calculation were considered in relation to their peculiar hydraulic behaviour; North-west and South areas.

Survey error

- **Measurement error**: can be linked to the pressure transducers; to manual reading of the measured water level or in drilling deviating from the true value in the aquifer due to partial clogging around the filter, etc. All together the measurement errors, were quantified as **5-30 cm**.
- **Elevation error** the error due to topographic elevation determined from a topographic map. If topographic elevation is determined using differential GPS uncertainties will typically be of magnitude of centimetre. In the case study the topographic map scale is 1:10000; the intervals between contour lines be 10 m, with a precision of 2 m, considering the bore approximate location, the aggregate standard deviation at measuring point quota be around **3-5 m.**

Scale error

Scale effects lead to an additional uncertainty in the data. Scale effects occur because finite size numerical cells are used to describe the continuous physical reality. The error will depend on factors as filter length, the vertical discretization and geological structure of the aquifer. They have been subdivided in:

- interpolation error: topography variation within the numerical cells can give rise to discrepancies between observed and simulated head level. Scaling errors related to well position, that may be located randomly within the 100 m^2 model grid. This error takes in consideration the model scale and the water table trend. This error is estimated as a typical hydraulic gradient multiplied by half the grid size;

- **geological heterogeneity:** geological heterogeneity has a decisive influence on simulation of groundwater flow. The fundamental question is how to deal with this heterogeneous reality as it is necessary to develop quantitative descriptions of flow in large-scale aquifer systems. More specifically, we would like to know how to find appropriate average parameters which can be applied to large-scale flow models and at the same time, these parameters could be able to influence of unmodelled heterogeneity on the quality of predictions from such models. Such evaluations of the reliability of the large-scale models are necessary if we are to realistically portray the predictive capabilities of groundwater flow models (Gelhar, 1986).

Two issues that have had a high profile since the mid-1970:

- which value could have an equivalent (effective) hydraulic conductivity, which can represent the integrated effect of a heterogeneous media;
- how to propagate the uncertainty due to the geologic heterogeneity (consider in the equivalent hydraulic conductivity) to the uncertainty in water table head.

Scaling error are due to geological heterogeneity within a model grid. Heterogeneity, which can not be mapped and hence not included directly in the model will cause a significant proportion of the

total deviation between observed and simulated head level. Uncertainty in head level is not only due to modelled heterogeneity, but is also a function of the gradient of the hydraulic pressure level variances, of log transform hydraulic conductivity and correlation length. The question, however, is where large deviations in the medium can be expected between observed and simulated head level in the individual measuring points? For instance, how large Root Mean Squared of the residuals (observed head minus simulated head) can be expected because heterogeneity has not been modelled. This has practical relevance in precision of a groundwater model.

However, it is possible to quantify this error, if statistical information are available on hydraulic conductivity (K) of the modelled area. According to Gelhar (1986), heterogeneity error σ_h^2 ,to be assessed as the autocorrelation length scale for log K multiplied to the standard deviation of log K and the average hydraulic gradient. It is necessary to have values for the correlation length (λ) and for lnK, $\sigma_{\ln K}^2$. These values can rarely be obtained for a specific area, but using the empirical values (Gelhar, 1993) it is possible to make guess on lnK geostatistical characteristics.

$$\sigma_h^2 = C \times \sigma_{\ln K^2} \times \lambda^2 \times J^2 \qquad \text{[m]} \qquad \text{Eq. 4.1}$$

Where:

$\sigma_{\ln K^2}$ is the standard deviation of log K;

λ is the hydraulic conductivity (K) correletion lenght

J is the hydraulic gradient

and with $C = 0.37 \ln\left[1.21 B / J\lambda\right]$ [dimensionless] for a 2D free aquifer Eq. 4.2

where B is the thickness of the free aquifer and J is the hydraulic gradient;

or $C = 0.46$ [dimensionless] for a 2D artesian aquifer Eq. 4.3

To evaluate the heterogeneity component error in the case of Bracciano Lake basin, it was used the equation related to a free aquifer (4.2). It was calculated the heterogeneity scale error considering three different cases: a general one, consisting in the evaluation of the entire Bracciano basin, and a focus on two areas with a "homogeneous" hydraulic behaviour, the northwest and the south. Values of the hydraulic gradient and of average thickness of the aquifer inserted in the calculation are shown in Table 4.7 are shown. The problem arise with λ and σ component, since it was not found sufficient experimental information about these values for volcanic contexts, so were taken as "good" the values proposed by Gelhar (1993) for an alluvial aquifer. The deposit sequence of sand,

clay and gravel could be consider as “similar” to the volcanic sequence deposits. Considering the scale of the model it was assigned a value to the correlation length of 480 m and a σ (slnK) of 0.7.

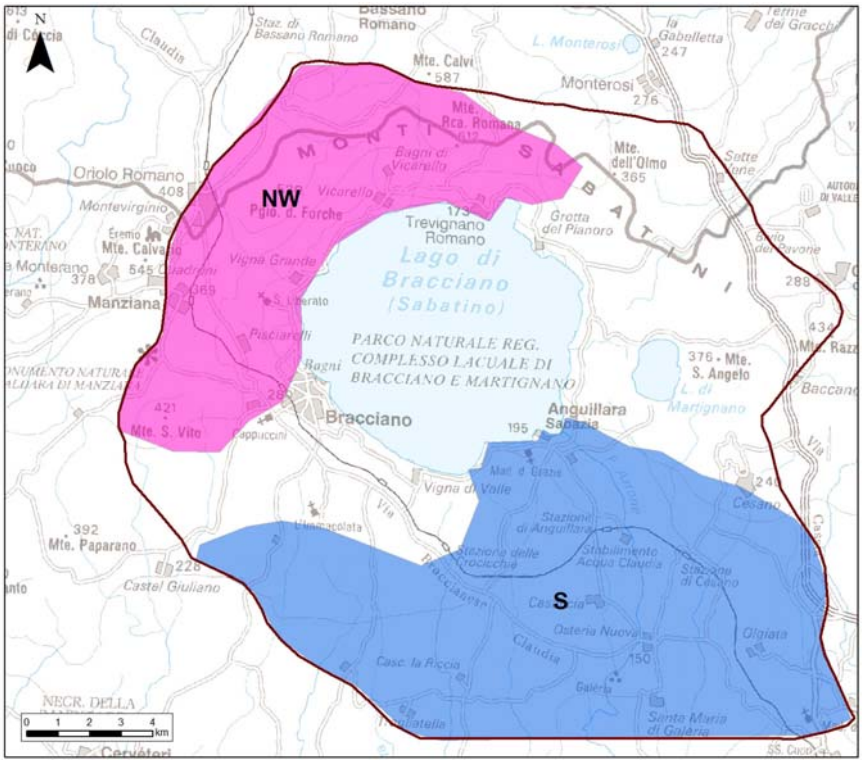

Figure 4.7: Schematic map with the indication of the two identified areas, where the uncertainty has been evaluated.

Table 4.4 – Calculation of the component of error due to the heterogeneity

Zone	B	J	λ	C= 0.37ln[1.21*B/J*λ]	σ= (SlnK)	Heterogenity scale error
Unit	**m**	**dimensionless**	**m**	**dimensionless**	**m**	**m**
NW	150	0.0424	480	**0.810**	0.7	12.817
S	80	0.0116	480	**1.058**	0.7	3.996
general situation	100	0.0187	480	**0.962**	0.7	6.164

B is the mean thikness of the aquifer in the consider area

J is the hydraulic gradient

σ is the standard deviation of log K. λ is the correlation lenght of log K. C is a constant whose value dipends from the flow system

Time scale effects

-**Error due to non-stationarity.** Observed data belong to different seasons. The time scale effects can be a source of error when using a stationary groundwater model. Use of observational data, which represent non-stationary state, in a a stationary model will result in discrepancies between observed and simulated head level that cannot be eliminated. If the time series of head level measurements were available, data can be analyzed and a value that represents the stationary state can be calculated. This allows the non-stationary error to be minimized to a level which is determined by time series length and by the analytical method used. In many cases, however, there is only a single or a few measurements available from most of the installed wells, and in this cases it will be difficult to filter the non-stationary power off. The seasonal variations will affect the data with considerable uncertainty, which can be quantified using time series of pressure level measurements from this region. This allows an estimate of the seasonal variations and hence the uncertainty of the data points are estimated. The error may be assessed as half the typical annual fluctuation. In the study cases, from the analysis of data it was estimated the value of **0.75** m.

Table 4.5: Summary of the estimated uncertainties

		Survey errors		Scale effect errors		Non stationarity errors		Overall Uncertainty S_{obs}	Accurancy requirements RMS	Criterion comparison
Zone	**Δx**	**Measura-ment**	**Eleva-tion**	**Interpola-tion**	**Heterogeneity**	**Seasonal variations**	**Other effects**	**$\sqrt{\sum}\square s^2$**		**$\sqrt{\sum}\square s2 * \beta2$**
	m	**m**	**m**	**0.5*Δx*J [**	**$C^{1/2}\lambda_{slnk}J$ [m] 1)**	**Δht/2 [m] 2)**	**m**	**m**	**dimensionless**	**m**
NW	100	0.15	5	2.12	12.82	0.75	0.75	13.96	(β2 = 2.5)	34.90
S	100	0.15	2	0.58	4.00	0.75	0.75	4.63	(β2 = 2.5)	11.58
general situation	100	0.15	5	0.94	6.16	0.75	0.75	8.06	(β2 = 2.5)	20.16
$\square s^2 = \Delta x^2$ + (Measurament Err)^2 + (Elevation Err)^2 + (Interpolation Err)^2 + (Heterogeneity Err)^2 + (Seasonal Variation Err)^2 + (Other Effects Err)^2										
2) Δht indicates the amplitude of seasonal variations in hydraulic pressure level										

The table 4.5 shows that the heterogeneity error is by far the most dominating error source in the presented model, furthermore, NW has a much higher overall uncertainty compared to S, that is due to the higher hydraulic gradient.

4.7.2 Numerical criteria

The performance criteria were chosen to reflect the objectives of the model, i.e. to simulate the hydraulic heads in different places, and to test if the numerical model could fulfil those criteria during validation processes using data not introduced in the calibration.

The criteria chosen arel:

Criterion 1. Head level criterion, based on the mean error. Mean error of the head (ME), related to the maximum variation in the observed heads within the model or sub models selected.

$$ME = \frac{1}{n}(X_{obs,i} - X_{cal,i}) \qquad \text{[m]} \qquad \text{Eq. 4.4}$$

$$\text{with} \quad \left| \frac{ME}{\Delta h_{\max}} \right| \leq \beta_1 \qquad \text{[dimensionless]} \qquad \text{Eq. 4.5}$$

where:

$X_{obs,i}$ is the head observed,

$X_{sim,i}$ is the head simulated,

$\Delta h_{\max}$ is the difference between the maximum and the minimum head observed and

β_1 is the reference value (see Table 4.6)

Criterion 2. Head level Criterion that relate to the RMS overall uncertainty (σ obs). The criterion requires a specific assessment of both, stationary and transitory state.

$$RMS = \sqrt{1/n} \sum_{i=1}^{n} (X_{obs,i} - X_{cal,i})^2 \qquad \text{[m]} \qquad \text{Eq. 4.6}$$

$$\text{with} \qquad RMS/\sigma_{obs} \leq \beta_2 \qquad \text{[dimensionless]} \qquad \text{Eq. 4.7}$$

where:

σ_{obs} is the total uncertainty of observational data and

β_2 is the reference value (see Table 4.6)

Criterion 4. Head level criterion, based on the variation of head for the model area

$$RMS/\Delta h_{\max} \leq \beta_4 \qquad \text{[dimensionless]} \qquad \text{Eq. 4.8}$$

where:

$\Delta h_{\max}$ is the difference between the maximum and the minimum head observed and

β_4 is the reference value (see Table 4.6)

In Table 4.6 the proposal reference values in relation to the model approach, as reported in Refsgaard et al., 2010, these performance criteria are recommended values based on experiences mostly from Denmark. Different objectives are listed and different ambitions are related to different model detail: screening/basic, estimate calculation/intermediate and detailed modelling/high. Values of B_1, B_2 and B_4 have been proposed by the same authors and in this work of study, it was consider the model to go for screening model ambition, as already mentioned in the beginning of this chapter.

Since criterion 2 require the most rigorous evaluation of the single terms that influence the performance of the model e.g. measurement errors of observations, grid size, seasonal variations, heterogeneity etc. it gives the best feedback to the modeller about what can be expected. Numerical criteria should always be evaluated based on the available data, quality of data, heterogeneity, topographical variability etc. There will always be subjectivity in evaluation of performance criteria. Beside the numerical criteria, qualitative criteria are equally important to include in the full evaluation of model performance

Table 4.6: Numerical targets accuracy (requirement values for the beta) (Refsgaard et al., 2010)

	SCREENING	***ESTIMATE CALCULATION***	***DETAIL MODELING***
CRITERION 1 β_1	0,05	0,025	0,01
CRITERION 2 β_2	**2,6**	**2**	**1,65**
CRITERION 4 β_4	0,1	0,05	0,025

5. CALIBRATION

In the first part of this chapter the theme will be on the VMF Bracciano model calibration, the steps followed to arrive to a calibrated model will be explained. The second part of the chapter will deal with the GWV Bracciano model calibration. The calibration approach presented has different characteristics in the two models presented.

In the two models two different approaches have been used: in VMF model the focus was put on the method proposal to compare the results with the uncertainty and performance criteria estimation (with all the themes related to it, like the heterogeneity role in the uncertainty extimation, ecc.)

In the GWV model the focus is on the lake package implementation, with focus on the lake budget. Here it was necessary to review and update the conceptual model to better understand the quantification of several terms of the budget. Another aspect that was considered with the second model was the introduction of flux targets as part of the inverse model calibration (PEST) and the estimation of the weight for the targets (targets with different unit) in the objective function.

5.1 VMF BRACCIANO MODEL CALIBRATION AND TENTATIVE VALIDATION

5.1.1VMF Bracciano model, steps followed

- First step. Simulation of the model with hydraulic parameters (conductivities K) *starting values*.

The observation dataset refers to 2009 measurements. The number of observation points for the model area was 127. These points were divided into observation data groups, as explained in Section4.7. Fig 5.1 shows the distribution of the observation points in the area; they are much more concentrated in the southern area (U2-U3 group). The water level of Lake Bracciano is monitored by a hydrometric station placed near the town of Anguillara. To consider the entire lake area, 22 observation points were arbitrarily distributed along the lake perimeter.

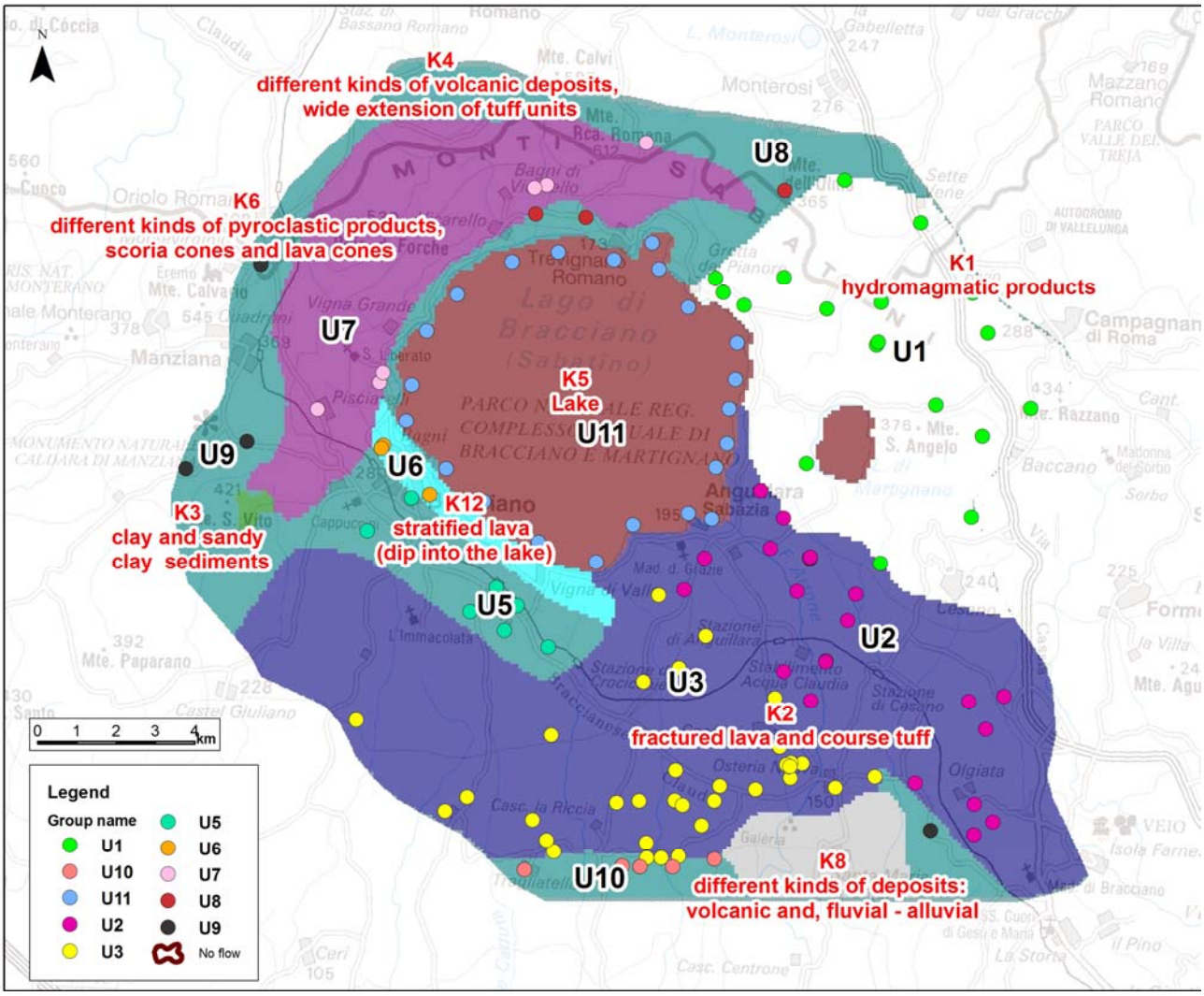

Figure 5.1: observation points divided into subgroups (U1-U11).

The results from the first step of the model setup and calibration process are shown in Table 5.1. The root mean square residual values (RMS) range from 14.30 m for the "Lake" group to 45 m for the U6 group. Considering criteria 1 and 2, described in Section 4.7.2, the first criterion is far from satisfied; only the values of the U5-U8-U9-U10 groups are acceptable for a screening model. A screening model based on a steady state groundwater flow model, e.g. a rather low ambition for the testing of the model performance, has been chosen, since the purpose is to describe the characteristics of the groundwater flow system in order to test the data, geological interpretations, assumptions about processes and model structures (Brown, 1992). The other values are higher. Refsgaard et al. (2005) distinct between (1) basic (rough calculations), (2) intermediate (moderately complex calculations) and (3) comprehensive (sophisticated, detailed calculations). A screening model viewed from this terminology is comparable to (1) basic (rough calculations).

Criterion 2 is satisfied for all the groups; this is due to the fact that uncertainty is very high (owing to geologic heterogeneity).

The output values for the Lake Bracciano level range between 177.31 and 173.94 m, as against an average level for the year 2009 of 162.17 m above sea level (a.s.l).

Table 5.1: calibration statistics report (first simulation)

								Crit 1 β1 < 0.05			Crit 2 β2 <2.5		Crit 4 β4<0.10	
Group_New	Number of head targets selected for calibration	Delta h max	Max Residual (m)	Min Residual (m)	Abs. Residual Mean (m)	Residual Mean (m)	ME/dH_{max}	RMS Root Mean Squared (m)	S_{obs} Overall Uncertainty *	RMS/S_{obs}	Standard Error of the Estimate (m)	RMS/dH_{max}	Correlation Coefficient
U1	**18**	99	-61.27	-1.97	20.80	-4.24	**0.043**	**27.80**	20.16	**1.379**	6.66	**0.281**	0.172
U11	**22**	0	15.14	11.77	14.28	14.28		**14.30**	20.16	**0.709**	0.18	**1.000**	0.000
U2	**22**	65	17.19	0.99	7.51	5.35	**0.082**	**8.76**	11.58	**0.756**	1.51	**0.134**	0.961
U3	**34**	64	52.41	2.35	18.38	18.22	**0.285**	**22.72**	11.58	**1.962**	2.36	**0.355**	0.695
U5	**7**	37	31.74	-1.58	9.07	6.17	**0.167**	**13.38**	20.16	**0.664**	4.85	**0.361**	0.591
U8	**4**	234	33.00	12.85	22.03	11.43	**0.049**	**23.17**	34.90	**0.664**	11.64	**0.099**	0.994
U9	**5**	233	35.77	-0.89	15.12	12.30	**0.053**	**21.81**	20.16	**1.082**	9.01	**0.094**	0.981
U10	**5**	13	50.82	-1.79	20.88	20.16	**1.551**	**26.67**	20.16	**1.323**	8.73	**2.072**	0.296
U6	**3**	7	50.44	32.97	44.22	44.22	**6.318**	**44.94**	20.16	**2.229**	5.64	**7.088**	0.168
U7	**7**	147	-41.00	8.16	20.84	2.13	**0.014**	**23.78**	34.90	**0.681**	9.67	**0.161**	0.927
TOTAL	**127**	291	-60.75	-0.89	16.45	10.82	**0.037**	**21.19**	20.16	**1.051**	1.62	0.073	0.932
*** values taken from the table 4.5, respectively for northwest area, south and for the general situation**													

With regard to the mass balance, in the outflow volume, the drains reach a value of 1.136 m3/s, which is considered to be too high with respect to the collected field data (the value of all the out-flows of the stream network of the area is around 0.74 m3/s, see Fig. 5.3) .

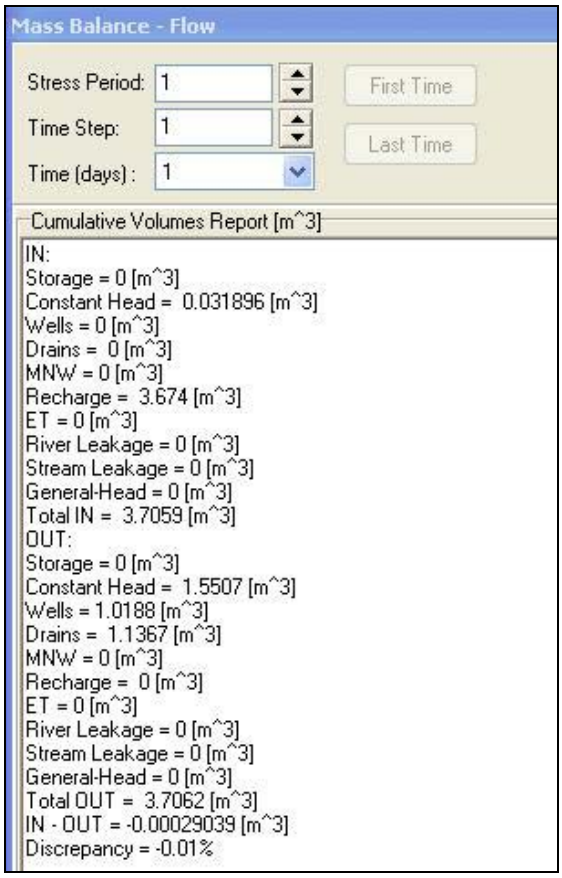

Figure 5.2: Mass balance in the first simulation

- Second step. In this step, use was made of PEST to calibrate hydraulic conductivities by automatic calibration (inverse modelling). The calibration was carried out by considering groups of two hydraulic conductivities together, starting from the K values pertaining to the starting model. Table 5.2 displays the results. The RMS values lie between 3.34 m for the "Lake" group and 28.29 m for the U1 group; the range of values was narrowed down with respect to the first step. Criterion 1 is satisfied for U1, U2, U8, U9, U7 and for the overall model and acceptable for a screening model / basic model (rough calibrations). The other values are higher than those required for criterion 1.
Criterion 2 is again satisfied for all the groups. In this second step, the output values for the Lake Bracciano level range between 166.6 and 162.65 m a.s.l., and the value of the outflow volume from the drains (0.624 m3/s) is closer to the measured one (Chapter 2) . Criterion 4 was improved for the overall model and for some of the sub-areas.

Table 5.2: calibration statistics report (second simulation)

							Crit 1 β1 < 0.05			Crit 2 β2 <2.5		Crit 4 β4<0.10	
Group_New	**Number of head targets selected for calibration**	**Delta h max**	**Max Residual (m)**	**Min Residual (m)**	**Abs. Residual Mean (m)**	**Residual Mean (m)**	**ME/dH$_{max}$**	**RMS Root Mean Squared (m)**	**S$_{obs}$ Overall Uncertainty ***	**RMS/ S$_{obs}$**	**Standard Error of the Estimate (m)**	**RMS/dH$_{max}$**	**Correlation Coefficient**
U1	**18**	99	-60.75	0.86	20.80	-2.32	**0.023**	**28.30**	20.16	**1.404**	6.84	**0.286**	0.292
U11	**22**	0	4.43	0.48	3.20	3.20		3.34	20.16	**0.166**	0.22	**1.000**	0.000
U2	**22**	65	-15.94	-1.37	5.39	-3.26	**0.050**	**6.56**	11.58	**0.567**	1.24	**0.101**	0.964
U3	**34**	64	41.30	0.16	11.26	9.33	**0.146**	**15.75**	11.58	**1.361**	2.21	**0.246**	0.691
U5	**7**	37	-30.64	-9.27	19.74	-19.74	**0.534**	**21.22**	20.16	**1.052**	3.17	**0.572**	0.791
U8	**4**	234	-37.68	-1.00	20.68	1.34	**0.006**	**26.59**	34.90	**0.762**	15.33	**0.114**	0.978
U9	**5**	233	15.83	4.01	9.15	4.94	**0.021**	**10.58**	20.16	**0.525**	4.68	**0.045**	0.997
U10	**5**	13	41.83	-2.27	15.37	14.46	**1.112**	**20.86**	20.16	**1.035**	7.52	**1.621**	0.269
U6	**3**	7	6.77	-0.16	3.05	2.94	**0.420**	**4.11**	20.16	**0.204**	2.03	**0.649**	0.258
U7	**7**	147	42.96	-2.28	18.83	-5.82	**0.040**	**25.59**	34.90	**0.733**	10.17	**0.173**	0.907
TOTAL	**127**	291	-60.75	-0.16	11.33	1.61	**0.006**	17.22	20.16	**0.854**	1.53	**0.059**	0.940
*** values taken from the table 4.5, respectively for northwest area, south and for the general situation**													

- Third step. Starting from the K values resulting from the second step, a PEST calibration was run on six parameters together (Kxy1; Kxy2; Kxy4; Kxy5; Kxy6; Kxy12). During this step, PEST was run multiple times and a "weight" was also introduced into the observation groups. In particular, a higher weight was associated with the "Lake" group, forcing the lake level observations so that the model would better compare with the lake water table and the effects on parametrisation could be assessed. The results from this step are shown in Table 5.4 below. The RMS values are more or less the same as in the second step; only the Lake group values decrease. The values for the Lake Bracciano level range between 163.42 and 162.84 m a.s.l, and the outflow volume from the drains (0.699 m3/s) is closer to the actually observed data, as noted in the second step.

Table 5.4 displays both the initial and the calibrated parameter values, which fall within the expected ranges and are consistent with a volcanic setting, Ky are maintained 1 order lower than Kxy.

Table 5.3 – Calibration statistics report (third simulation)

							Crit 1 β1 < 0.05			Crit 2 β2 < 2.5		Crit 4 β4<0.10	
Group_New	**Number of head targets selected for calibration**	**Delta h max**	**Max Residual (m)**	**Min Residual (m)**	**Abs. Residual Mean (m)**	**Residual Mean ME (m)**	**ME/dH$_{max}$**	**RMS Root Mean Squared (m)**	**S$_{obs}$ Overall Uncertainty ***	**RMS/ S$_{obs}$**	**Standard Error of the Estimate (m)**	**Normalized RMS (%)**	**Correlation Coefficient**
U1	**18**	99	-61.27	0.23	20.41	-3.15	**0.032**	**28.37**	20.16	**1.408**	6.84	0.287	0.305
U11	**22**	0	1.25	0.67	1.08	1.08		**1.09**	20.16	**0.054**	0.03	1.000	0.000
U2	**22**	65	-16.04	0.85	5.62	-3.85	**0.059**	**6.83**	11.58	**0.590**	1.23	0.105	0.965
U3	**34**	64	40.39	-0.18	10.77	8.44	**0.132**	**15.25**	11.58	**1.317**	2.21	0.238	0.689
U5	**7**	37	-32.45	-11.21	21.33	-21.33	**0.576**	**22.69**	20.16	**1.126**	3.16	0.612	0.798
U8	**4**	234	36.83	-3.87	18.66	1.93	**0.008**	**23.80**	34.90	**0.682**	13.69	0.102	0.979
U9	**5**	233	18.82	-5.47	12.69	7.88	**0.034**	**13.85**	20.16	**0.687**	5.70	0.059	0.998
U10	**5**	13	41.10	-3.13	15.16	13.91	**1.070**	**20.47**	20.16	**1.015**	7.51	1.590	0.275
U6	**3**	7	4.50	0.01	2.24	0.76	**0.109**	**2.90**	20.16	**0.144**	1.98	0.457	0.285
U7	**7**	147	47.08	1.08	18.93	-5.17	**0.035**	**25.16**	34.90	**0.721**	10.05	0.170	0.911
TOTAL	**127**	291	-61.27	0.01	10.89	0.81	**0.003**	**17.03**	20.16	**0.845**	1.52	0.059	0.941
*** values taken from the table 4.5, respectively for northwest area, south and for the general situation**													

Table 5.4: initial vs. calibrated parameter values

STEP	*FIRST*	*SECOND*	*THIRD*
Kx1-Ky1 m/s	**$1*10^{-5}$**	**$5.82*10^{-6}$**	**$5.72*10^{-6}$**
Kx2-Ky2 m/s	**$1*10^{-4}$**	**$1.69*10^{-4}$**	**$1.77*10^{-4}$**
Kx3-Ky3 m/s	**$1*10^{-7}$**	**$1*10^{-7}$**	**$1*10^{-7}$**
Kx4-Ky4 m/s	**$1*10^{-5}$**	**$2.47*10^{-5}$**	**$2.56*10^{-5}$**
Kx5-Ky5 m/s	**$1*10^{-3}$**	**$1*10^{-3}$**	**$7.69*10^{-3}$**
Kx6-Ky6 m/s	**$1*10^{-6}$**	**$5.26*10^{-7}$**	**$4.78*10^{-7}$**
Kx8-Ky8 m/s	**$1*10^{-6}$**	**$1*10^{-6}$**	**$1.67*10^{-5}$**
Kx12-Ky12 m/s	**$1*10^{-6}$**	**$6.59*10^{-6}$**	**$6.46*10^{-6}$**

Some points can be summarised based on the results of the calibration process:

- The RMS values of the U1 group in the three steps show that the change in Kx-y1 does not affect the residuals values; the RMS values in the three steps do not vary. This finding was in some way "expected". In effect, the simplified representation of one aquifer related to all volcanic deposits does not consider the occurrence of a perched aquifer as in Camponeschi and Lombardi (1968) and Capelli et al., 2005 (containing Lake Martignano and covered by hydromagmatic deposits) in the southern area. Most of the head values measured in this area are related to very shallow wells which draw water from the perched aquifer which was not taken into consideration. Therefore, it was not the purpose to obtain a satisfactory performance in head values for this area.
- The lake area is very important for several reasons, including the general public interest in the conservation of Lake Bracciano. The calibration was aimed at reaching a decrease in the RMS values of the Lake observation data in order to have a good performance for the lake area. Actually, the values passed from 14.28 m in the first step to 1.09 m in the third one.

From Table 5.1 to Table 5.3, the values for the overall model decrease as follows: from 0.037 to 0.003 (< criterion 1: 0.05), from 1.05 to 0.845 (< criterion 2: 2.5) and from 0.073 to 0.059 (< criterion 4: 0.1). For some of the sub-areas (RMS/Sobs), the values are above 1 but in general quite satisfactory. The normalised RMS value for the overall model is acceptable; however, for some of the sub-areas, the required criterion (0.010) is far from satisfied.

Table 5.5: Mass balance values in the three steps

	Mass Balance (m^3/s)					
FIRST STEP	IN Recharge	IN Constant head	IN Wells	IN Drain	IN ET	IN TOTAL
	3.674	3.19E-02				3.7059
	OUT Recharge	OUT Constant head	OUT Wells	OUT Drain	OUT ET	OUT TOTAL
		1.5507	1.0188	1.1367		3.7062
SECOND STEP	IN Recharge m3	IN Constant head m3	IN Wells	IN Drain	IN ET	IN TOTAL
	3.6421	3.55E-02				3.6776
	OUT Recharge	OUT Constant head	OUT Wells	OUT Drain	OUT ET	OUT TOTAL
		2.0021	1.0516	0.6241		3.6779
THIRD STEP	IN Recharge m3	IN Constant head m3	IN Wells	IN Drain	IN ET	IN TOTAL
	3.653	8.75E-02				3.7406
	OUT Recharge	OUT Constant head	OUT Wells	OUT Drain	OUT ET	OUT TOTAL
		2.0181	1.0178	0.7057		3.7416

Table 5.5 shows the mass balance results from the three-step model. The outflow values from the drains vary from 1.1367 m3/s in the first simulation to 0.706 m3/s in the third one; the last value appears to be consistent with the measured values. Fig. 5.3 indicates the location of the discharge stations whose flows were measured in the 2009 survey; summing all the flow values measured in the streams, the total amount is around 0.740 m3/s.

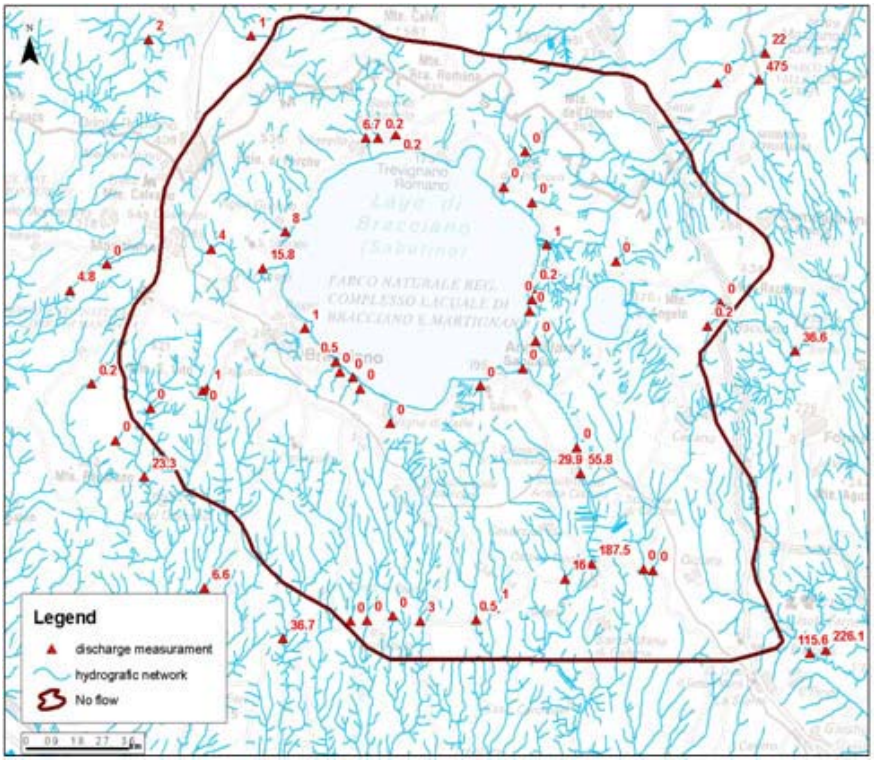

Figure 5.3: location of discharge stations whose flow was measured in the 2009 survey

The calibration process included several water budget zones where the model calculated the flow rate. Fig. 5.5 shows the inflows that the Lake Zone receives from the other zones; zone 10 provides the highest contribution. The flows from the eastern and western zones to the Lake are minimum (negligible?) and zone 12 receives the flow from the Lake. Zones 13 and 14 were introduced in order to quantify the outflow from the basin to its southern boundary.

The zone budget results indicate that the flow direction is consistent with the one of the conceptual model. The water mainly flows from the northern part of the basin to the lake and from the lake to the southern part of the basin. There is an amount of water stored in the lake, which should be analysed in more detail. The flow rate from Zone 13 to Zone 14 ranges from 1.369 m3/s in the first step to 1.794 m3/s in the third one. The value calculated in chapter 2 for the groundwater outflow from the study area in the south direction (Fig. 2.27) seems to be consistent with the one obtained from the second and third steps of the calibration process.

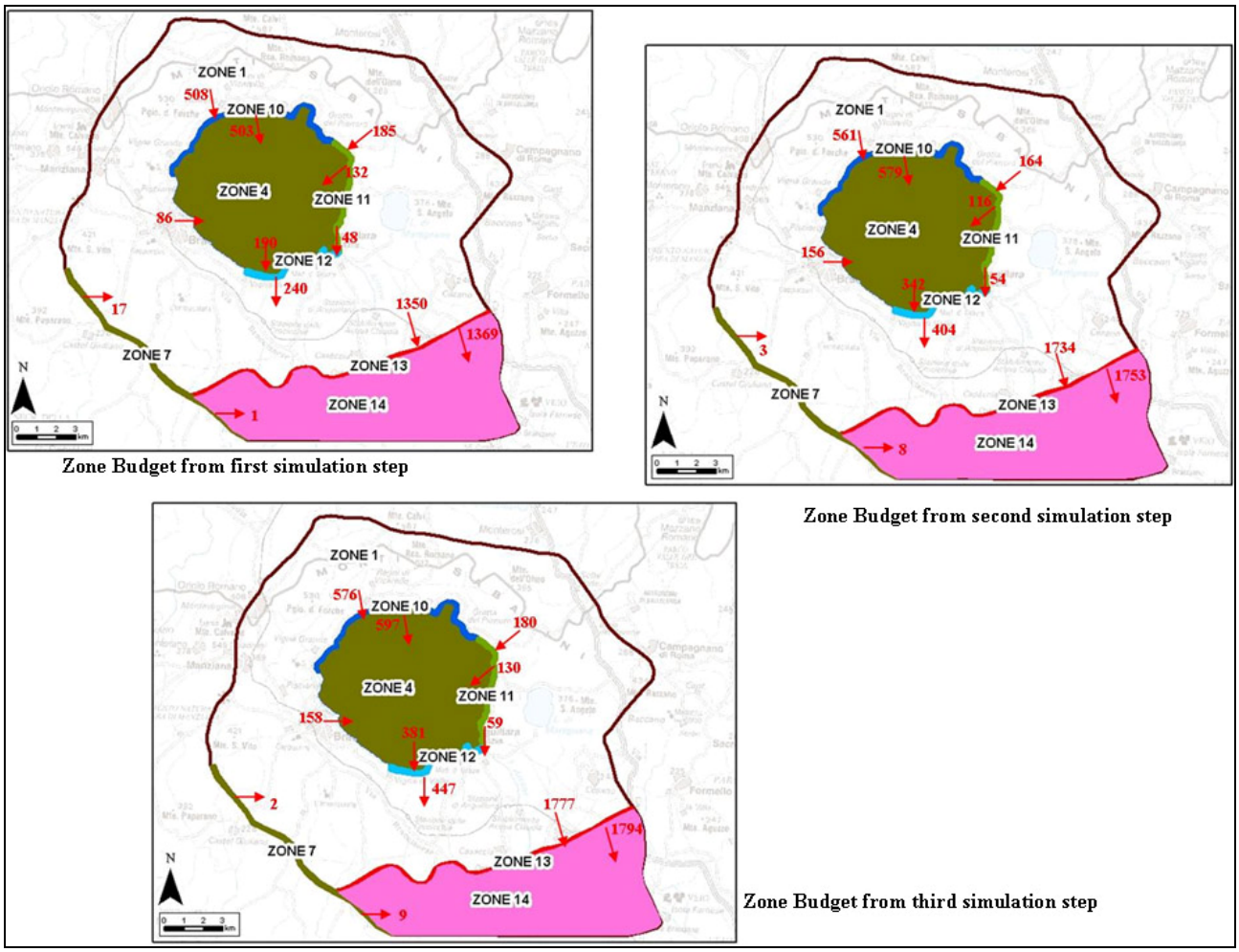

Figure 5.4: Zone Budgets

5.1.2 Tentative model validation

At the end of the calibration process, it was decided to use the calibrated model with another set of data, not used for calibration, with a view to making a tentative validation of the model. Model validation is an important step in the modelling process. This step consists in introducing recharge, abstraction and head values from another set of historical data into the calibrated model and in subsequently analysing the results. If the statistics reports are satisfactory, then the model has been validated and thus confirmed the conceptual model. For the study area, the 2002 scenario was selected for the validation test. In 2002, a piezometric survey (Capelli et al., 2005) of all the volcanic deposits of Latium was conducted. The survey made available about 60 head data on the study area. The 2002 lake levels were derived from the data collected by the SIMN hydrometric monitoring station (as explained in Chapter 2). Withdrawal from Lake Bracciano was obtained from the reports of the ACEA company on withdrawal in the past decade. Table 4.3 lists the data used for the model validation process. The statistics report of the validation is shown in Table 5.6. The RMS values and those under the three criteria are not very different from the values calculated in the calibration process for the calibration period, but the Lake level ranges from 142.23 to 142.8 m asl, i.e. differs

about 20 m from the observed values (20 meter lower). In figure 5.5 it is possible to see the model output from the third step of calibration and from the tentative validation…

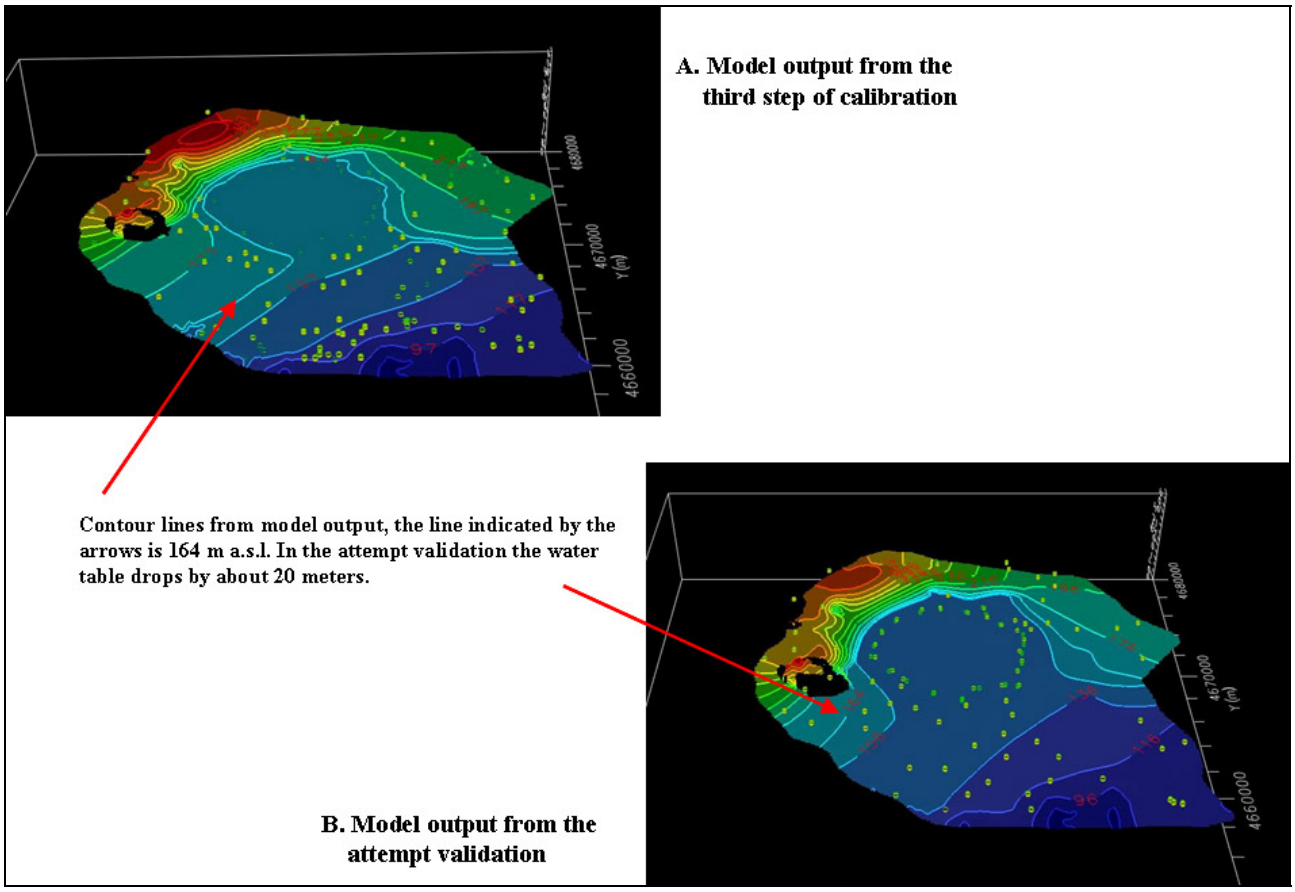

Figure 5.5: comparison between output water table of the third calibration and of the attempt validation

These results of the validation process were not satisfactory, so the validation test show that the model perform very poor regarding the simulated lake level. This means that the validation test can not prove the goodness of the model (Refsgaard et al., 2005). The validation showed that a "good" statistical value for the main part of the basin (RMS of 20 m) was not consistent with the Lake observations, which are the fundamental ones for any use of the model for assessments of regional flow and water balance near and in the surroundings of the lake.

Assuming that the poor validation test is an indicator for something must be wrong regarding the conceptual model, considering that a conceptual model consist of the following elements (Refsgaard et al., 2010):

- a geological model
- specification of process equations that are used e.g. 2D versus 3D, porous media versus fractured media, approximation for unsaturated zone etc.

- specification of, how the model domain are subdivided in structural elements with constant parameter values (e.g. zoning of parameters)
- specification of boundary conditions
- specification of which input data that drive the model (e.g. net precipitation, recharge, abstraction)
- an overall understanding of the regional flow and water balance of the area

What appears is that the boundary condition (or process description if viewed as the interaction between the lake and the groundwater) chosen for Bracciano Lake is not satisfactory and it conditions model results. Lake was represented as an aquifer with a higher hydraulic conductivity compared to the other areas, but it should be reviewed and it should be found other solutions.

Table 5.6 – Calibration statistics report (tentative validation)

								Criterion 1 (β1 < 0.05)			**Criterion 2 (β2 < 2.5)**		**Criterion 4 (β4<0.10)**	
Group_New		**Number of head targets selected for validation**	**Delta h max**		**Max Residual (m)**	**Min Residual (m)**	**Abs. Residual Mean (m)**	**Residual Mean ME (m)**	**ME/dH$_{max}$**	**RMS Root Mean Squared (m)**	**S$_{obs}$ Overall Uncertainty ***	**RMS/ S$_{obs}$**	**Standard Error of the Estimate (m)**	**Normalized RMS (%)**	**Correlation Coefficient**
U1		**12**	74		-57.96	10.44	30.99	-26.88	**0.363**	**33.75**	20.16	**1.674**	6.15	0.456	0.345
U11		**22**			-19.94	-19.37	19.51	-19.51		**19.51**			0.03	1.000	0.000
U2		**24**	100		-43.02	1.11	13.63	-7.35	**0.073**	**17.67**	13.43	**1.316**	3.35	0.177	0.845
U3														0.000	
U5		**4**	24		-52.54	-32.98	40.50	-40.50	**1.688**	**41.16**	20.16	**2.042**	4.23	1.715	0.538
U8		**6**	181		35.40	1.95	22.13	10.35	**0.057**	**25.56**	33.87	**0.755**	10.45	0.141	0.930
U9		**6**	222		-27.18	3.13	13.42	-0.40	**0.002**	**15.30**	20.16	**0.759**	6.84	0.161	0.983
U10		**3**	19		26.49	-4.53	14.50	11.47	**0.604**	**17.10**	20.16	**0.848**	8.97	0.900	0.581
U6		**2**	9		-29.37	24.63	27.00	-27.00	**3.000**	**27.10**	20.16	**1.344**	2.37	3.011	1.000
U7		**4**	58		-51.66	3.01	16.62	-9.21	**0.160**	**26.25**	33.87	**0.775**	14.19	0.457	0.219
TOTAL		**85**	345		-57.96	1.11	20.05	-13.22	**0.038**	**23.62**	20.16	**1.171**	2.14	0.092	0.929
*** values taken from the table 4.5, respectively for the north-west area, the south and a value for the general situation**															

5.2 GWV BRACCIANO MODEL CALIBRATION

5.2.1 Two layer starting model

It was considered to build a two layer model using Groundwater Vistas software, with the aim to better represent the Lake using Lake Package and to better analyse the lake-aquifer interactions.
A two layers GWV Bracciano model was compiled. As explained in chapter 4 the first layer was initially a thin layer (a constant thickness layer of 40 meters all over the area, except in the Lake Bracciano area, in which it assumes the appropriate lake thickness). This version of the model had some problems; many of first layer cells went dry during in the simulations (Fig. 5.6) and this fact brings a lot of instability to the numerical simulation of the groundwater table. The presence of dry cells was in itself not a problem, from a conceptual point of view; the water table level, in several areas of the model, is 40 meters below the topographic surface. This version of the model arrived at a solution and at an acceptable value of mass balance error, but the ground water table was very "unstable" and thus lacked robustness.

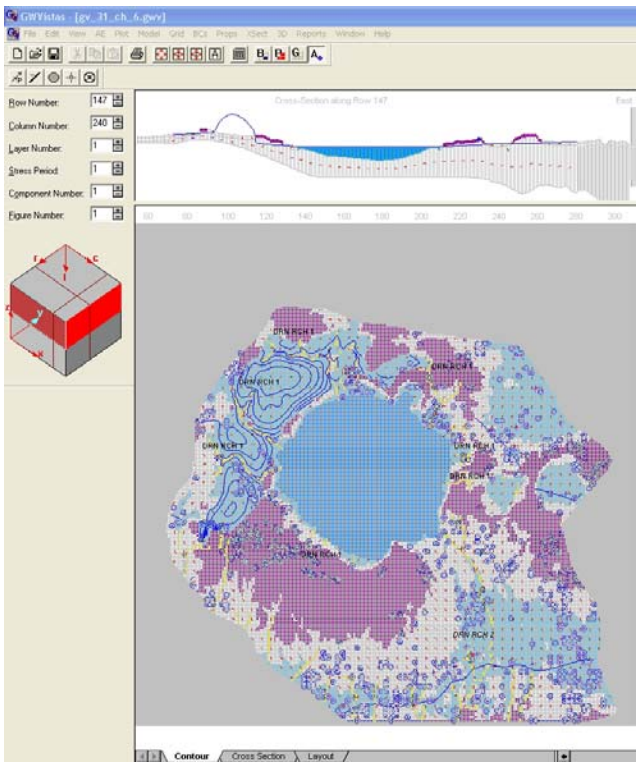

Figure 5.6: first GWV Bracciano model, with a thin upper calculation layer

It was decided to increase the thickness of layer 1 and decrease the thickness of layer 2, in order to reduce or to eliminate the problem with dry cells. The whole aquifer was divided in two layers of

the same thickness, in this way the problem of dry cells was solved because the water table could fall to the appropriate depth and still lie above the bottom of layer 1.

5.2.2 Selection of calibration targets

In the GWV Bracciano model, the approach to the calibration was further improved compared to the VMF model. The GWV model has been calibrated using both: water level and flow measurements which is important and provides a better utilisation of observation data from the area. In GWV model only two observation head groups were considered, water level measurement included:

Water level measurement for 98 wells during the spring and summer of 2009,

24 water level points were arbitrarily distributed along the Bracciano Lake perimeter.

Flow measurement included:

8 Streamflow gains on Arrone river and other streams during the summer of 2009

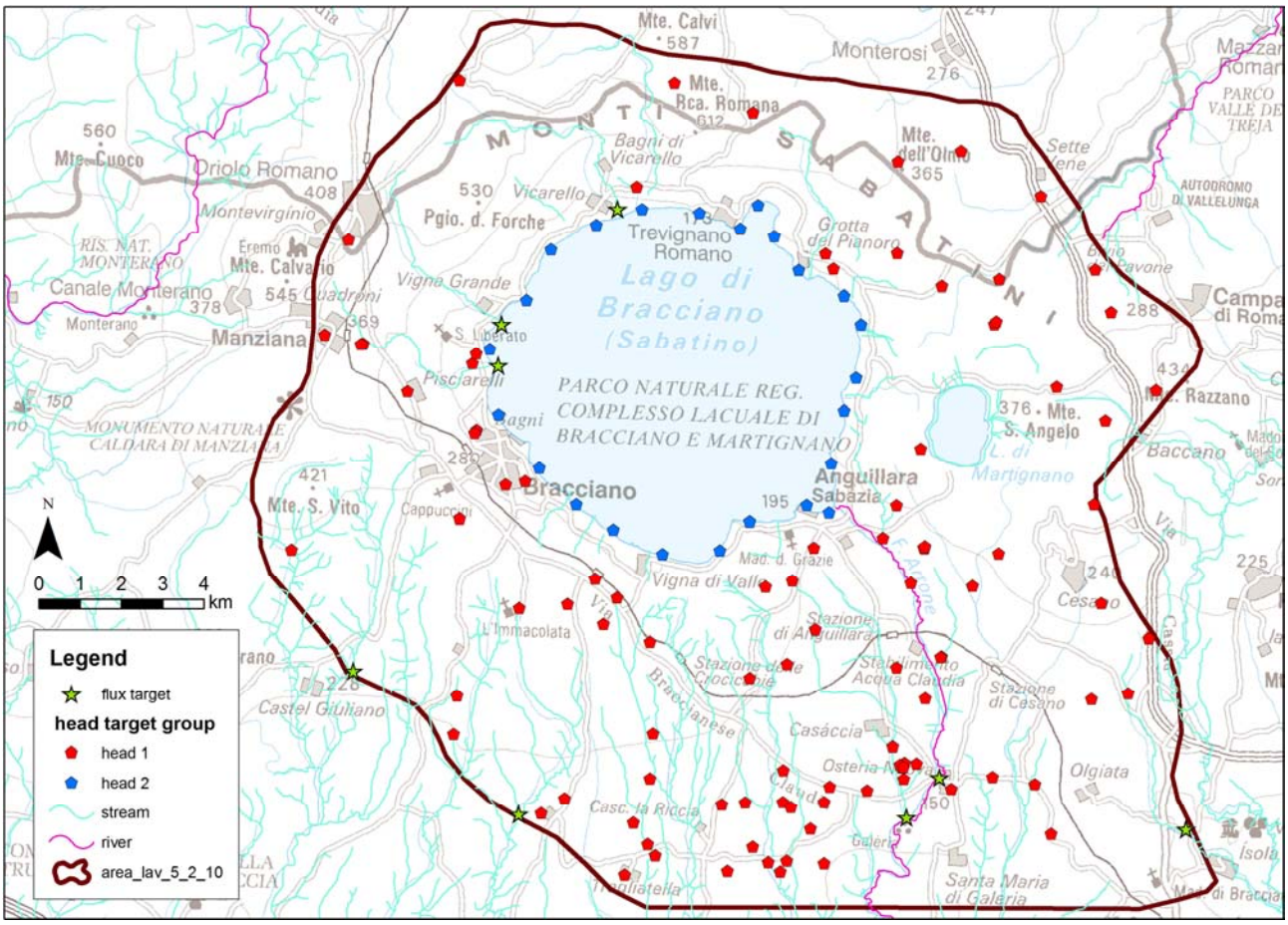

Figure 5.7– GWV Bracciano model head and flux targets

5.2.3 Overview of the main steps followed

In this section is presented an overview of the main steps followed in the GWV model calibration process. In the table 5.6a, for every main step is reported the model name, the characterization of the calibration and the target used. Detailed information on each of these steps are provided in the following paragraphs.

Table 5.7: scheme of the calibration process

	MODEL A	***MODEL B***	***MODEL C***	***MODEL D***
step	starting model	first PEST calibration	second PEST calibration	manual re-arrangement of the
preliminary actions	refining layers thickness, solved the dry cells problems			
calibration process	focus on the trial and error calibration of the lakebed conductance			
	trying autosensitivity analysis, with hydraulic conductivities, drain hydraulic conductivities and recharge parameters	PEST calibration on K (aquifer hydraulic conductivities) and Cd (drain conductance) parameters	PEST calibration on K (aquifer hydraulic conductivities), Cd (drain conductance) and R (recharge) parameters	manual re-arrangement: change of the unreasonable values of drain hydraulic conductivities, re-arrange on the recharge
use of head targets	Yes	Yes	Yes	Yes
use of flux targets	No	4 flux targets introduced	8 flux targets introduced	Yes

5.2.4 Model A

Model A is the starting model, where equal thickness of layers 1 and 2 was assigned in order to avoid problems with dry cells. Based on this model the subsequent calibration process was carried out, including the following concerned actions:

Introduction of a new Hydraulic conductivity zone, in the southern part of the first layer. It was considered important to differentiate between upper and lower sediments in this part of the model; in fact, in this zone, there is a water circulation between the upper volcanic aquifer and the underlying sand and gravel aquifer. The volcanic aquifer feeds the sand and gravel aquifer. A new hydraulic conductivity zone was introduced, named K7 (Fig. 5.7).

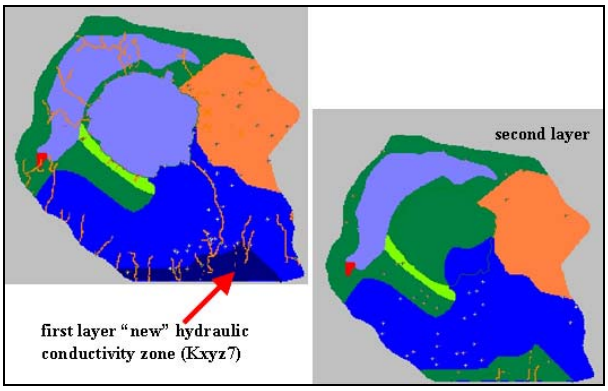

Figure 5.8: hydraulic conductivity zones, focus on the new zone, characterized by Kxyz7 hydraulic conductivity

***Trial and error* calibration on the Lake hydraulic conductivity.** As was explained in the chapter 3, the lake package considers the lake as an area of no-flow cells except the aquifer-lake interface cells through which the water exchange is calculated. For this reason particular attention has been given to calibrating the lakebed conductance.

Taking in consideration the equation n. 14 (chapter 3), for the steady state case:

$$h_l = \frac{p - e + rnf - w - sp + Q_{si} - Q_{so}}{A_s} \qquad \text{[m]} \qquad \text{Eq. 3.14}$$

where

h_l^n and h_l^{n-1} are the lake stages [m] from the present and previous time steps;

Δt is the time step length [s]

p is the rate of precipitation [m^3/s] on the lake during the time step;

e is the rate of evaporation [m^3/s] from the lake surface during the time step;

rnf is the rate of surface runoff to the lake [m^3/s] during the time step;

w is the rate of water withdrawal from the lake [m^3/s] during the time step (a negative value is used to specify a rate of augmentation);

Q_{si} is the rate of inflow from streams [m^3/s] during the time step;

Q_{so} is the rate of outflow to streams [m^3/s] during the time step;

A_s is the surface area of the lake [m^2] at the beginning of the time step; and

sp is the net rate of seepage between the lake and the aquifer [m^3/s] during the time step (a positive value indicates seepage from the lake into the aquifer), and is computed as the sum of individual seepage terms for all M lake/aquifer cell interfaces:

$$sp = \sum_{m}^{M} c_m \left(h_l - h_{am}\right) \qquad \text{[m}^2\text{/s]} \qquad \text{Eq. 3.15}$$

where

h_{am} is the head in the aquifer cell across the m^{th} interface;
c_m is the conductance across the m^{th} interface (Fig. 3.16A)

and

$$c_m = \frac{A}{\frac{b}{K_b} + \frac{\Delta l}{K_a}} \qquad [m^2/s] \qquad \text{Eq. 3.16}$$

So the simple sensitivity analysis consisted in change the K_b value several times and observing the effects on the c_m term and consequently on the lake head level solution.
In the numerical modelling context, Δl is half the grid cell dimension in the appropriate coordinate direction (fig. 3b, the distance between the edge of the aquifer grid cell that is the interface with the lakebed and the aquifer grid cell center), A is the cross-sectional area of the grid cell in a plane perpendicular to the travel distance Δl, and Ka is the aquifer hydraulic conductivity in the direction of Δl (either horizontal, Kh, or vertical, Kv). The lakebed Bracciano thickness b of 2 m was considered reasonable and not changed as part of calibration This trial and error calibration consisted in several steps, in which the terms of equation 5.1 (*p, e, rnf, w*) were changed according to the reasonable ranges of values of those parameters and the resulting simulation lake level were then analysed.

Table 5.8: calculation of c_m , the conductance across the m^{th} interface

A	***b***	***Kb***	***Δl***	***Ka***	***c_m = A/[(b/Kb)+(Δl/Ka)]***	***h lake***
m^2	**m**	**m/s**	**m**	**m/s**	**m^2/s**	**m a.s.l.**
10000	2	8.00E-08	70	2.56E-05	0.000360563	162.05
10000	2	8.00E-08	70	6.46E-06	0.00027905	162.05
10000	2	8.00E-08	70	6.72E-06	0.000282353	162.05
10000	2	8.00E-08	70	1.77E-04	0.000393771	162.05
10000	2	1.00E-06	70	2.56E-05	0.002112211	155.36
10000	2	1.00E-06	70	6.46E-06	0.000779064	155.36
10000	2	1.00E-06	70	6.72E-06	0.000805369	155.36
10000	2	1.00E-06	70	1.77E-04	0.004174528	155.36

Looking to the table 5.7, in the last column are reported the lake level in m a.s.l., calculated from the model simulations in relation to data inserted. After several attempts, it was found as a satisfactory value of 8.00E-08 for the lakebed hydraulic conductivity. Model A can be considered “stable” in relation to the lake level. Using the calibrated lakebed hydraulic conductivity, it is possible to vary other parameters without causing strong variations of the lake level (this was one important objective). In the Fig. 5.8 are reported two sections of the model (row 129), that represent the two situations listed in the table 5.7.

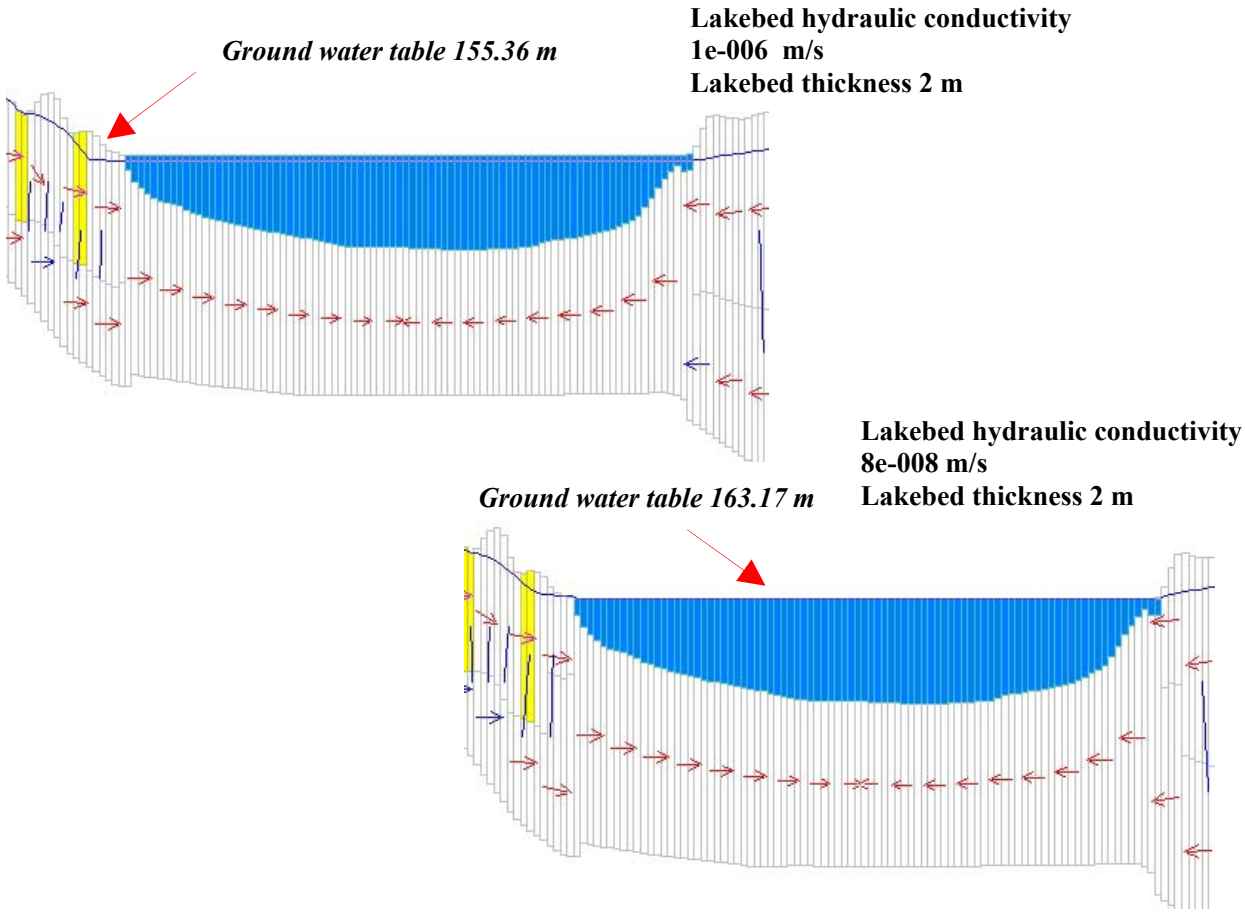

Figure 5.9: two sections from Model A, related to different lakebed hydraulic conductivity

Autosensitivity analysis. One of the most important steps in any calibration procedure is a quantitative understanding of parameter sensitivity and parameter correlation. We evaluated sensitivities and correlations using a conventional approach that varies one parameter value at a time in each MODFLOW run. Groundwater Vistas provides a tool for conducting this analysis called "autosensitivity". It permits us to determine quickly which parameters are sensitive to the available targets and which parameters are closely linked because raising the value of one requires lowering the value of the other to minimize the sum of squared residual. Sensitive parameters, with high priority, should then be subjected to a manual inverse parameter estimation analysis or to an automated algorithm (e.g., using the code PEST) applied to the other parameters. Autosensitivty was made on the **Model A** , introducing only head targets. The Fig. 5.9 reports the graph, it can be seen that the simulated values at target locations are most sensitive to parameters are: Kxy4; Kxy5; Kxy7 and cond 9; The head target values are also somewhat sensitive to Recharge 6 and Recharge 2.

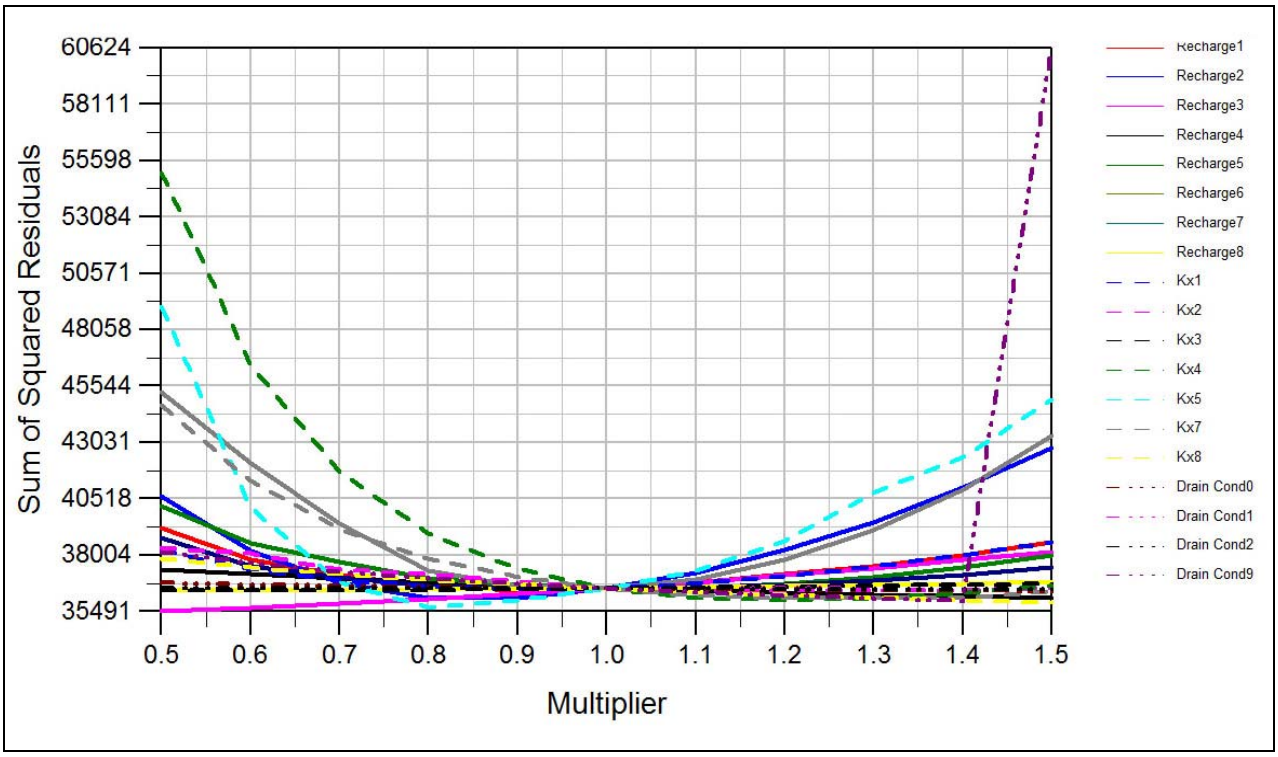

Figure 5.10: result from the autosensitivity analysis, carried out after the calibration of Model A.

5.2.5 MODEL B

Starting from the Model A, it was decided to introduce 4 flux targets (Fig. 5.11), in addition to the head targets and to calibrate the model, PEST was used for the inverse calibration. It was also decided to estimate a subset of the model parameters. The estimated parameters are the values for each hydraulic conductivity zone and the drain conductance for groups (called "reaches") of drain cells representing the following surface-water features: (see Fig. 5.10):

- *drain reach 0*: all streams flowing eastward
- *drain reach 9* streams flowing toward the lake in the northwest sector
- *drain reach 1*: streams flowing toward the lake in sectors other than the northwest sector
- *drain reach 3*: streams flowing toward the southwest.
- *drain reach 2*: the Arrone river and its tributary streams

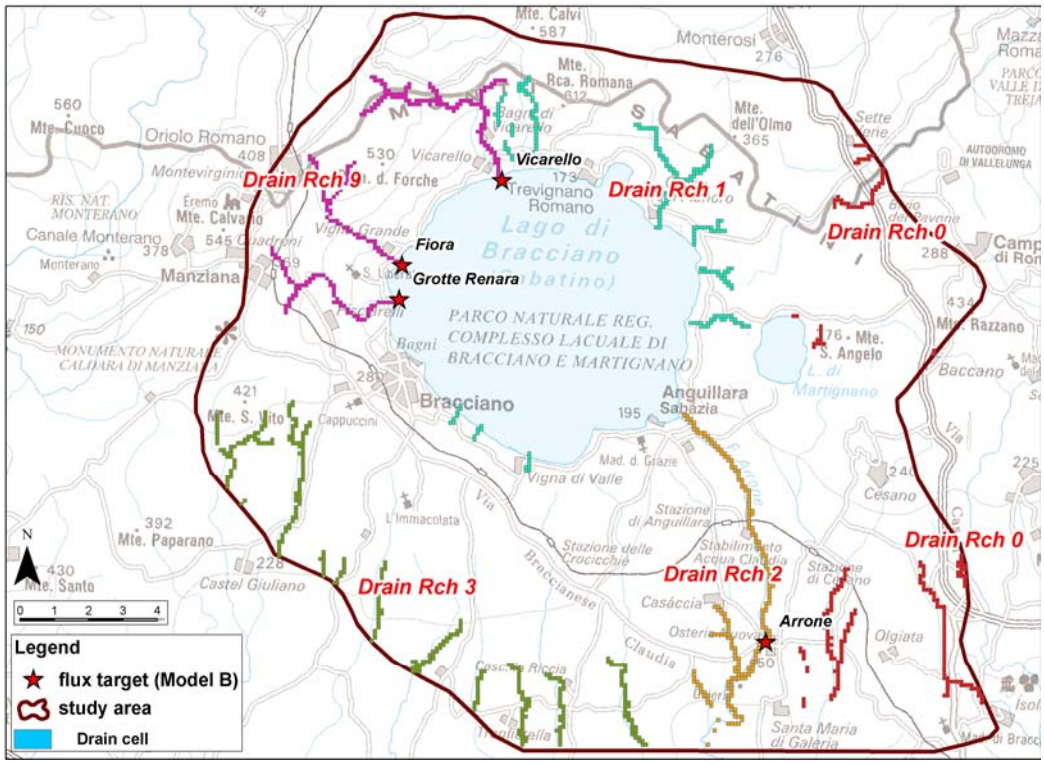

Figure 5.11: Drain reach distribution and location of the 4 flux targets.

In order to properly apply the PEST algorithm, it is necessary to assign weights to the targets in order to determine their relative importance in the parameter estimation process as measured by the objective function, that is the sum of squares of weighted residuals. In particular, it was necessary to decide how much the flux targets have to contribute relatively to the other groups of head targets. In this decision the judgment of the modeller has a big role e.g. it is to some extent a subjective decision (or a decision which requires expert knowledge). It was considered that "close to lake" head targets should have an important weight in the objective function, on the order of 40% of its total value when expected average residual values are assumed. Therefore weights was adjusted so that the expected contribution to the objective function was around 40%. Similarly, were adjusted the weights assigned the aquifer head targets so that they also contributed around 40% of the total value of the objective function, and adjusted the weights of the flux targets given their expected residuals so that collectively they would be expected to account for the remaining ~20% of the objective function. It was used a spreadsheet in order to test possible weights (table 5.8). The spreadsheet has a line for each of the 3 groups of targets. It was assigned an expected average residual for the targets in each group and a trial weight for each target in each group. Then was calculated the contribution to the value of the expected total objective function of each group using the formula reported in the table as sum of squares of weighted residuals. By trial and error it was found the weight for every target group that contributed the percentages previously established. Table 5.8 shows in the middle column the trial weight that was used in the PEST simulation of Model B and later of Model C.

Table 5.9: spreadsheet for the evaluation of a trial weight

	Target type	*Number targets*	*Expected average absolute residual*	*Trial Weight*	*Sum of squares of weight residuals*	*Target Percent*	*Percent contribution to OBJ function*
MODEL B	aquifer heads m	98	11.50	1.00	12960.50	43	43.07
	near lake heads m	23	2.70	8.00	10730.88	36	35.66
	stream baseflow m/s	4	0.08	500.00	6400.00	21	21.27
				TOTAL	**30091.38**	**100**	**100.00**
	Sum of squares of weight residuals = Number targests*(Weight)^2*(Expected average absolute residual)^2 Percent contribution to OBJ function = (Sum of squares of weighted residuals / TOTAL Sum of square of squares of weighted residuals)*100						
MODEL C	*Target type*	*Number targets*	*Expected average absolute residual*	*Trial Weight*	*Sum of squares of weight residuals*	*Target Percent*	*Percent contribution to OBJ function*
	aquifer heads m	98	12.00	0.60	5080.32	41	41.29
	near lake heads m	23	3.00	5.00	5175.00	42	42.06
	stream baseflow m/s	8	0.02	800.00	2048.00	17	16.65
				TOTAL	**12303.32**	**100**	**100.00**

Target head statistics from simulation of Model B are reported in table 5.9 where is possible to see the Model B absolute residual mean and the RMS Error of the head 1 (in both layers) and the head target statistics for the head 2 group ("close to lake" head) have values around 2.17 m, more then the values related to the starting Model A. This is due to the PEST implementation, in which parameters of calibration are aquifer hydraulic conductivity and drain conductance and not the lake-bed conductance as in Model A. Target statistics of Model A results has been inserted to be compared with less emphasis then the following model's results. Moreover the lake level cannot be included directly as a head target in the PEST simulation; for this reason were used as proxy for lake level the "near lake" head targets to represent the lake level.

In table 5.10 values of hydraulic conductivities of different areas (Fig 5.11) are reported; Model A has the hydraulic conductivity values coming out from VMF Bracciano model calibration, while the values reported for the Model B and Model C steps are the calibrated values.

Table 5.10: head 1 and head 2 groups target statistics

Layer	*Group target*	Target statistics	Model A	Model B	Model C	Model D
Layer 1	Head 1	Absolute Residual Mean (m)	12.35	9.72	9.82	10.45
Layer 1	Head 1	Residual Sum of squares (m2)	18800	12900	12900	12400
Layer 1	Head 1	RMS Error (m)	18.34	15.18	15.16	14.9
Layer 1	Head 1	Number of target	56	56	56	56
Layer 1	Head 2	Absolute Residual Mean (m)	1.89	2.17	2.55	1.9
Layer 1	Head 2	Residual Sum of squares (m2)	117	147	201	123
Layer 1	Head 2	RMS Error (m)	2.21	2.47	2.89	2.26
Layer 1	Head 2	Number of target	24	24	24	24
Layer 2	Head 1	Absolute Residual Mean (m)	16.77	14.19	13.69	14.57
Layer 2	Head 1	Residual Sum of squares (m2)	17700	13800	13700	14800
Layer 2	Head 1	RMS Error (m)	20.52	18.11	18.07	18.79
Layer 2	Head 1	Number of target	42	42	42	42
Layer 1 & Layer 2	Head 1	Absolute Residual Mean (m)	14.25	11.64	11.48	12.22
Layer 1 & Layer 2	Head 1	Residual Sum of squares (m2)	36500	26700	26600	27300
Layer 1 & Layer 2	Head 1	RMS Error (m)	19.3	16.5	16.47	16.68
Layer 1 & Layer 2	Head 1	Number of target	98	98	98	98
Layer 1 & Layer 2	Head 1 & Head 2	Absolute Residual Mean (m)	11.96	9.89	9.48	10.19
Layer 1 & Layer 2	Head 1 & Head 2	Residual Sum of squares (m2)	36700	26900	26900	27300
Layer 1 & Layer 2	Head 1 & Head 2	RMS Error (m)	17.35	14.85	14.85	14.98
Layer 1 & Layer 2	Head 1 & Head 2	Number of target	122	122	122	122

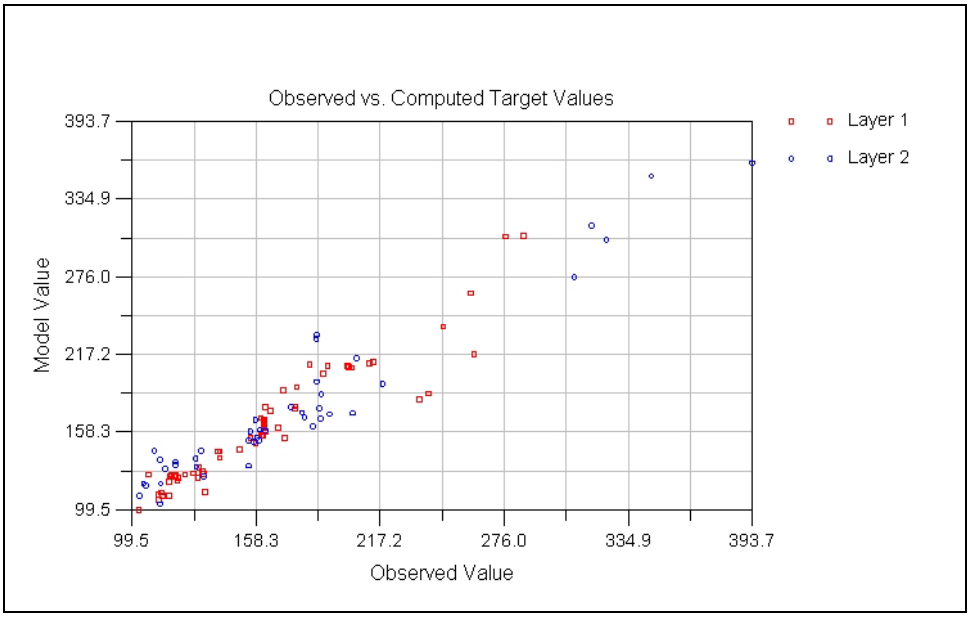

Figure 5.12: observed versus simulated head (Model B).

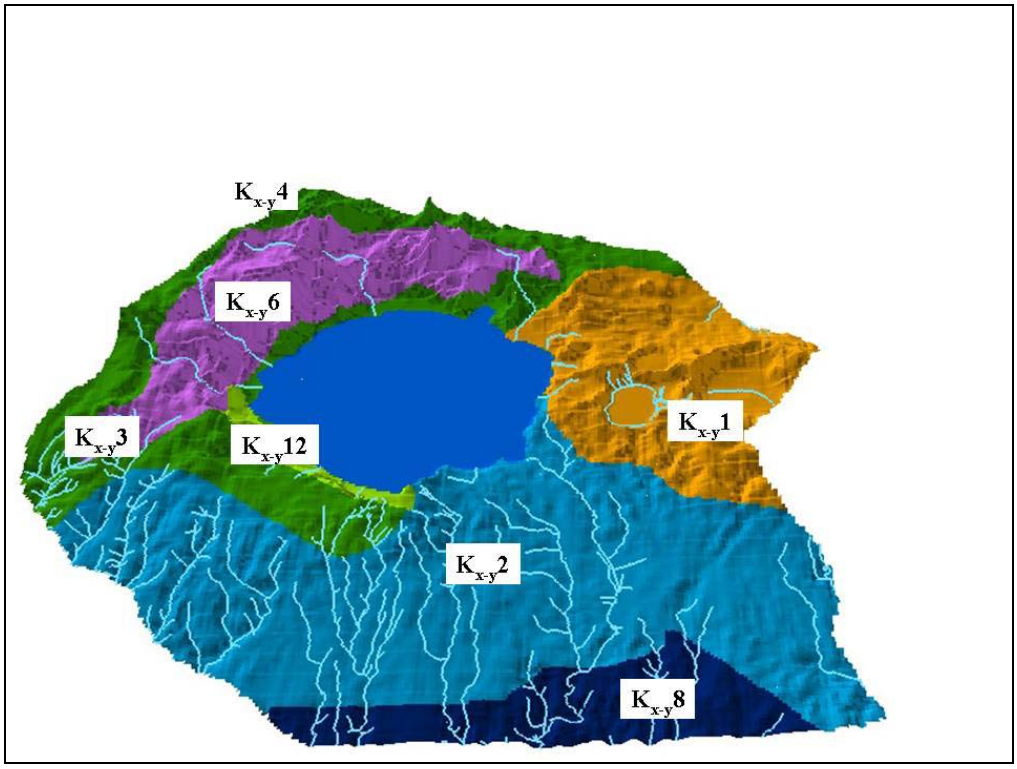

Figure 5.13 homogeneous hydraulic conductivity areas.

Table 5.11: hydraulic conductivities values in the calibration steps

K	***Model A***	***Model B***	***Model C***
	m/s	**m/s**	**m/s**
Kx-y1	6.72E-06	3.63E-06	3.98E-06
Kx-y2	0.000177	7.28E-05	9.22E-05
Kx-y3	1.00E-07	1.00E-07	1.00E-07
Kx-y4	2.56E-05	1.63E-05	1.70E-05
Kx-y6	3.78E-07	4.76E-07	3.96E-07
Kx-y8	0.000177	7.50E-05	0.000197843
Kx-y12	6.46E-06	4.38E-06	4.47E-06
Kx-y1	6.72E-07	3.63E-07	3.98E-07
Kx-y2	7.70E-06	7.28E-06	9.22E-06
Kx-y3	1.00E-08	1.00E-08	1.00E-08
Kx-y4	2.56E-06	1.63E-06	1.70E-06
Kx-y6	3.78E-08	4.76E-08	3.96E-08
Kx-y8	1.77E-05	7.50E-06	1.97843E-05
Kx-y12	6.46E-07	4.38E-07	4.47E-07

Final values of hydraulic conductivities are reasonable, all these values fall into the establish range considered.

Next we considered the four flux targets introduced in MODEL B and their residuals, as shown in table 5.11, It can be seen that simulated fluxes are higher than estimated baseflow for Vicarello, Fiora, Grotte Renare, while for the Arrone river the simulated value is about a third of the estimated value. In table 5.12 is reported total model drain outflow (divided in different drain reach components), the total amount of drain outflow is too high (1.999 m3/s), compared to the observed drain outflow (chapter 2..); the main source of error is due to the outflow of drain reach 0 (all streams eastward), that is not consistent with the observed situation.

Table 5.12: flux target statistics.

MODEL B			
flux target name	**flux target**	**computed**	**weighted residual**
Vicarello	-0.030	-0.130	0.100
Fiora	-0.040	-0.130	0.090
Grotte Renara	-0.075	-0.125	0.050
Arrone	-0.240	-0.140	-0.100
TOTAL	**-0.385**	**-0.525**	

MODEL C			
flux target name	**flux target**	**computed**	**weighted residual**
Vicarello	-0.080	-0.001	-0.079
Fiora	-0.028	-0.031	0.003
Grotte Renara	-0.075	-0.113	0.038
Arrone	-0.240	-0.232	-0.010
Vaccina	-0.025	0.000	-0.025
Tavolato	-0.030	0.000	-0.030
Piordo	-0.100	-0.137	0.037
Casaccia	-0.016	0.000	-0.016
TOTAL	**-0.594**	**-0.514**	

target statistics	***Model B***
Absolute Residual Mean (m)	0.080
Residual Sum of squares (m2)	290.000
RMS Error (m)	0.090
Number of target	4.000

target statistics	***Model C***
Absolute Residual Mean (m)	0.040
Residual Sum of squares (m2)	163.000
RMS Error (m)	0.050
Number of target	8.000

target statistics	***Model D***
Absolute Residual Mean (m)	0.030
Residual Sum of squares (m2)	0.009
RMS Error (m)	0.030
Number of target	8.000

MODEL D			
flux target name	**flux target**	**computed**	**residual**
Vicarello	-0.080	-0.035	-0.045
Fiora	-0.028	-0.021	-0.007
Grotte Renara	-0.075	-0.092	0.017
Arrone	-0.240	-0.224	-0.016
Vaccina	-0.025	0.000	-0.025
Tavolato	-0.030	-0.007	-0.023
Piordo	-0.100	-0.171	0.071
Casaccia	-0.016	0.000	-0.016
TOTAL	**-0.594**	**-0.550**	

Table 5.13: total drain outflow for different drain conductance values.

Drain Reach	*Model A*	*Model B*		*Model C*		*Model D*	
	Conductance m^2/s *	**Conductance m^2/s**	**Drain outflow m^3/s**	**Conductance m^2/s**	**Drain outflow m^3/s**	**Conductance m^2/s**	**Drain outflow m^3/s**
Drain Reach1	2.11E-05	1.00533E-10	0.000	1.00E-10	0.000	1.00E-05	-0.004
Drain Reach2	2.11E-05	8.48256E-05	-0.055	5.04E-04	-0.231	5.04E-04	-0.224
Drain Reach 3	2.11E-05	0.001276963	-0.787	1.00E-10	0.000	1.00E-05	-0.007
Drain Reach 9	2.11E-05	0.000376333	-0.129				
Drain Reach 0	2.11E-05	0.012770063	-1.028	2.20E-01	-0.138	2.20E-04	-0.104
Drain Reach15				3.44E-07	-0.001	3.44E-04	-0.035
Drain Reach13				1.32E-02	-0.032	1.32E-02	-0.021
Drain Reach11				1.60E-02	-0.113	1.60E-02	-0.092
Drain Reach 6				1.00E-10	0.000	1.00E-05	0.000
Drain Reach 8				1.00E-10	0.000	1.00E-05	-0.007
Drain Reach 20				7.85E-05	-0.033	7.85E-05	-0.032
Drain Reach 10				1.54E-08	0.000	1.54E-04	0.000
Drain Reach 14				1.00E-10	0.000	1.00E-05	-0.013
Drain Reach 16				2.25E-01	-0.233	2.25E-04	-0.047
Drain Reach 12				2.85E-01	-0.137	2.85E-01	-0.171
		TOTAL	**-1.999**	**TOTAL**	**-0.919**	**TOTAL**	**-0.757**
*** conductance starting value**							
Fixed Conductance has been consider, assaigning a value of hydraulic conductivity and a value of 1 m to width, lenght of the drain and 1m to thickness of drain bed							

5.2.6 Model C

The next step in the analysis was to introduce 4 additional flux target (total 8 flux targets), because the values coming out from the MODEL B were not satisfactory. In MODEL C it was refined the grouping of drain reaches, as can be seen in the Fig. 5.12. It was also reviewed the weight of group targets (table 5.8), considering an expected average absolute residual of 0.02. Based on a critical review, other changes were made to the flux target values. The Vicarello target value was updated to 0.08 m^3/s, consider to be a more realistic value due to the presence of several spring which feed Traiano aqueduct. The flux target for the Arrone river were updated too, because the observed flux of 0.157 m^3/s was measured in a gauge station placed some kilometres upstream of the edge of the model domain. A value of 0.240 m^3/s for the whole outflow of the Arrone inside the study area was judged reasonable.

In the Model C PEST simulation it was implemented the recharge, besides the hydraulic conductivity and conductance parameters. So, the importance of flux targets as a way of adjusting recharge without it being correlated to K, flux targets which served to break the correlation between recharge and K.

gives good results in term of the agreement between estimated and simulated drain outflow. In table 5.12 it can be seen the total value of –0.919 m^3/s, is much closer to the total volume estimated to discharge to these reaches. Head target statistics are simular to the Model B results. In the table 5.11 the values of residuals are considered adequate;, the only one showing a large residual is the Vicarello flux target. It could be interesting to manually increase drain conductance of drain reach 15 and to observe if the Vicarello flux target go better.

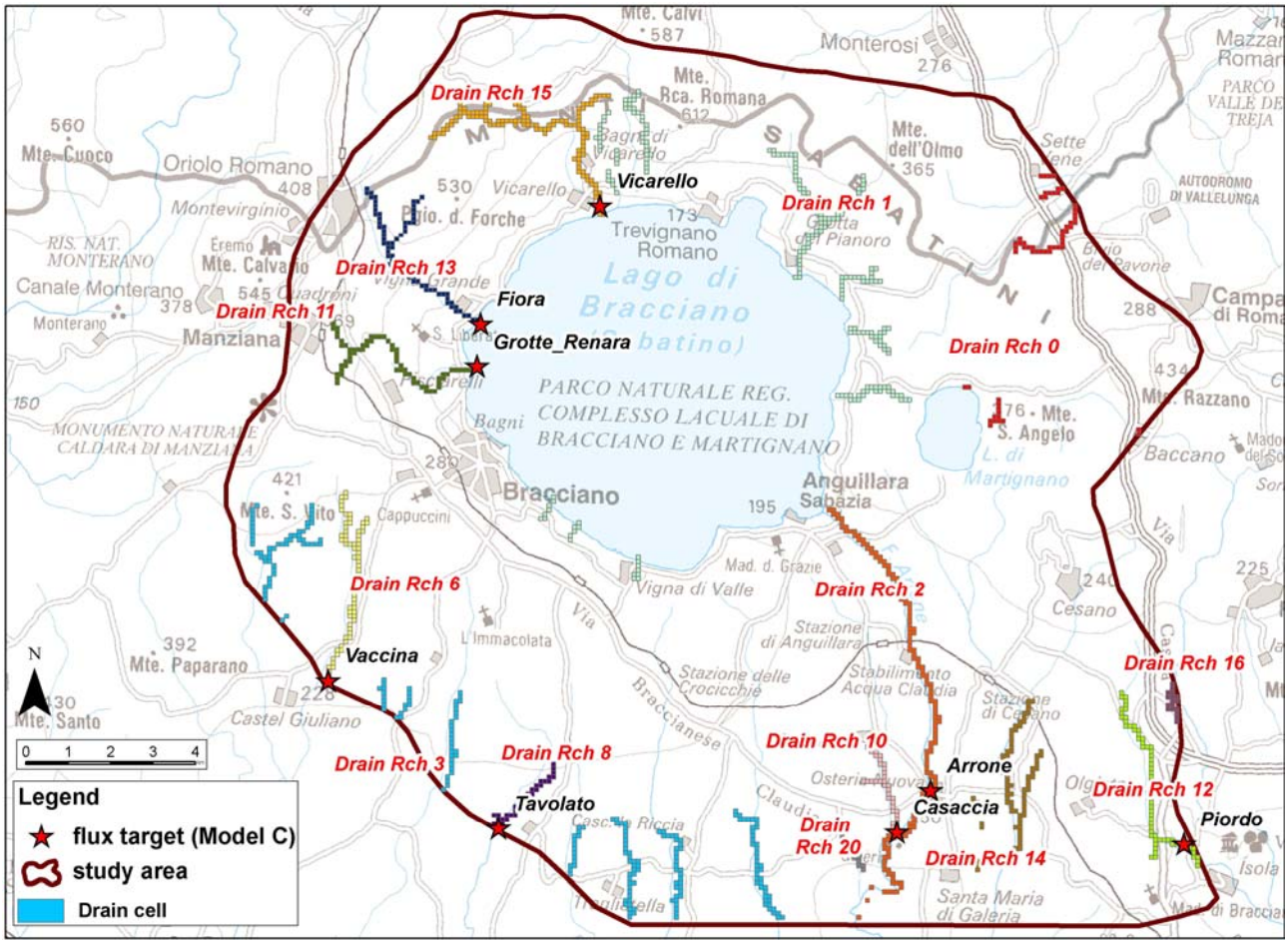

Figure 5.14: Drain reach distribution and location of the 4 flux targets.

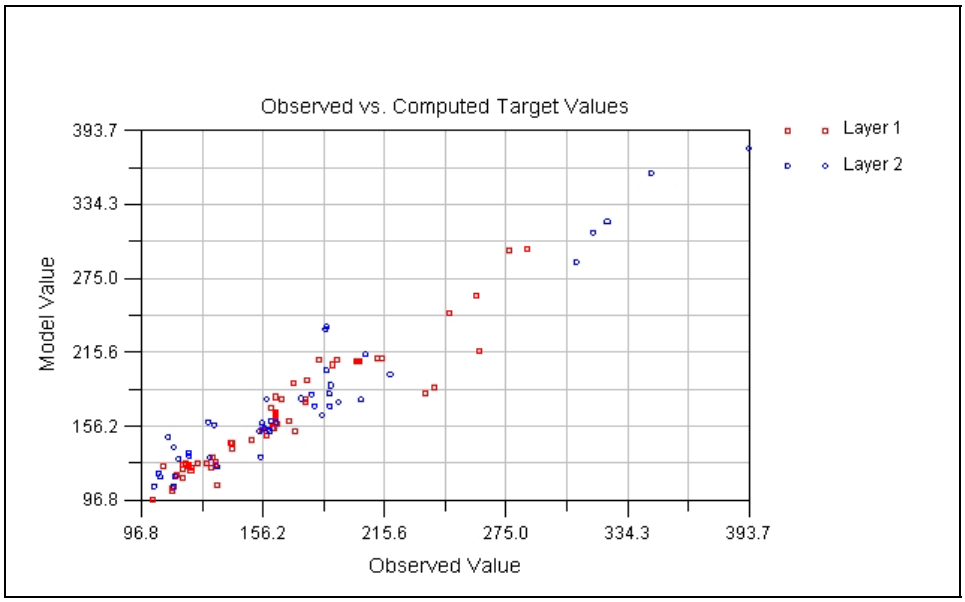

Figure 5.15: observed versus simulated head (Model C)

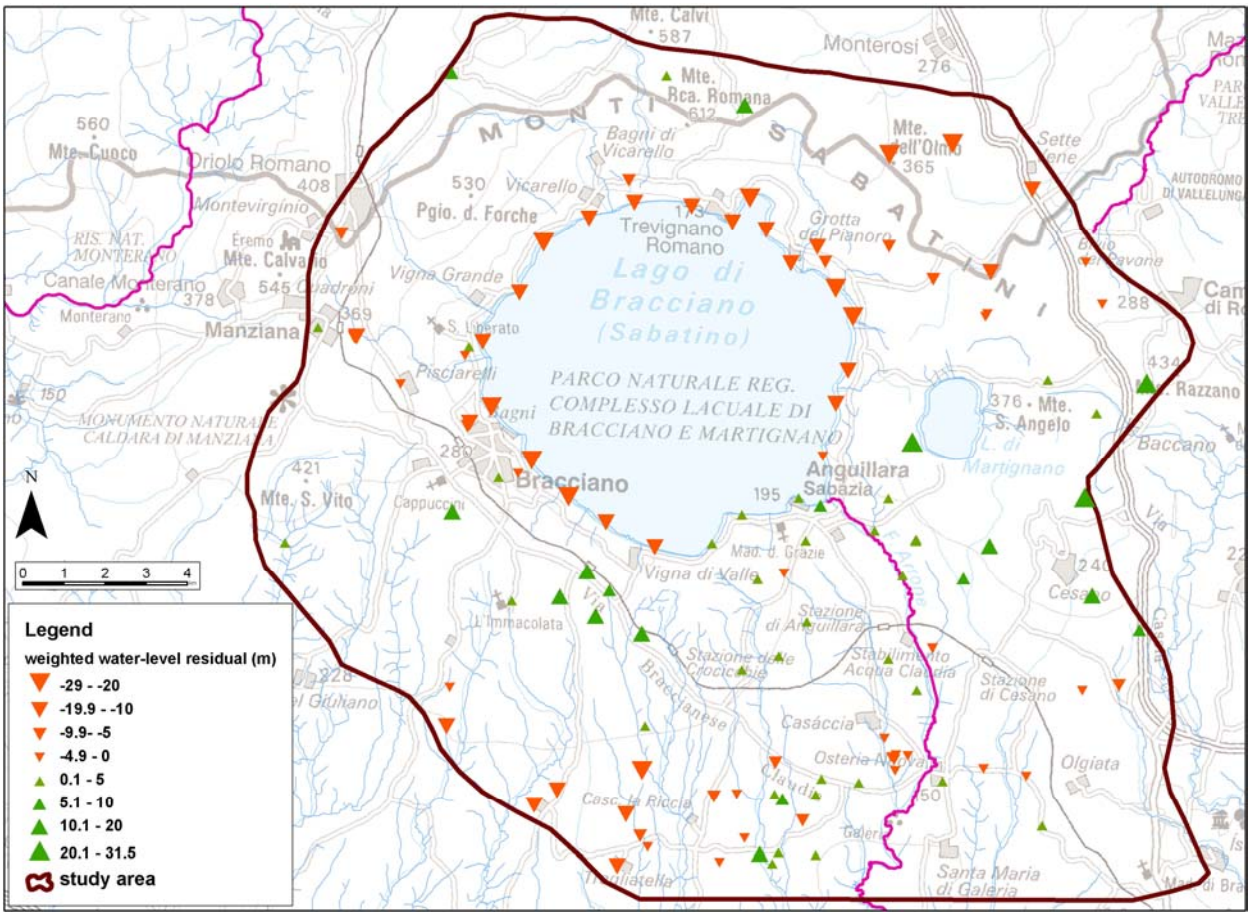

Figure 5.16: weighted water level residuals in Model C

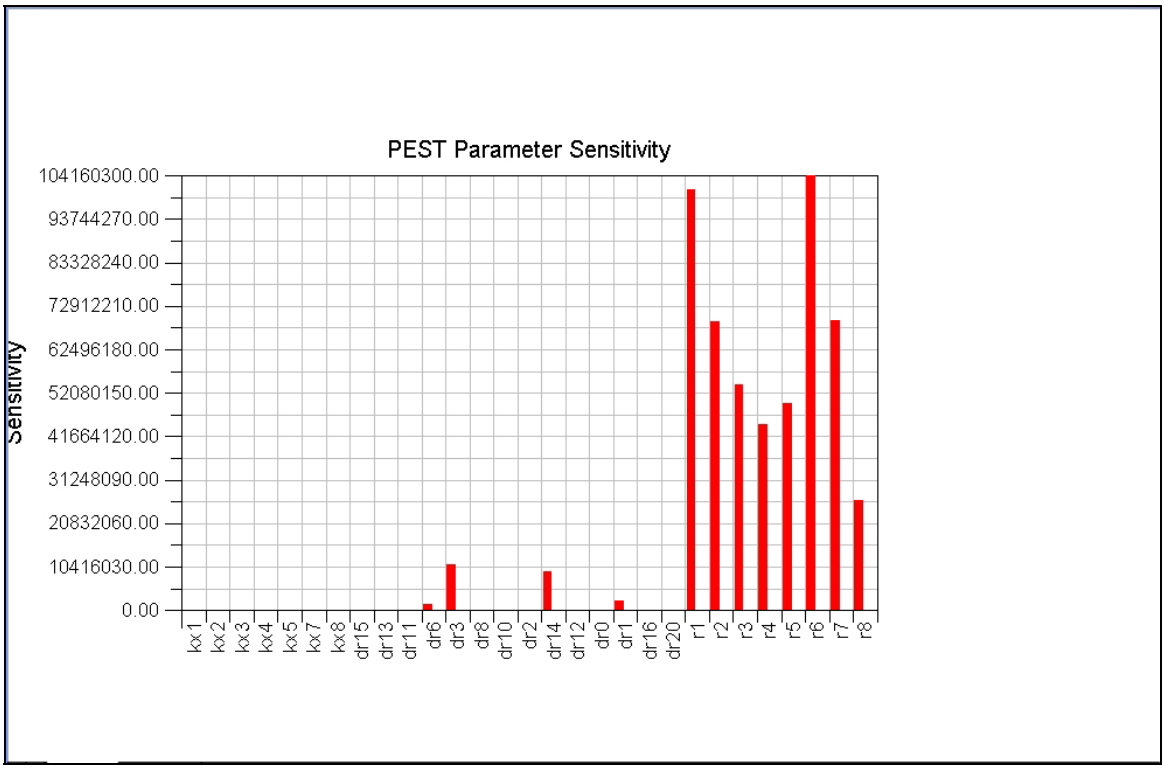

Figure 5.17: weighted water level residuals in Model C

5.2.7 Model D

A model D was built, starting from previuos models. Was tried a PEST calibration of the recharge values and on the strenght of PEST sensitivity values coming out from Model C (recharge parameters are the most sensitivity, Fig. 5.17) and in Model D recharge values were updated from these results. Another change was to introduce more reasonable drain conductance values than those coming out from Model C PEST calibration (see table 5.12) and with the aim of finding a better fit of the drain outflow volume.

Values inserted in model D resulted in acceptable results, where the amount of drain outflow is around 0.7 m3/s and correspond to the estimated value for the study area.

Simultated head contours were compared with man-drawn contours relative to 2009 survey campaign (see Fig. 5.17a). In the northwest area of the basin, the comparison between the two water table appears as quite good, the simulated one is characterized by a higher gradient than the other; it could be that the hydrogeological model interpretation is wrong, or that the man-drown contours even could be wrong in this area (is a wooded area, few target points here). Different anisotropy in the area could be another explanation or groundwater recharge estimate could also be wrong.

Also in the southern part of the basin the comparison seems to be satisfactory. In the southwest area the simulated contours have a trend very different from the drawed, the simulated contours are not affected by the drains, it could be related to the not good fit of the drain flow in this area. Looking

to the table 5.12 values of drain outflow from drain reach 6, 8 and 3 has a whole value of 0.014 m3/s, while the sum of 6 and 8 flux target is 0.055 m3/s. This can be a reason, another reason could be the presence of a border of no flow cells boundary that induce the water table to mantain a more "regular" trend.

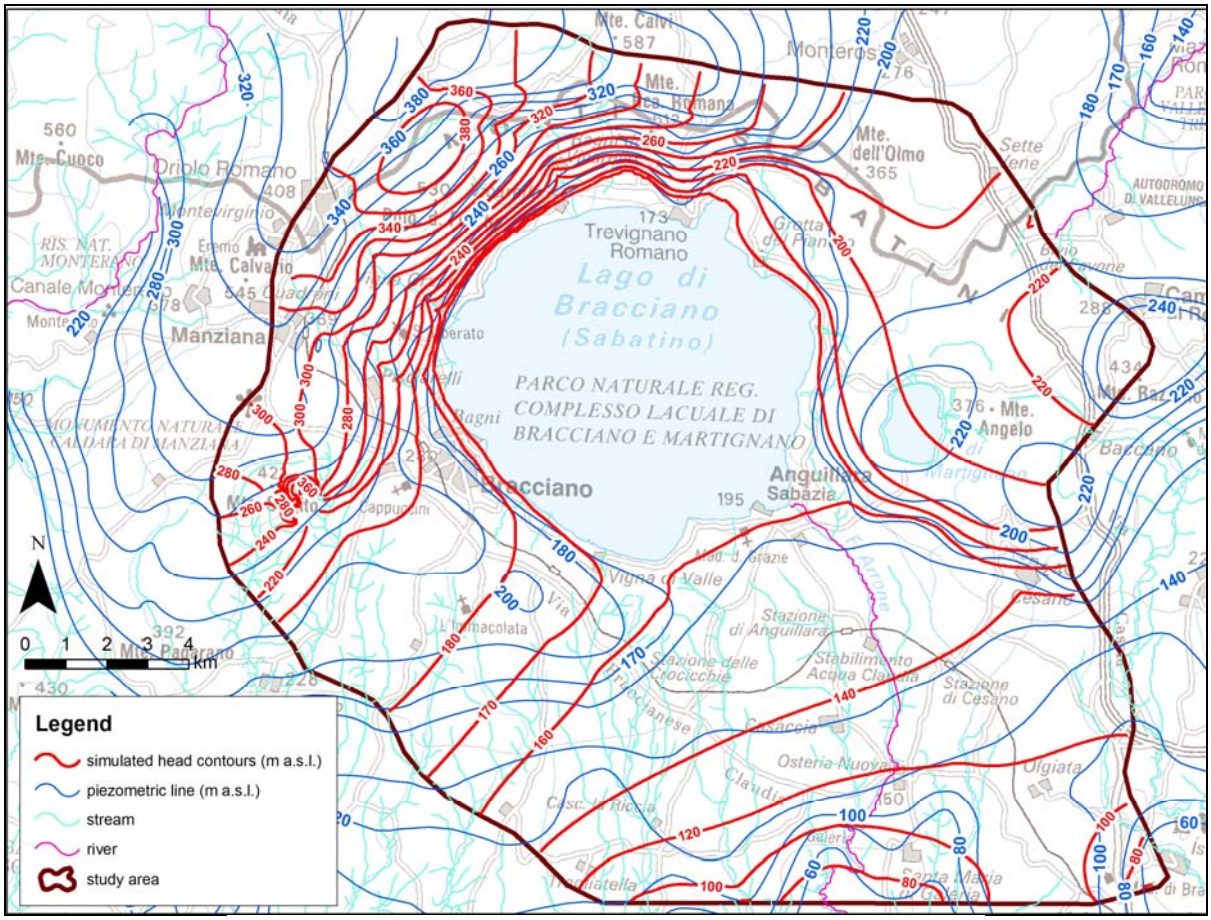

Figure 5.18: simulated head contours versus man-hand contours

5.2.8 Discussion

Some points can be summarised based on the results of the calibration process and looking to the mass balance results listed in table 5.13:

- Recharge simulated by Model A is too high, it is 19 % more than the estimated value (chapter 2) and so it is considered to be less representative, while the recharges simulated by the other models are acceptable within the range of most likely magnitudes.
- Net Constant head outflow can be compared with the basin outflow toward south direction, estimated in chapter 2, para…Model A CH net outflow values is too high (coherently with the recharge value). On the other side Model B CH net outflow is too low, compared to the estimated 1.5 m3/s. Model C and Model D net outflow results are satisfactory both.

- Drain outflow relative to Model A and to Model C are high, the amount of total drain outflow observed (survey campaign 2009) and integrated with other information achieved (see para 2..) is 0.75 m3/s as a maximum value. Model B drain outflow volume is too high, and thus not acceptable. Model D drain outflow has a satisfactory value.

Before to evaluate the results of the calibration, let us have a look at the lake balance and critically analize it.

Table 5.14: Models mass balance

		Model A	*Model B*	*Model C*	*Model D*
WELL	**INFLOWS**				
	OUTFLOWS	0.4512	0.4397	0.4397	0.4397
CH	**INFLOWS**	0.1256	0.3193	0.1842	0.1825
	OUTFLOWS	2.1504	0.5139	1.5943	1.5427
Drain	**INFLOWS**				
	OUTFLOWS	0.9511	1.9988	0.9190	0.7572
Recharge	**INFLOWS**	4.1274	3.3340	3.4997	3.2435
	OUTFLOWS				
Lake	**INFLOWS**	0.3176	0.1007	0.1518	0.1419
	OUTFLOWS	1.0604	0.8446	0.9098	0.8773
Total	**INFLOWS**	4.5707	3.7540	3.8358	3.5680
	OUTFLOWS	4.6132	3.7971	3.8629	3.6169
Percent Error		-0.9254	-1.1423	-0.7038	-1.3607
Lake level (m)		162.0500	163.1700	163.4000	162.4400
Percent Error = (INFLOWS-OUTFLOWS)*100/INFLOWS					
INFLOW and OUTFLOW unit is m^3/s					

In table 5.15 are reported the values which composed the lake balance as they appear in the lak spreadsheet of Groundwarter Vistas software. The value of Error Lake is reported and the calculation formula is indicated. Being “fixed” the precipitation, runoff, evaporation and withdrawal (see lake budget in chapter 2) values that determined the error are groundwater inflow and outflow. A more detailed lake-aquifer interaction understanding is necessary and a close examination on the lake balance components.

Table 5.15: Lake balance and error estimation

Model	Precipitation	Runoff	Groundwater inflow	Error-Lake *	Evapora-tion	Groundwater outflow	Withdrawal	pct-Error **
	m^3/s	m^3/s	m^3/s	m^3/s	m^3/s	m^3/s	m^3/s	
Model A	1.701	0.300	1.061	-0.0379	2.264	0.318	0.518	-1.2378
Model B	1.701	0.300	0.845	-0.0367	2.264	0.101	0.518	-1.2903
Model C	1.701	0.300	0.910	-0.0227	2.264	0.152	0.518	-0.7794
Model D	1.701	0.300	0.877	-0.0454	2.264	0.142	0.518	-1.5759
*** Error Lake = (Precipitation + Runoff + Groundwater inflow) - (Evaporation + Groundwater outflow + Withdrawal)**								
**** pct Error = 100 x Error Lake/(Precipitation + Runoff + Groundwater inflow)**								

Model D volume values seems to be the most acceptable, also even though the percent error is higher than 1 and for this quite high. What appears is that the calibration process could obtain an improving of the model and it gives indication that this model could be a starting model for a forward research study.

6. MODEL DISCUSSION AND CONCLUSIONS

The work of study presented can be retraced in the following main phases:

Comprehensive work of examination and interpretation of several field campaign data and literature data: well log stratigraphies, geological maps. From a detailed starting approach, in which the comprehensive volcanic sequence has been analyzed and each deposit's hydraulic behaviour has been considered, to a simplified re-organization with the definition of main hydrogeological complexes.

Conceptual model building: geological and hydrogeological framework has been investigated, a volumetric reconstruction of the aquifer has been made, were areas with different hydraulic behaviour were identified and media type defined (porous media and fractured). Then the identification of the sources and sinks: summarised in the elaborated water budget.

Some issues linked to the conceptual model have to be highlighted:

- The evaluation of the geologic heterogeneity effect on the hydraulic behaviour at the model scale. Volcanic deposits are characterized by a high heterogeneity which conditions groundwater flow patterns. So, which value could have an equivalent (effective) hydraulic conductivity, which can represent the integrated effect of a heterogeneous media? A more detailed analysis of pumping test; including data coming from other zones of the latium volcanic complex should be useful. Heterogeneity plays a key part in the uncertainty estimation (Section 4.7.1); it has to be improved for the proper evaluation of the two key parameters, correlation lenght λ and the σ (standard deviation of lnK).
- There was applied a methodology, suggested by Sonnenborg & Henriksen (2005), to determine the uncertainty of observational head data in relation to the model. The purpose of quantifying the uncertainty of observational head data (σ obs) is to achieve a measure of how accurately the model can reproduce the data. This should in principle be an objective criterion for how data weighted approximation and more importantly, how data of different types must be relatively weighted (important when using objective functions).
- It was revealed that the component due to geologic heterogeneity on the whole observational head uncertainty value, played a major role for such performance assessments and that the lack of experimental data suggested that this aspect should be further analysed in more depth when doing future model analysis of volcanic aquifers.

From the conceptual model a numerical groundwater flow model (mathematical model) was set up using a finite-difference code MODFLOW2000 and in a first step the graphical interface Visual Modflow 2009-1®. In this first two dimensional, steady state numerical groundwater model, the

aquifer system was represented by a one layer model describing the groundwater flow systems in 2 dimensions. Bracciano Lake area together with the underlying aquifer was represented as a simplified single aquifer system, with a higher hydraulic conductivity for the lake area compared to the surrounding areas. Results from calibration and tentative validation of this simplified model did not satisfy the initial performance criteria and objectives identified, e.g. it was not possible to evaluate lake-aquifer interactions (see chapter 1) in the required details with this first model. Next step consisted in setting up a new mathematical model based on a numerical integrated groundwater flow and lake model by use of Groundwater Vistas®5.41 (ESI), which allowed incorporation of the implemented lake package in this software, thus it was possible explicitly to include Lake Bracciano and its interaction with the underlying volcanic aquifer within this package. In order to keep the model as simple as possible, the whole aquifer was divided in two layers having the same thickness, except in Lake Bracciano area. In the lake area the upper layer was defined by the lake depth, whereas the lower layer was comprised by the aquifer.

Calibration and tentative validation tests were carried out on the VMF model. PEST was used for the inverse calibration, with head targets. The methodology allowed for a comparison of the residual statistics (difference between simulated and observed head). Hereby, head observational uncertainty when referring to model scale and other target values could be evaluated for three adopted quantitative accuracy Criteria (Refsgaard et al., 2010). Criteria value ranges were related to the established model detail that is a function of the objectives and the ambition level, as reported in Refsgaard et al., 2010. Ambition level can be considered as: 1) screening/basic (rough calculations), 2) intermediate and 3) high (aquifer simulation/detailed modelling). In this work of study it was decided, based on the available knowledge and data, to go for a screening model (as a first step): ”A screening model describes the regional characteristics of the ground-water-flow system without including the hydrogeologic detail or data density that would be necessary for answering site-specific questions. A calibrated screening model can be used with confidence to simulate a regional ground-water-flow system, but with less confidence to simulate local-scale flow. A screening model is a tool that can be used to improve the overall understanding of the hydrology of a basin by testing alternative conceptual models of the ground-water-flow system. Additionally, a screening model can be used to highlight areas where more hydrogeologic or water-quality data are needed”. (Feinstain et al., 2005)

Calibration carried out using the Groundwater Vistas 5.41® MODFLOW interface was initially focused on a sensitivity analysis to obtain an acceptable value of the lakebed hydraulic conductivity. A second step was the “autosensitivity” analysis (Groundwater Vistas tool) that permits to determine in a detailed analysis which parameters are sensitive to the available targets and which parameters are closely linked. Then PEST was used to calibrate the model using automatic calibration (inverse routines). At the beginning the head dataset and four flux values were applied. Subsequently eight flux values were used in combination with the

head data. Head targets were divided in two groups: one representing water table level nearby the lake and another representing targets all over the study area. Flux (flow in drainage systems) was then the third target group. When using inverse modelling (PEST) it is important to assign proper weights to the different targets in order to determine their relative importance in the parameter estimation process and understand by which weights the model is optimized with respect also to the objectives. Groundwater model results improved after the calibration process.

One of the objectives of the Bracciano groundwater model was that it should be a useful tool for testing the current understanding and assumptions established with the conceptual model. The use of inverse modelling (PEST) here allowed for understanding about whether the constructed model for the aquifer system and the lake interaction turned out as a credible and reliable model. If that is the case, then the model can be used in future management of the water resources for the volcanic basin. Thus two tests are important for evaluating the credibility and reliability: 1) Quantitative performance e.g. the simulated and observed water balance for aquifer and lake and results of validation tests (the 3 Criteria), when running the model with data not used for calibration and 2) Qualitative performance e.g. whether the calibrated parameters are within realistic ranges, whether the simulated head distribution is credible compared to manual mapped distributions etc.

During calibration process, the water budget values (Table 2.10) are constantly compared with the volumes estimation coming out from simulations (Table 5.3) to evaluate the results.

Table 2.10: Water budget (2002-2008)

Water Budget (mean values of the years 2002-2008) used for model 2009 simulation					
	Surface of the basin 380 km^2	**mm/year**	**Mm^3/year**	**m3/s**	**notes**
BASIN INFLOW	Rain	863.00	285.2	9.044	
	Evapotraspiration	373.00	123.3	3.909	
	Runoff	112.00	37.0	1.174	a percent of runoff goes to the lake (is an INFLOW to the lake)
	Recharge	330.00	109.1	**3.458**	
	sewage discharge inside the basin				water drained by sewage in the north of Bracciano Lake, is returned to the basin in the southern part (Cesano)
BASIN OUTFLOW	Water going out from the system, in the southern area	145.70	48.2	1.527	Estimation
	Total abstraction (Table 2.8)	109.65	41.7	1.323	Estimation
	Drain outflow			0.750	0.033 m3/s into Lake Bracciano, 0.1 m3/s feed Traiano aqueduct
	water drained by sewage system				Estimation
	TOTAL BASIN OUTFLOW	298.37	113.5	**3.600**	

Table 5.13: Models mass balance

		Model A	*Model B*	*Model C*	*Model D*
WELL	**INFLOWS**				
	OUTFLOWS	0.4512	0.4397	0.4397	0.4397
CH	**INFLOWS**	0.1256	0.3193	0.1842	0.1825
	OUTFLOWS	2.1504	0.5139	1.5943	1.5427
Drain	**INFLOWS**				
	OUTFLOWS	0.9511	1.9988	0.9190	0.7572
Recharge	**INFLOWS**	4.1274	3.3340	3.4997	3.2435
	OUTFLOWS				
Lake	**INFLOWS**	0.3176	0.1007	0.1518	0.1419
	OUTFLOWS	1.0604	0.8446	0.9098	0.8773
Total	**INFLOWS**	4.5707	3.7540	3.8358	3.5680
	OUTFLOWS	4.6132	3.7971	3.8629	3.6169
Percent Error		-0.9254	-1.1423	-0.7038	-1.3607
Lake level (m)		162.0500	163.1700	163.4000	162.4400
Percent Error = (INFLOWS-OUTFLOWS)*100/INFLOWS					
INFLOW and OUTFLOW unit is m^3/s					

The hydrogeologic system studied is characterized by the presence of four volcanic calderas, two of these still occupied by lakes (Lake Bracciano and Lake Martignano), there are two big water abstraction sites: one from lake (Paolo aqueduct) and the other fed by drains on the northwest side of the Lake Bracciano (Traiano aqueduct). At the same time the area is exposed to a continuous exploitation and dewatering from effect of the several public and private pumping wells from the groundwater aquifer put in action in the last twenty years.

The management of this complex system is challenging, and could surely benefit of the predictive capacities that a calibrated and validated model would enable and provide. It should be an interest and preference of the public administration to implement a stronger tool as a groundwater model, since a quantitative understanding of the whole system and its interactions are needed in order to exploit the groundwater aquifer in a sustainable way. Also for the different water users it is important to manage their own wells based on a better understanding of the whole system, and how their groundwater abstraction and land use affects the recharge, water balance of the aquifer, interaction with lake, wetlands near the lake and runoff from the area.

Lections learned with this work of study are:

- The use of the “lake package” to study aquifer-lake interactions appears to be promising and needed in order to properly address the conceptual model and the objectives defined.

- The MODFLOW model (final Groundwater Vistas model) could be a “basic” model that could be further improved if running a new model cycle in order to arrive to a starting model useful for the water resources administrator (with a special focus to Lake Bracciano, which constitute a site of environmental and economical interest); to reach an intermediate level useful for credible and reliable predictive simulations of the regional Bracciano aquifer-lake system for practical water management purposes

- The actual model should be improved by introducing a “zonation” of values of the lakebed hydraulic conductivity, considering influencing factors as the wave energy, the slope of the bottom surface, etc. This would probably require additional field investigations of the groundwater – lake interactions

- Simulation in transient conditions should be considered. This would enable more possibilities for validating the model, because time series of head and flow including the storage terms in groundwater and lake could be explicitly included. Lake budget data should be inserted at a time scale relevant (e.g. monthly): so rain, evaporation, runoff and lake elevation could be elaborated with this transient model approach. It could be another way to improve Bracciano groundwater model and to test also the input data (the calculation of monthly net precipitation and groundwater recharge to the model).

-A three or more layer model could be considered, with the aim of representing the presence of the aquitards, perched water tables etc. There are several challenges, and feasibility of different model codes with respect to describing ‘perched water tables’, unsaturated zone, overland flow, river and drainage flow etc. needs to be further evaluated before an high ambition model level could be met.

8. BIBLIOGRAPHY

ACQUAITAL S.R.L., 1997. *Studi preliminari per il Piano di Bacino. ST8 Modello di gestione del Lago di Bracciano*. Relazione inedita

Alvarez, W, 1972. *The Treia valley north of Rome: volcanic stratigraphy, topography evolution, and geological influences on human settlement.* Geol. Rom., 11, 153-176

Alvarez, W. 1973. *Ancient course of the Tiber river near Rome: an introduction to the Middle Pleistocene volcanic stratigraphy of Central Italy*. Geol. Soc. Am. Bull., 84, 749-758

Anderson, M.P. & Woessner, W.W., 1992. *Applied Groundwater Modelling*. Academic Press, San Diego.

American Society for Testing and Materials, 95-2006. *Guide for Documenting a Ground-Water Flow Model Application*. ASTM 5718, Philadelphia, Pennsylvania

American Society for Testing and Materials, 93-2008. *Standard Guide for Comparing Ground-Water Flow Model Simulations to Site-Specific Information*. ASTM 5490, Philadelphia, Pennsylvania

American Society for Testing and Materials, 04-2010. *Standard Guide for Application of a Ground-Water Flow Model to a Site-Specific Problem.* ASTM. 5447, Philadelphia, Pennsylvania

Baldi, P.; Civitelli, G.; Funiciello, R.; Lombardi, G.; Parotto, M. & Serva, L., 1978. *Study of the stratigraphy and mineralization of teh deep wells in Cesano geothermal field (Rome, Italy).* ENEL, Studi e ricerche, la geotermia nell'alto Lazio, 35, p. 71-86.

Bestini, M.; D'Amico, C.; Deriu, M; Bavaglini, S. & Vernia, L., 1971. *Note illustrative alla Carta Geologica d'Italia.* F. 143 Bracciano (Roma, IGM, 1971)

Boni, C., 1992. Unpublished report

Borghetti, G., Sbrana, A. & Sollevanti, F., 1981. *Vulcano-tettonica dell'area dei Monti Cimini e rapporti cronologici tra vulcanismo cimino e vicano*. Soc. Geol. Ital. Sed. Sci. "Vulcanismo e tettonica" Gargnano.

Brown, D.M. (1992) *The fidelity fallacy*. Ground Water, Vol. 30, No. 4, 1992

Bruno G. & Raspa G., 1994. *La pratica della Geostatistica non Lineare*. Il trattamento dei Dati Spaziali. Ed. Guerini.

Buonasorte, G., Carboni, M.G.e Conti, M.A., 1991. *Il substrato plio-pleistocenico delle vulcaniti sabatine: considerazioni stratigrafiche e paleoambientali*. Boll. Soc. Geol. It., 110: 35-40.

Camponeschi, B. & Lombardi, L., 1968. *Idrogeologia dell'area vulcanica Sabatina*. Mem. Soc. Geol. It., 8, 25-55

Capelli, G., Mazza, R. e Gazzetti, C., 2005. *Strumenti e strategie per la tutela e uso compatibile della risorsa idrica nel Lazio. Gli acquiferi vulcanici*. Quaderni di Tecniche di protezione ambientale. Protezione delle acque sotterranee, 78. Pitagora, Bologna, 186 pp.

Chilès & Delfiner, 1999. *Geostatistics. Modelling Spatial Uncertainty*. Wiley Series in Probability an Statistics.

Cioni, R., Laurenzi, M.A., Sbrana, A.e Villa, I.M., 1993. *40Ar/39Ar chronostratigraphy of the initial activity in the Sabatini Volcanic Complex (Italy)*. Boll. Soc. Geol. It., 112: 251-263.

Civitelli, G. & Corda, L., 1993. *The allochthonous succession of the Sabatini area in: note illustrative della carta "Sabatini volcanic Complex"*. Quaderni della Ricerca Scientifica 114, V. 11 CNR, Roma.

Dagan, G. (1986). *Statistical theory of groundwater flow and transport: Pore to laboratory, laboratory to formation and formation to regional scale*. Water Resources Research, 22(9), 120S-134S.

De Rita, D.; Funiciello, R.; Rossi, U & Sposato, A., 1983. *Structure and evolution of the Sacrofano-Baccano caldera, Sabatini volcanic complex, Rome.* J. Volcanol. Geotherm. Res., 17, 219-236

De Rita, D., Funiciello, R., Corda, L., Sposato, A. e Rossi, U., 1993. *Volcanic Units*. In: M.D. Filippo (Editor), Sabatini Volcanic Complex. Quaderni de "La Ricerca Scientifica" N°114 - Progetto Finalizzato "Geodinamica" - Monografie Finali - Vol. 11. C.N.R., Roma, pp. 33-79.

De Rita, D.; Di Filippo, M. & Sposato, A, 1993 a. *Carta geologica del Complesso Vulcanico Sabatino. In "Sabatini Volcanic Complex",* Edited by Michele Di Filippo, Quaderni de "La Ricerca Scientifica", CNR, 114, Carta fuori testo alla scala 1:50.000.

De Rita D., Di Filippo M. & Rosa C., 1996.*Structural evolution of the Bracciano volcano-tectonic depression, Sabatini Volcanic Sistrict, Italy*. In: McGuire W.J., Jones A.P. & Neuberg J. (eds) "Volcano Instability on the Earth and Other Planets". Geological Society Special Publication No 110, pp 225-236.

ENEL-VDAG-URM, 1994. *Aggiornamento delle caratteristiche geologiche di superficie e profonde del Lazio settentrionale.* Relazione inedita, ENEL, Università di Studi "La Sapienza", Dipartimento di Scienze della Terra, pp 110.

Feinstein D.T., Buchwald C.A., Dunning C.P. and Hunt R.J., 2006. *Development and Application of a Screening Model for Simulating Regional Ground-Water Flow in the St. Croix River Basin, Minnesota and Wisconsin*. U.S. Geological Survey Scientific Investigations Report 2005–5283, pp 50.

Fazzini, P.; Gelmini, R.; Mantovani, M.P. & Pellegrini, M., 1972. *Geologia dei Monti della Tolfa (Lazio settentrionale provincia di Viterbo e Roma*). Mem. Soc. Geol. Ital., 11, 65-144.

Funiciello R. & Parotto M., 1978. *Il substrato sedimentario nell'area dei Colli Albani: considerazioni geodinamiche e paleogeografiche sul margine tirrenico dell'Appennino centrale*. Geol. Rom., 17, 233-287.

Funiciello, R.; Mariotti, G.; Parotto, M.; Preite Martinez, M.; Tecce, F.; Toneatti, R. & Turi, B., 1979. *Geology, mineralogy, and stable isotope geochemistry of the Cesano geothermal field (Sabatini Mts. volcanic system, northern Latium, Italy).*Geothermics, 8, 55-73

Gasparri, A., 1987. *Idrologia e idrogeologia dell'apparato vulcanico dei monti della Tolfa e del piccolo bacino rappresentativo del Cinque Bottini*. Tesi di Laurea in Scienze della Terra, Università degli Studi di Roma "La Sapienza", Roma.

Gelhar, L.W. (1986) *Stochastic subsurface hydrology from theory to applications*. Water Resources Research, 22(9), 135S-145S.

Gelhar, L.W. (1993) *Stochastic Subsurface Hydrology*. Englewood Cliffs, NJ, Prentice Hall.

Harbaugh, A.W., McDonald, M.G., 1996. *User's Documentation for MODFLOW-96, an update to the US Geological Survey Modular Finite-Difference Ground-Water Flow Model*. US Geologic Survey, Open-File Report 96-486, Reston, Va.

Henry Darcy, *Les Fontaines Publiques de la Ville de Dijon ("The Public Fountains of the Town of Dijon"*), Dalmont, Paris (1856).

Henriksen HJ, Troldborg L, Nyegaard P, Sonnenborg TO, Refsgaard JC, Madsen B., 2003. *Methodology for construction, calibration and validation of a national hydrological model for Denmark*. J Hydrol; 280(1–4):52–71.

Hill, M.C.; Cooley, R.L.; Pollock, D.W.,1998. *A Controlled Experiment in Ground Water Flow Model Calibration*, Ground Water, Vol. 36, Issue 3, pp 520–535, May 1998.

Hunt, R.J.; Haitjema, M.H.; Krohelski, J.T. & Feinstein, D.T., 2003. *Simulating Ground Water-Lake Interactions: Approaches and Insights*. Ground Water, Vol. 41, No. 2, 227-237.

Indelman, P., Fiori A., Dagan G., 1996 *Steady Flow Toward Wells in Heterogeneous Formations: Mean Head and Equivalent Conductivity*. Water Resources Research, Vol. 32, No. 7, PP. 1975-1983.

ISTAT census of 2001 (population and industry) and census 2000 (agriculture)

Lauro, C., 1963. Nota riassuntiva sulle ricerche geopetrografiche sulla regione della Tolfa, Ric. Sci.

Lauro, C. & Negretti, G.C., 1969. *Contributo alla conoscenza delle vulcaniti delle regioni Tolfetana, Cerite e Manziate. Il vulcanismo nella Tuscia Romana: le manifestazioni vulcaniche acide del settore centro-occidentale*. Quad. CNR, 5, 1-39.

LeVeque, R.J., 2002. *Finite Volume Methods for Hyperbolic Problems*. Cambridge University Press, 2002.

Lombardi G., Morbidelli, L. & Negretti, G.C., 1965 a. *Lineamenti geopetrografici e strutturale degli affioramenti vulcanici del settore Tolfetano (Lazio)*. Rend. Soc. Mineral. Ital., 21, 157-164.

Lombardi G., Morbidelli, L. & Negretti, G.C., 1965 b. *Gli affioramenti eruttivi della Tolfaccia (Monti della Tolfa)*. Rend. Soc. Mineral. Ital., 21, 157-164.

Lombardi, L. & Giannotti, G.P., 1969. *Idrogeologia della zona a Sud-Est del lago di Bracciano*. Boll. Soc. Geol. It., 88: pp 107-121.

Matheron G., 1973. The intrinsic random functions and their applications. Advances in Applied Probability, 5, pp 439-468.

Mattias, P.P. & Ventriglia, V., 1970. *La regione vulcanica dei monti Cimini e Sabatini.* Mem. Soc. Geol. Ital., 9, 331-384.

Maxey, G. B., 1964. *Hydrostratigraphic units*. Journal of Hydrology, v. 2, p. 124-129.

Negretti, G.C., 1963. *Osservazioni vulcanologiche e petrografie sui "tufi caotici" e le ignimbriti dei Monti del Sasseto (Tolfa.,* Rend. Soc. Mineral. Ital., 19, 171-186.

Negretti, G.C. &Morbidelli, L., 1963. *Studio geopetrografico del complesso vulcanico tolfetano cerite (Lazio*). 3: Le manifestazioni vulcaniche acide del settore cerite, Quad. CNR, 3, 1-91.

Negretti, G.C.; Lombardi, G &Morbidelli, L., 1966. *Studio geopetrografico del complesso vulcanico tolfetano-cerite (Lazio)*. IV: Le manifestazioni vulcaniche acide del settore civitavecchiese tolfetano, Quad. CNR, 4, 1-173.

Neuman, S.P., 1994. *Generalized scaling of permeabilities*. Validation and effect of support scale, Geophysical Research Letters, 21 (5), 349-352.

Nilsson, B., Højbjerg, A.L., Refsgaard, J.C. & Troldborg, L. 2007. *Uncertainty in geological and hydrogeological data*. Hydrology and Earth System Sciences 11, 1551-1561

Oosterbaan R.J., Boonstra J. and Rao K.V.G.K., 1996. *The energy balance of groundwater flow applied to subsurface drainage in anisotropic soils by pipes or ditches with entrance resistance*. International Institute for Land Reclamation and Improvement (ILRI), Wageningen, The Netherlands.

Refsgaard, J.C., Henriksen, H.J., 2004. *Modelling guidelines e terminology and guiding principles*. Advances in Water Resources 27, 71e82.

Refsgaard, JC, Henriksen,HJ, Harrar, WG, Scholten, H and Kassahun, A., 2005.*Quality assurance in model based water management – review of existing practice and outline of new approaches*. Environmental Modelling and Software 20: 1201-1215

Refsgaard, J.C.; van der Sluijs, J.P.; H.J, Hojberg; Vanrolleghem, P.A., 2007. *Uncertainty in the environmental modelling process e A framework and guidance*, Environmental Modelling & Software 22, 1543-1556.

Refsgaard, JC., Troldborg, L, Henriksen, HJ, Højberg, AL, Møller, RR and Nielsen, AM (2010) *God praksis i hydrologisk modellering. Geovejledning 7*. GEUS (In Danish) 56 pp.

Rosa, C., 1995. *Evoluzione geologica quaternaria delle aree vulcaniche laziali: confronto tra il settore dei Monti Sabatini e quello dei Colli Albani.* Tesi Dottorato di Ricerca in Scienze della Terra - VII ciclo, Università degli Studi di Roma "La Sapienza", Roma, 224 pp.

Rushton, K.R., 2003. *Groundwater Hydrology: Conceptual and Computational Models*. John Wiley and Sons Ltd. ISBN 0-470-85004-3.

Sacco, F., 1930. *Dati geologici di trivellazioni nella vulsinia (Bolsena) e nel Sabatino (Bracciano)*. Boll. Serv. Geol. d'Italia, 49 (1), 145-160.

Scherillo, A., 1943. *Studi su alcuni tufi gialli della regione sabazia*. Period. Mineral., 14, 1-11.

Schulze-Makuch, D., Carlson, D.A., Cherkauer, D.S., Malik, P., 1999. *Scale dependency of hydraulic conductivity in heterogeneous media*. Ground Water, 37(6), 904-919.

Seaber, P.R. 1988. *Hydrostratigraphic Units*. In: Hydrogeology, the Geology of North America (W. Back, J.S. Rosenshein, and P.R. Seaber, Eds.), V.0-2, Geol. Soc. Amer., pp 9-14.

Sollevanti, F, 1983. *Geologic, vulcanologic and tectonic setting of the Vico-Cimini area, Italy*. J. Volcanol. Geotherm. Res., 17, 203-217.

Sonnenborg, T.O. & Jensen, K. H., 2005. *Handbog grundvandsmodellering, Kapitel 11*, *Skalaforhold heterogenitet*. GEUS (In Danish), 80 pp

Sonnenborg & Henriksen (2005). *Definition of requirements for RMS with specific assessment of uncertainty of observational data, Sobs*. Appendix D, Handbook of Goundwater Modelling. GEUS report 2005/80.

Tarantino L., 1991. *Bacino "Cinque Bottini" (Allumierre): bilancio idrologico del periodo maggio 1986-aprile 1987*. Tesi di Laurea in Scienze della Terra, Università degli Studi di Roma "La Sapienza", Roma.

Toro, E. F., 1999. *Riemann Solvers and Numerical Methods for Fluid Dynamics*. Springer-Verlag.

Wakernagel, 1995. *Multivariate Geostatistics*. Sprinter

Walker, W.E., Harremoe¨s, P., Rotmans, J., Van der Sluijs, J.P., Van Asselt, M.B.A., Janssen, P., Krayer von Krauss, M.P., 2003. *Defining uncertainty a conceptual basis for uncertainty management in model-based decision support*. Integrated Assessment 4 (1), 5e17.

A.1 APPENDIX A: DETAILED GEOLOGIC SEQUENCE

A 1.1 PREVULCANIC STRATIGRAPHIC SEQUENCE

Basal carbonate succession: (Upper Noric –Rhaetic- Oligocene age). This succession , in part contemporaneous with the flysch that covers it tectonically, includes the oldest terrains outcropping in the area or encountered in deep drill holes it constitutes the substratum of the entire area. Its presumable autochthony is based on observation of both the outcrops (Monte Soratte) and the deep drill holes (Valle del Baccano): in these latter almost 2000 meters of apparent thickness of the continuous series have been observed. They are not much disturbed.

Lithologically, the succession includes from marls to calcareous-marls in its upper portion.

This series consists mainly of alternations of limestone marl, marl and limestone with schist; details were then two distinct members tectonically superimposed (Fazzini et al, 1972): the upper part, called "Formation of Pietraforte (Aptian-Upper Cretaceous.) consists of alternating layers clayey-arenaceous and schist thickness of about 100-150 m, while at the less known as "Flysch Tolfetano" is dominating the area with limestone alternating calcareous clay, limestone and marly calcarenitic top (Sup Cretaceous-Oligocene). Other authors (Civitelli & Corda, 1993) propose a series stratigraphic and tectonic contacts locally interrupted by eteropie side, which goes by terms as schist-limestone and the base (which is incorporated in the lens of Pietraforte) in terms limestone, calcareous sandstone and marl-up.

The Allochthonous Succession

Allochthonous tectonic units rely on the carbonate basement, emerging abundantly in the western and north-west of the volcanic Sabatini District. The genesis of the rocks that make up these units is due to the evolving Ligure-Piemontese Ocean during a passive margin sedimentation.

The succession is composed by pelitic –arenaceus, calcareous- and caly sediments

The sequence is allochthonous in outcrop on the right bank area of the river Mignone and around Bassano Romano, also found evidence of coverage under the allochthonous volcanic deposits throughout the Sabatini area. Instead in the South East the volcanic deposits are in contact with the allochthonous sandy clay Plio-Pleistocene sediments.

Sediment cycle neo-indigenous Neogene

During the Pliocene and Pleistocene, the area has been subjected to clastic sedimentation in shallow water environment.

The evolution of this sedimentary phase can be outline in 6 phases:

1. Marine ingression in the lower Pliocene (Globorotalia zone puncticulata) (Fazzini et al, 1972) in western areas, and there after the retreat of the coastline, will affect even the most eastern areas of the Sabaini untill the high Pliocene.
2. Marine sedimentation until the middle Pliocene (biozone to Globorotalia gr. Crassaformis) (Fazzini et al, 1972), with a particle size passing through the clay basal part to coarse at the top of the deposit. The outcrops of this formation are limited and only present in areas of marked erosion (ditches within the Eastern area of Sabatini) or in areas where the pre-volcanic basement was exhumed. This second series is well represented in the western where outcrops of these sediments are in contact with the dominant acids related to the volcanic Tolfa - Cerite and Manziana. The intrusion of these acids has altered the dominant clay substrate.
3. Stratigraphic gap in the Late Pliocene (biozone to Globorotalia inflata (Fazzini et al, 1972) accompanied by tilting, Pleistocene deposits are found in eastern areas in unconformity with the preceding sediments. This gap has been interpreted as a phase of general emergence that affected the whole area covered by study.
4. New phase of marine sedimentation until the Early Pleistocene
5. Marine regression before the Middle Pleistocene, the age of this regressive phase varies slightly from the inner regions to the western ones.
6. Beginning of sedimentation represented by continental fluvial deposits in paleo valleys (found through surveys) and lacustrine deposits also interspersed at various volcanic stages.

A 1.2 VOLCANIC UNITS

Many authors have analyzed the stratigraphic sequence of Sabatini context, here it has been consider the detailed reconstruction of stratigraphic sequence made by De Rita et al. (1993),from bottom to top.

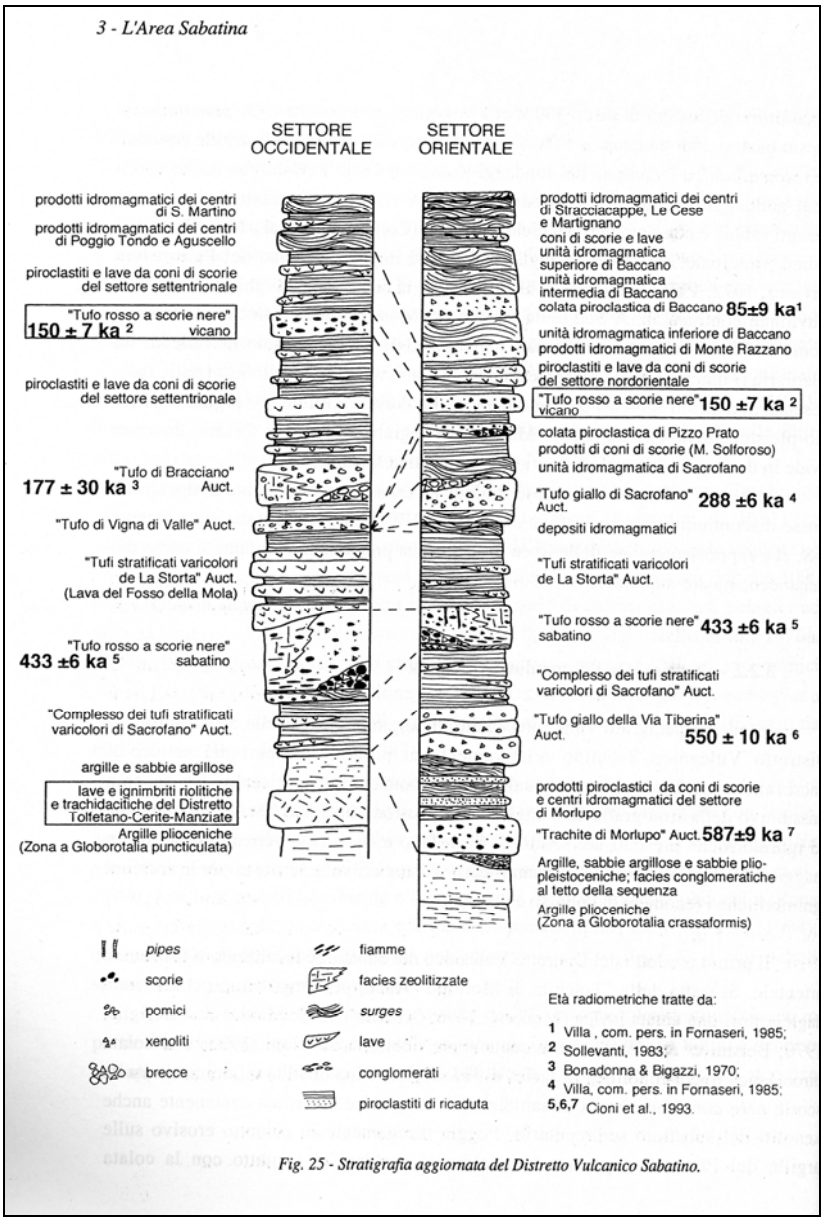

Figure 2.7: Stratigraphic log of the Sabatini volcanic complex (De Rita, 1993)

Acid volcanites of the Tolfetano-Cerite and Manziate complexes

They are located on the western edge of the Sabatini volcanic complex and represent the oldest volcanites in the area. They rest on clayey-sand deposits of the Pliocene and on a volcanic conglomerate of the Pleistocene. Volcanites include domes and ignimbrites with a compositional range from hypo to holocrystalline quarztlatites to liparite to latite. (Negretti, 1963; Negretti &Morbidelli, 1963; Lauro, 1963; Lombardi et al., 1965a,b; Negretti et al., 1966; Lauro & Negretti, 1969).

"Peperini listati" Auct. Pyroclastic flow unit

The "Peperini listati" Auct. Pyroclastic flow unit crops out only in the far western sector of the Sabatini volcanic complex, along the Mignone valley and to the south near Bagni di Stigliano. It is

constituted by grey volcanic welded ashes very enriched on altered leucite phenocrysts and with frequent lava and rare sedimentary lithics, pumices and gray and blanckish tipically flattened and riched in leucite and sanidine phenocrysts scoria.
Its thickness ranges from 10 to 30 m.

Pyroclastic fall products from Morlupo edifice

The Pyroclastic fall products of Morlupo crop out in the eastern sector of the complex with maximum thickness around Morlupo and Castelnuovo di Porto towns. The sequence is mainly composed of fall levels but many ash rich in accretionary lapilli layers could be hydromagmatic flow deposits. Generally it is composed of pumice lyers with grain size pumices ranging from 5 to 10 cm and containing crystals of sanidine and rich in accretionary lapilli ashy layers. Often the accretionary lapilli have lava nuclei. These levels contain also frequent carbonatic and marly sedimetnary lithics. The upper levels are constituted of scoria and of chaotic breccia.made up of pyroclastics, holocristalline, lava and sedimentary elements in an ashy matrix compacted to the top and altered into soil on which the Morlupo pyroclastic flow unit is present.At the base of the pyroclastic sequence, in the valley underlying the inhabited area of Morlupo a discontnuous trachytic lava crops put. It has scoriaceous microvesicles and it is strongly altered by the lateral transition to chatic agglomerates of scoria.

Sacrofano lower pyroclastic flow unit

This unit includes the “Tufo giallo della Via Tiberina” (Mattias & Ventriglia, 1970). It crops out in the eastern and southeastern edge of the Sabatini volcanic complex, from the Treia river valley to Ponte di Roma, but drill holes data point out that it is also present under the younger volcanic cover, with considerable thickness all over the eastern sector of the Sabatini volcanic complex.
The unit emplacement has been strongly affected by the pre-existing topography and its maximum thickness is reached along the Tevere valley that had a more western course and that was deviated to its actual position (Alvarez, 1972; 1973).
The unit shows homogeneous characateristics: due to zeolitizzation processes generally shows a lithified yellow matrix rich in orangey-yellow, altered, small sized pumices.
The isopach map show a ranging thickness from 50-60 m in the Riano area to 30 m near Calcata to less in the more eastern area; maximun thickness correspond to the Tevere valley and the minimum to the Monte Mario structural high. The general trend is gradually decreasing from Sacrofano edifice.

In the northern and southern sectors, the Sacrofano lower pyroclastic flow rests directly on the Plio-Pleistocene sediments. In the area of Mazzano and Calcata towns it rests on the conglomerate alluvial deposits of the Paleotevere river (Alvarez, 1972). In the area of Castelnuovo di Porto the unit rests on the pyroclastic fall products from Morlupo. Far southeast the pyroclastic flow unit rich a predominantly sedimentary lithics and with similar chemico-petrographical characteristics called "Peperino della via Flaminia" (Mattias & Ventriglia, 1970).
The Sacrofano lower pyroclastic flow is covered for almost all its extent by products of the pyroclastic fall activitty of Sacrofano whereas in the Morlupo-Castelnuovo di Porto area it is covered by the pyroclastic flow of Morlupo.

Morlupo pyroclastic flow unit

This unit crops out extensively in the surrounding areas of Morlupo town. The unit is consituted by several flow units and by different facies that seems to be the response of the flow to the pre-existing topography. In the valley it shows a massive unstratified and lithified aspect and it is constituted by yellow ashy matrix containing sedimentary and volcanic lithics. Otherways the ashy matrix is unconsolidated and shows planar and cross-laminations of discontinuos pumice layers. Inside the matrix accretionary lapilli and sedimentary lithics are present.
Locally reworked fall and hydromagmatic levels are also included in the unit. They are consituted by thin pumices, lapilli and ashy layers, locally reversal graded and with cross laminations. This unit partially includes the "Castelnuovo tufo" (Mattias & Ventriglia, 1970). It is superimposed on both Morlupo pyroclastic fall products and on the Sacrofano lower pyroclastic flow unit. At the Morlupo pyroclastic fall sequence contact soil ashy layer is present. Thickness (5-10 m) rapidly decrease towards south and towards north.

"Red tuff with black scoria" pyroclastic flow unit

The unit crop out extensively in almost all the peripherical Sabatini area with rather homogenous characteristics and with considerable thickness (10-30 m). It has not been found in the drilling performed in the Baccano-Cesano area and in the structural high of Monte Mario it is outcropping with considerable reduced thickness. It is also interesting to note that two drill holes drilled west of Bracciano Lake near Manziana do not encounter pyroclastic units with the "Tufo rosso a scorie nere" characteristics (Sacco, 1930).
The unit with an alkaline-trachytic composition (vulsinite:Scherillo, 1943) is generally constituted by a loosely sandy-pomiceous continuous black scoria. Locally the matrix appears lithified and the micro-pumiceous matrix is altered to yellowish-red colour inside which are distinticly visible black

pomices. The black pomices contain sanidine and leucite crystals; generally the pumices show a medium diameter of 20 cm but sizes up to 70-80 cm have been observed.
In the western sector is covered by the Bracciano pyroclastic flow unit.
The pyrocalstic flow was emplaced from a crater probably located south of Bracciano lake.

Pyroclastic fall products from Sacrofano and local scoria cones

The pyroclastic frin the explosive activity of Sacrofano include two pyroclastic sequences defined by AA as "Tufi stratificati varicolori di Sacrofano" and "Tufi stratificati varicolori di La Storta" (Mattias & Ventriglia, 1970). Locally the two sequences are interbedded with the "Tufo rosso a scorie nere" pyroclastic flow unit. The pyrocalstic fall deposits of Sacrofano are interbedded with scoria cone products on the sides and at the edge of the edifice (Monte Musino, Monte Cucco, Monte Solforoso, Monte Aguzzo, Casale Francalancia, Monte Maggiore and Monte Ficoreto).
The sequence is composed of graded alternating scoria-lapilli layers that are rich in pumiceous elements towards the top. The series is topped by thin stratified ashy layers with accretionary lapilly, that indicate a final hydromagmatic activity of the Sacrofano caldera.This unit corresponds, in the western sector, to the reworked series underlying the pyroclastic flow of Bracciano, and, in the sector north of Bracciao lake, it is interbedded with the explosive activity of local ceneters.

Sacrofano upper pyroclastic flow unit

This unit crops out with homogenous characteristics around the rim of the present caldera.It shows different facies that are the response of the flow to the pre-existing topography. Inside the valleys the flow loses the structures and becomes chaotic, massive, often lithoid and made up of alteres pumices in a pinkish-yellow ashy matrix.
The emplacement characteristics of this unit indicate that when its explosive event happened, the Sacrofano caldera was in part alredy formed. In fact, the unit rests on several scoria cones developed on the caldera rim and the flow partically emplaced back into the Sacrofano depression. Where this happened, the unir shows accumulation of both lava and sedimentary blocks; rapidly moving towards the outside og the caldera rom the unit loses structural characteristics and its granular sizes seem to become much finer. The unit always rests on the pyroclastics of the Sacrofano edifice and in the northeast sector it is covered by a hydromagmatic sequence. Its maximum thickness has been found in te valleys South of the inhabited area of Formello (Fosso della Mola) which are reccongnized as paleomophology. The Sacrofano upper pyroclastic flow totally filled up these valleys assuming lithoid and massive facies. Locally in these valleys at the base of the unit flow structures can be recognized. Locally the unit has the apparence of the lahar.

Pizzo Prato pyroclastic flow unit

This unit crop out along the southeastern edge of Bracciano lake and along the upper part of the Arrone valley. The unit shows several different facies that probably are the response of the flow to the pre-existing morphology. The prevailing facies, massive and chaotic, has dark grey scoriaceous matrix with scattered pumices and abundant sanidine crystals.The thikness is variable with a maximum of about 10 m. Because of the unit thickness values and of the morphology of the pre-existing topography, the vent area has been hipothesized as a fracture system with N-S direction located between Pizzo Prato and Mola Vecchia di Anguillara.

Vigna di Valle pyroclastic flow unit

This unit crops out onlyh in the southern sector, west of Anguillara Sabazia town. It is made up of a greyish, semicoherent sandy vitric and vesciculated matrix with a thickness of about 10 m. The emission point, according to Mattias & Ventriglia (1970) is the Vigna di Valle crater (west of Anguillara town) of which only southern rim remains.

At the base of this unit there is a lava flow of considerable thickness (10-15 m) with a petrographical composition similar to that of the pyroclastic flow. The units of Vigna di Valle pyroclastic flow, the unit of Bracciano and Pizzo Prato pyroclastic flow seem to be very similar as structure and depositional characteristics, even if they show different chemico-petrographical characters. Their emplacement had to happen almost contemporaneously after or during Bracciano basin collapse. It is possible that their eruptions occurred from fracture systems bordering the collapsing area.

Bracciano pyroclastic flow unit

This unit is extensively outcropping all over the western sector of Bracciano Laje. In the western area the unit rests on the “Peperini listati” and on the sabatinian “Tufo rosso a scorie nere” Auct., while in the southern and southernern area it rests on reworked pyroclastic products related to the fall activity from Sacrofano. The Bracciano pyroclastic flow unit is a pyroclastic flow deposit with a phonolitic tefritic composition (Bertini et al., 1971) and with a mean thickness of more than 50 m. It is costituited by a sandy-pumiceous matrix rich in lava and in sedimentary clasts.

As many other huge pyroclastic flow of the Latian volcanoes this unit shows different facies characteristics that are the response of the flow to the pre-existing topography on which it emplaced. Inside paleovalleys it assumes a lithoid aspect (probably due to zeolitization processes) and massive apparence, whitout the slightest indication of stratification. Generally it is semicoherent to incoherent with sandy-lapilli particle size.

By the alignment of a local agglomerate facies constituted by many considerable size (about 30-35 cm) lava clast it has been possible to hypotesize one or perhaps more alimentation fracture, oriented roughly in a N-S direction. It is interesting to note that Bracciano pyroclastic flow unit seems to be erupted contemporaneously to Vigna di Valle pyroclastic flow unit as both are immediately after the Bracciano Lake basin volcano-tectonic collapse.

Hydromagmatic products of the Vigna di Valle center

This unit crops out near the station of Vigna di Valle with thickness of 4-5 m; the stratigraphic base even though it is never visible by direct contact, is represented by the Vigna di Valle pyroclastic flow unit. The unit is made up of light grey, coarse ash quite rich in altered leucite and with lava fragments.

The Vico units

All over the northern sector, a pyroclastic flow unit characterized by a reddish ashy matrix with black scoria crops out. Thins unit is very similar to the sabatinian "Tufo rosso a scorie nere" Auct. has been distinguished by its different stratigraphic position as it has been dated 0.155 + 0.01 (Borghetti et al., 1981; Sollevanti, 1983) and it has to be superimposed to the Bracciano pyroclastic flow unit even if the contact is rarely visible.

The Vico "Tufo rosso a scorie nere" has a tephritic phonolitic composition and in the Sabatini area the unit shows homogenoeus characteristics: the base is often characterized by the presence of two pumice layers; most of the deposits is constituted by a pomiceous lithified sandy matrix containing big black scoria and rare sedimentary and volcanic lithics. Locally the unit enters deep erosional valleys and oblique contacts with the underlying pyroclastic fall deposits are visible. The median thickness of the unit is around 20-30 m but a maximun of 50 m has been observed. The "Tufo rosso a scorie nere" Auct. from Vico is interbedded with pyroclastic fall deposits from the same edifice. These fall deposits correspond to the "Tufi stratificati varicolori vicani" (Mattias & Ventriglia, 1970) that in the Sabatini area crop out discontinuously in the most northern part of the map.

Pyroclastic fall deposits from local centers of the northern sector (Monterosi, Monte Guerrano, Monte Calvi, Trevignano)

This unit is mainly consituted by fall levels of magmatic origin and includes products of many local centers erupted over a long period of time. By drill holes data it has been possible to deduce that in the northcentral sector of the Sabatini area volcanism was active contemporaneously with Sacrofano edifice grouwing up. Some of the scoria cones or lava flows had to be already present in this sector

to stop the lower and upper Sacrofano pyroclastic flow expansion. The fall sequence is directly on the sedimentaty substratum represented by thin thickness of Pliocene sandy-clays and has lateral transition to Sacrofano fall deposits. At the top it is interbedded with hydromagmatic levels from the same centers. The Monterosi products include scoriaceous-lapilli levels interbedded with ashy pyroclastic flow levels. The Monte Guerano and Monte Calvi products are consituted by bad sorted and chaotic levels with bombs and lapillu interbedded with 50 cm thick pomiceous levels. Chemico-petrographical analyses made up on some lava lithics og the Trevignano tuff (Sciotti, 1966) indicate different types of lava flows as leucitites, tephritic leucitites, leucititic tephrites and trachytic phonolotes leucite bearing. At the top of the Trevignano sequence thin sandy lapilli levels are interbedded with pomiceous ashy levels and with thin yellow pyrocalstic flow deposits. The sequence is interested by local reverse faulting with small displacement.

Hydromagmatic products from Monterosi, V.S. Maria, S. Martino, Aguscello, Trevignagno, Pizzopiede, Tre Querce craters

These products of phreatic and hydromagmatic origin from different craters, have been grouped togheter because erupted almost contemporaneously and interbedded with fall deposits from other centers of the same sector. The hydromagmatic products from Aguscello crater seem to be the oldest. The rest directly on the “Tufo rosso a scorie nere” Auct. from Vico and more or less contemporaneous, or just a little previous to the scoria cones products from Monte Guerrano and Monte Calvi, northwest of Bracciano Lake.

On the pyroclastic products of Monte Guerrano and Monte Calvi a sequence of hydromagmatic layhers from different small centers coalesced and aligned in a NW-SE direction are present in the area of V.S. Martino. The products of V.S. Martino are more or less contemporaneous with those of another hydromagmatic center located in the vicinity of V.S. Maria. In this case, too, there are thynly stratified pyroclastic with sandwaves structures and levels rich in accretionary lapilly and impact sags. The lithics that are generally lava are of considerable size; the grain size of the layers is rather coarse. The stratigraphic relationship between the products of Pizzo Piede and Tre Querce centers are not clear. These phreatic thinly stratified pyroclastic with parallel and cross laminations and impact sags rest in a pyroclastic sequence partly reworked and probably related to the Sacrofano activity. It is difficult to define exactly the stratigraphic relations of the products of Trevignano with the units of the neighboring centers. After mainly pyroclastic and lava activity Trevignano as the other centers located further north, ended its activity with hydromagmatic explosions that generated well straified products with structures characteristics of the “base surge”.

Sacrofano hydromagmatic dry surge

This unit is consituted of fine grey ashes, thinly stratified, characterized by cross and planar laminations and occasional impact sags. This unit crops out with limited extent around the border of the Sacrofano caldera, it rests directily on the upper pyroclastic flow unit of Sacrofano from which it is separeted by only a thin layer of discontinuity.

It 'difficult to attribute to an eruptive center, but could come from Sacrofano area, given its position, in any case it is not sure the position of the vent. Could belong to the first phase of activity of Baccano or Monte Razzano but lack certain elements.

Pyroclastics products from local centers on the eastern side of the Sacrofano caldera (Monte S. Silvestro, Casale Nuovo, Monte Rosi, Fosso Cisterna e Li Porcini)

These units lie over the upper pyroclastic flow of Sacrofano. Due to the activity of the small, local, explosive craters they are mainly fall and phreatic pyroclastics. One center, with a diameter of about 600-700 m is located near Monte S. Silvestro, 1 km east of Sacrofano caldera. Monte S. Silvestro has emitted alternating layers of thinly stratified ashes and of scoria-lapilli characterized by the presence of small sized bombs that sometimes form impact sags structures. A second explosive center of modest dimension is located further south in the Casale Nuovo area. Its pyroclastic sequence of limited thicknes, is quite similar to that of Monte S. Silvestro. A third center is located about 2 km NE od Monte Solforoso, in the vicinity of Monte Rosi, and seems to be associated with the activity of two other small centers, located immediately further south: one in the vicinity of Fosso Citerno, the other in the area of Li Porcini. These three small centers have had similtar and probably contemporaneous activity; their products are limted in thickness and are only distributed at a few hundred of meters around the emission point. The series are made up of a grey thinly stratified ashes rich in lithics of leucititic lavas. These pyroclastics are connected to an explosive activity that followed the caldera collapse phase of Sacrofano.

Monte Razzano hydromagmatic deposits

Monte Razzano is a small edifice grown up inside the Sacrofano caldera on its western edge. The lithological characteristics of its products and its morphological shape allow to classify Monte Razzano as a tuff cone. Its pyroclastics have a considerable distribution going from the inhabited area of Campagnago to the edge of Baccano. The products are generally massive, lithoid rich in subvolcanic and lava clasts and sedimentary lithics with abundant crystals of biotite, piroxene and leucite. Very rounded pumices with weak vescicular structures are present in small amounts.

Near the summit of Monte Razzano the dimension of the lithics reach 70 cm. The tuff cone products dip slightly toward ENE in te eastern part. They dip sharply toward WSW in the western part. The actual summit of Monte Razzano seems, then, to be the eastern part of the older tuff cone crater rim. It had to be collapsed a little further to the west during the Baccano caldera sinking. On the north-eastern slopes of Monte Razzano the products are covered by a successive hydromagmatic unit and by the pyroclastic flow of Baccano whose thickness decreases rapidly towards the summit of Monte Razzano.

Lower hydromagmatic unit from Baccano

The products of Baccano are largely outcropping all around the morphological depression of Baccano valley that has benn identified as a caldera. The morphological relatinoship between Baccano and Sacrofano depressions demonstrates that the activity of Baccano began after the Sacrofano caldera collapse and after the Monte Razzano growing up. The lower hydromagmatic unit from Baccano seems the first deposit related to this center. It is consituted by a series of hydromagmatic explosions that developed mainly to the south of Baccano and sporadically east, inside of the Sacrofano caldera and in valley of Baccano as it is possible to hypotesize by the deepining of the beds and also by the relationship between the products reconstructed trough deep drillin data (De Rita et al., 1983). This unit show all the typical depositional structures of hydromagmatic products such as planar and cross laminations, layers with accretionary lapilli. The extent and the concentration of the "ejecta" in this unit allow to hypothesize a vent area located in the southern zone of the valley of Baccano.

Baccano pyroclastic flow unit

This unit extends to the south and to the SW of the present caldera of Baccano. It's areal distribution was strongly influenced by the pre-existing morphology. In particular the structure of Monte Razzano obstructed the flow expansion eastward forcing the flow to move SE. The Baccano pyroclastic flow is always on the lower Baccano hydromagmatic unit and it is coverd by the intermediate Baccano hydromagmatic unit. Different stratigraphical relationship can be observed only on the eastern side of Baccano caldera, where the unit is directly in contact with the Monte Razzano units (probably the flow tried to climb up the tuff cone) and inside the Sacrofano caldera where the Baccano unit flowed up on the side of the ancient caldera emplacing directly on Sacrofano deposits. At the contact an ashy soil level is present. Everywhere the unit is very rich in whitish, trachytic pumices in sizes that vary from 2 to 15 cm, according to their distance from the Baccano center, in leucite crystals that are often analcime and, to a lesser extent, in biotite and in pyroxene. The unit can

be divided into an upper predominantly cineritica with low and high content of pumice stone and leucite.

Monte S. Angelo hydromagmatic deposits

These deposits crop out along the road from Baccano valley to the summit of Monte S. Angelo. They are consituted by massive, lithoid rich in subvolcanic and lava clasts and sedimentary lithics asches.

At the top of the deposits ashy cross-laminated levels predominates; bomb sags structures are evident. These depositis are very similar to those consituting Monte Razzano tuff cone and they have been considered by the Authors products of the same activity drom Baccano. The morphological shape of Monte S. Angelo, the dipping of the levels and the grain size of the ejecta have allowed to hypothesize that also Monte S. Angelo is a small tuff cone, younger that Monte Razzano as its products are on the Baccano pyroclastic flow unit. The Monte S. Angelo western and eastern sides are truncated by the Baccano and Martignano caldera collapse faults.

Hydromagmatic products of Polline, La Conca e Lagusciello

Above the pyroclastic flow of Baccano along the eastern edge of Bracciano Lake and aligned in a N-S direction the centers of Polline, La Conca and Lagusiello are present. The products related to the Polline center rest on the products of Pizzo Prato unit, locally interbedded with reworked pumices of the Baccano pyroclastic flow. The discontinuous outcrops show chaotic layers rich in lava lithics from the underlying units. Toward the top there are ashy, thinly stratified levels with impact sags and cross-bedding structures. Inside the crater the products of Polline are covered by the hydromagmatic pyroclastiscs of Martignano.

The products of La Conca are present only in te eastern rim of the crater where it is possible to observe a chaotic layer, made up solely of clasts from the underlying lava units, which changes towards the top to thinly stratified layers with small lava lithics (max 1 cm).

The products of Acquarello crater are rarely visible as they are almost totally masked by younger deposits. They are consituted by ashy levels rich in lava lithics and by thin levels of sandy-lapilli size with planar and cross laminations.

The products of Lagusiello, cropping out along the southwestern rim of the crater do not have a clear straigraphic relationship with the surrounding products; there are thinly stratified ashes with accretionary lapilly, impact sags and frequent lava and “Tufo rosso a scorie nere” lithics.

Baccano intermediate hydromagmatic unit

This unit is characterized by an ashy-sandy matrix rich in analcime, sedimentary and lava lithics with a grain size from 2 to 10 cm. The acrretionary lapilli are scattered, appearing only in the upper part of the unit. The unit mainly extends towards the E and SE; westward it is covered by successive products and crops out only at the bottom of the deepest valleys. The emplacement of the intermediate unit caused the Baccano caldera collapse. An ashy lens of paleosoil locally enriched in manganese oxides is present at the base of the unir, indicating that after the emplacement of the pyroclastic flow of Baccano there was a short pause.

Baccano upper hydromagmatic unit

This unit represents the last product from the Baccano center. It crops out inside the caldera (where it has not been re-covered by lacustrine sediments), north of Baccano valley, on the slopes of Monte Razzano. It has a thikness of about 10 m. Westward it is masked by the hydromagmatic products of Martignano. Lithologically, it is ashy with clear parallel and sanwaves laminations and impact sags and is rich in accretionary lapilly. This lithics have dimensions of 10 cm and are of both lava and sedimentary types. The areal distribution of the products indicate that the last center of explosion was located in the presently most depressed part of Baccano valley.

Hydromagmatic products of the final stage from the activity of Stracciacappe, Le Cese and Martignano

The activity of Martignano consisted of several hydromagmatic explosions which emplaced huge thickness of gery, semilithoid ash, with alva, pyroclastic, and infrequently, sedimentary lithics with accretionary lapilli and with parallel and cross laminations. The few existing outcrops do not permit ta complete stratigraphical recontruction of the different centers that are morphologically evident; very probably the activity of Martignano began before the end of the activity of Baccano or the "Tuff cone of Monte S. Angelo". The last pyroclastics of Martignano eastward rest on the last unit of Baccano, westward on the pumices related to the pyroclastic flow of Baccano and on the unit of Pizzo Prato; they cover the inner part of the Polline crater and the products of La Conca. On the southern edge og the Martignano Lage the hydromagmatic products rest in the pyroclastic flow of Baccano, which encircles a preceding scoria cone. The last evidence of magmatic activity in the area of Martigano has never been noted unitll now.

The last hydromagmatic explosions seem to have occurred at the Stracciacappe and Le Cese craters. Both craters have produced the hydromagmatic units that are emplaced above the Martignano unit and the upper Baccano unit. The products are easily vistible in proximity to the two centers and do not show obvious reciprocal relationships. Particularly at Stracciacappe where a well-laminated hy-

dromagmatic series can be observed, this series has impact sags and lithics of lavas and infrequent sediments of consideable size (up to a max of 2 m in diameter). It always has dip direction toward s the exterior of the crater. The upper part has an ashy sandy matrix, with small lithics with a maximun size of 30 cm and with parallel, cross-lamination. The type of lithics and the size of the center, which is quite small lead autors to assume that the explosions were superfical.

A.2 ANNEX B: TABLES RELATIVES TO ALL THE GAUGING STATIONS PRESENTED IN THE AREA OF STUDY

See Fig. 2.21 for the location of the gauging stations listed in the tables downhere.

Table 2.3.b: Streams with a centripetal direction towards the lake

Map Code	*Stream*	*Elevation (m a.s.l.)*	*Season*	*Year*	*Flow rate (l/s)*
B7	Pratone stream	165.5	winter	1995	0.0
B7	Pratone stream	165	summer	1995	0.0
B33	Vigna di Valle stream	165	winter	1995	0.0
B33	Vigna di Valle stream	165	summer	1995	0.0
B22	Fonte Lupo stream	180	winter	1995	0.0
B22	Fonte Lupo stream	180	summer	1995	0.0
B34	Lobbra stream	167	winter	1995	6.0
B34	Lobbra stream	167	summer	1995	4.0
B8	Sassone stream	165	winter	1995	0.9
B8	Sassone stream	165	summer	1995	0.4
B8	Sassone stream	165	summer	2009	0.5
B18	Grotte Renara stream	165	winter	1992	22.0
B18	Grotte Renara stream	165	winter	1995	14.0
B18	Grotte Renara stream	165	summer	1995	10.0
B18	Grotte Renara stream	165	summer	2009	15.8
B15	la Fiora stream	165	winter	1992	12.0
B15	la Fiora stream	165	winter	1995	7.0
B15	la Fiora stream	165	summer	1995	6.0
B15	la Fiora stream	165	summer	2009	8.0
B21	Vigna Orsini stream	166	winter	1992	37.0
B21	Vigna Orsini stream	166	winter	1995	25.0
B21	Vigna Orsini stream	166	summer	1995	25.0
B20	Val D'Aia stream	182	winter	1992	61.0
B20	Val D'Aia stream	169	winter	1995	4.0
B20	Val D'Aia stream	169	summer	1995	3.0
B20	Val D'Aia stream	177	summer	2009	6.7
B5	Bagnatore stream	178	winter	1992	1.0
B5	Bagnatore stream	169	winter	1995	0.3
B5	Bagnatore stream	169	summer	1995	0.0
B11	la Calandrina stream	172	winter	1992	4.0
B11	la Calandrina stream	172	winter	1995	0.8
B11	la Calandrina stream	172	summer	1995	0.0
B11	la Calandrina stream	172	summer	2009	0.2
B6	Pianoro stream	165	winter	1995	0.0
B6	Pianoro stream	165	summer	1995	0.2
B30	Sambuco stream	169	winter	1992	5.0
B4	Cognolo stream	169	winter	1992	1.0
B4	Cognolo stream	169	winter	1995	0.1
B4	Cognolo stream	169	summer	1995	0.0
B29	Polline stream	164	winter	1995	0.5
B29	Polline stream	164	summer	1995	0.0
B29	Polline stream	167	winter	1992	3.0
B29	Polline stream	166	summer	2009	1.0
B14	la Conca stream	167	winter	1992	5.0
B14	la Conca stream	165	winter	1995	1.2
B14	la Conca stream	165	summer	1995	2.0
B3	Casacci stream	167	winter	1995	0.9
B3	Casacci stream	167	summer	1995	0.1
B3	Casacci stream	167	summer	2009	0.2
B24	il Ginestreto stream	170	winter	1995	0.0
B24	il Ginestreto stream	170	summer	1995	0.0
B2	Campo Porcino stream	170	winter	1995	0.0
B2	Campo Porcino stream	170	summer	1995	0.0

Table 2.4.b: Streams draining the south-east side

Map Code	*Stream*	*Elevation (m a.s.l.)*	*Season*	*Year*	*Flow rate (l/s)*
B1	Stracciacappa drain	209	winter	1999	0.6
B1	Stracciacappa drain	209	summer	1999	0.0
B1	Stracciacappa drain	164	summer	2009	0.0
B16	la Merla stream	212	winter	1999	0.5
B16	la Merla stream	212	summer	1999	0.0
B25	La Mola stream	155	summer	1982	119.0
B26	Maestro Curzio stream	215	winter	1981	15.0
B26	Maestro Curzio stream	215	summer	1981	5.0
B26	Maestro Curzio stream	215	winter	1999	77.0
B26	Maestro Curzio stream	215	summer	1999	0.0
B26a	Maestro Curzio stream	195	winter	1999	216.3
B26a	Maestro Curzio stream	195	summer	1999	14.0
B23	Galeria stream	120	winter	1981	30.0
B23	Galeria stream	120	summer	1981	10.0
B23	Galeria stream	120	summer	2009	0.0
B35	Valchetta creek	93	winter	1981	327.0
B35	Valchetta creek	93	summer	1981	310.0
B35	Valchetta creek	41	summer	2009	226.1
B28	Piordo stream	90	winter	1981	56.0
B28	Piordo stream	90	summer	1981	56.0
B28	Piordo stream	45	summer	2009	115.6

Table 2.5.b: Streams draining southwest side

Map Code	*Stream*	*Elevation (m a.s.l.)*	*Year*	*Season*	*Flow rate (l/s)*
B12	la Caldara stream	260	summer	2009	0.2
B31	Vaccina stream	195	summer	2009	23.3
B32	Vaccinella stream	135	winter	1981	30.0
B32	Vaccinella stream	135	summer	1981	22.0
B32	Vaccinella stream	135	summer	2009	6.6
B9	Tavolato stream	95	winter	1981	10.0
B9	Tavolato stream	95	summer	1981	10.0
B9	Tavolato stream	95	summer	2002	17.0
B9	Tavolato stream	95	summer	2009	36.7
B19	Tagliatelle stream	140	winter	1981	1.0
B19	Tagliatelle stream	140	summer	1981	0.0
B19	Tagliatelle stream	140	summer	2002	0.0
B19	Tagliatelle stream	140	summer	2009	0.0
B17	Cadute stream	144	winter	1981	4.0
B17	Cadute stream	144	summer	1981	1.0
B17	Cadute stream	140	summer	2002	2.0
B17	Cadute stream	140	summer	2009	3.0
B27	Pietroso stream	146	summer	2002	0.0
B27	Pietroso stream	146	summer	2009	0.5
B10	la Cadutella stream	46	winter	1981	1.0
B10	la Cadutella stream	46	summer	1981	1.0
B10	la Cadutella stream	46	summer	2002	0.0
B10	la Cadutella stream	46	summer	2009	1.0
B13	la Casaccia stream	131	winter	1981	63.0
B13	la Casaccia stream	131	summer	1981	15.0
B13	la Casaccia stream	131	summer	2002	18.0
B13	la Casaccia stream	131	summer	2009	16.0